

REFERENCE ONLY

UNIVERSITY OF LONDON THESIS

Degree MD Year 2004 Name of Author VAINOVA, S. J.

LOAN

Institute of Cancer Research Library

Theses may not be lent to _____ at the University, _____ library may lend a copy to

A.

This copy has been deposited in the Library of ICR

This copy has been deposited in the University of London Library, Senate House, Malet Street, London WC1E 7HU.

**USE OF MAGNETIC RESONANCE SPECTROSCOPY
TO STUDY IN VIVO METABOLISM OF IFOSFAMIDE
AND RESPONSE TO CHEMOTHERAPY**

Thesis submitted to the

University of London

for the degree of

Doctor of Medicine

by

Dr Sucheta Jayant Vaidya

Department of Paediatric Oncology

The Royal Marsden NHS Trust &

The Institute of Cancer Research

Sutton

2004

Dedicated to

**Gangadhar R Sardesai
Radhabai G Sardesai
Sharad G Vaidya
Nirmala S Vaidya**

ABSTRACT

Ifosfamide and cyclophosphamide are extensively used in cancer therapy. These are both prodrugs, which produce active, inactive and toxic metabolites. There is considerable variation in the levels of metabolites of these prodrugs in plasma and their clinical response rates.

Magnetic Resonance Spectroscopy (MRS) can detect changes in tumour metabolism induced by chemotherapy. MRS may demonstrate tumour response earlier than volume response and this may allow us to tailor therapies to individual patients.

For this thesis, MRS was used to study uptake and metabolism of ifosfamide in the tumour and in the liver –the site of its activation. The role of MRS to assess chemotherapy response in a paediatric tumour model was also studied.

A review of literature about the basis of MRS, its role in tumour response assessment and ifosfamide metabolism was undertaken. A clinical study was performed. It was found that ifosfamide and cyclophosphamide could be detected by ^{31}P MRS signals in liver of paediatric and adult patients when the dose was over 1500 mg.

The pharmacokinetics of ifosfamide using ^{31}P MRS in a mouse model was then studied. The half-life of ifosfamide in liver and tumour was calculated using the decay of ifosfamide peak in vivo. MRS was not sensitive enough to permit measurement of most ifosfamide metabolites. The amount of ifosfamide and its metabolites in liver and tumour were measured using high performance liquid chromatography -mass spectrometry. Carboxy-ifosfamide

was significantly higher in liver tissues and keto-ifosfamide was higher in most tumour samples.

Finally, the effects of ifosfamide on phospholipid metabolism and high-energy phosphates as seen on ^{31}P MR spectra were evaluated in a xenograft model with a paediatric rhabdomyosarcoma cell line. On Day 8, in vivo, the ratios of phosphomonoesters (PME) and β -nucleotide triphosphate to inorganic phosphate were significantly raised in the ifosfamide-treated tumours compared with controls. In vitro findings confirmed that the phosphoethanolamine component of PME was responsible for the increase in the PME.

Our studies suggest that ^{31}P MRS could be used to evaluate ifosfamide metabolism in liver and tumour. Measurements with ^{31}P MRS could also be used as a non-invasive marker of tumour response with potential clinical applications.

TABLE OF CONTENTS

ABSTRACT	3
TABLE OF CONTENTS	5
DECLARATION	11
ACKNOWLEDGEMENTS	12
INDEX OF TABLES	14
INDEX OF FIGURES	16
LIST OF ABBREVIATIONS	19
CHAPTER 1	22
INTRODUCTION AND LITERATURE REVIEW	22
1.1 Background	23
1.2 Magnetic resonance	25
1.2.1 Historical perspectives	25
1.2.2 <i>Basis for the NMR phenomenon</i>	26
1.2.3 <i>Manipulations required to produce an NMR signal</i>	29
1.2.4 Chemical shift	32
1.2.5 Localisation	33
1.2.6 Interpretation of data.....	35
1.2.7 <i>³¹P Magnetic Resonance Spectroscopy</i>	36
1.2.8 Coupling and decoupling.....	38
1.2.9 <i>High-resolution Magnetic resonance spectroscopy</i>	39
1.2.10 <i>Magic angle sample spinning</i>	40
1.3 Applications of MRS to cancer	41
1.3.1 MRS of tumours	42
1.3.2 <i>Biological implications of ³¹P MRS</i>	46

1.3.2.i. Choline cycle	47
1.3.2.ii. Ethanolamine cycle.....	48
1.3.3. Study of tumour physiology.....	50
1.3.4. Potential role of MRS in assessment of tumour response in paediatric oncology.....	52
1.3.4.i. Introduction.....	52
1.3.4.ii. Examples of pre-clinical studies relevant to tumour response ..	52
1.3.4.iii. Examples of clinical studies	54
1.3.4.iv. Conclusion of literature review of MRS and tumour response .	60
1.4 Pharmacokinetic study of ifosfamide	62
1.4.1. History of oxazaphosphorines.....	62
1.4.2. Structures of ifosfamide and cyclophosphamide.....	63
1.4.3 Mechanism of action of ifosfamide.....	64
1.4.4. Metabolism of ifosfamide	65
1.4.5. Metabolic distribution of ifosfamide	69
1.4.6 Pharmacokinetic variations and factors affecting metabolism.....	71
1.4.7. Pharmacogenetics	75
1.4.8. Relationship between Ifosfamide metabolism and efficacy & toxicity	77
1.4.9. Ifosfamide and magnetic resonance spectroscopy	79
1.4.9.i Introduction.....	79
1.4.9.ii ³¹ P MRS.....	79
1.4.10. Therapeutic drug monitoring	85
1.4.11 : Overall aims	88
CHAPTER 2	90

CLINICAL STUDY TO DETECT IFOSFAMIDE AND CYCLOPHOSPHAMIDE IN LIVER AND TUMOURS OF PATIENTS.....	90
2.1 Introduction.....	91
2.2 Aims and objectives	92
2.3 Materials and methods.....	93
2.4 Results	96
2.4.1 Liver measurements	96
2.4.2 Tumour measurements	100
2.4.3 <i>Composition of the 'Ifosfamide' peak</i>	101
2.5 Discussion	102
CHAPTER 3	103
PRE-CLINICAL STUDY TO EVALUATE PHARMACOKINETICS OF IFOSFAMIDE IN AN ANIMAL MODEL.....	103
3.1 Introduction.....	104
3.2 Aims and objectives.....	105
3.3 Study design.....	106
3.4 Materials and methods.....	107
3.4.1 Tissue culture.....	108
3.4.2 <i>Growth of the tumour in nude mice</i>	109
3.4.3 <i>Preparation of animal prior to experiments</i>	110
3.4.3.i <i>Anaesthesia</i>	110
3.4.3.ii <i>Ifosfamide preparation</i>	110
3.4.3.iii <i>Tumour volume measurement</i>	110
3.4.3.iv <i>Ifosfamide injection</i>	110
3.4.4 In vivo animal experiments.....	111

3.4.5 Processing of tumours after spectroscopy experiments.....	114
3.4.6 In vitro ¹ H and ³¹ P MRS experiments.....	115
3.4.7 HPLC-MS analysis of tissue extract.....	116
3.4.8 Data analysis	117
3.4.8.i Analysis of spectra	117
3.4.8.ii Calculation of half-life.....	119
3.5 Results	120
3.5.1 Liver experiments.....	120
3.5.2 Tumour experiments	123
3.5.3 Ifosfamide metabolites	128
3.5.3.i Liver.....	128
3.5.3.ii Tumour	130
3.5.4 ³¹ P high resolution spectra.....	131
3.5.5 HPLC-MS data.....	133
3.5.6 Comparison of HPLC-MS data between liver and tumour.....	137
3.5.7 Correlation between HPLC-MS and MRS data.....	139
3.6 Discussion	143
3.7 Summary and future directions.....	148
CHAPTER 4	149
MAGNETIC RESONANCE SPECTROSCOPY (MRS) TO ASSESS	
RESPONSE TO CHEMOTHERAPY IN A PAEDIATRIC EMBRYONAL	
RHABDOMYOSARCOMA MODEL.	149
4.1 Introduction.....	150
4.2 Aims and objectives	151
4.3 Materials and methods.....	152

4.3.1 Ifosfamide injection	152
4.3.2 Saline injection.....	152
4.3.3 In vivo experiments	153
4.3.4 <i>Data analysis of in vivo spectra</i>	156
4.3.5 <i>Data analysis of in vitro spectra</i>	156
4.3.6 Response measurements	158
4.3.7 Statistical analysis.....	159
4.4 Results	160
4.4.1 <i>Comparison of volume change of tumours in IFO- treated Vs vehicle - treated (control) animals</i>	160
4.4.2 In vivo ³¹ P MRS data.....	162
4.4.3 <i>Effects of the treatment (IFO or saline) on ³¹P MRS ratios compared with pre-treatment values</i>	163
4.4.4 <i>Comparison of changes in the ratios following IFO treatment with changes in ratios following saline treatment</i>	166
4.4.5 <i>Comparison of in vitro ¹H MRS data between treated and control animals</i>	171
4.4.6 <i>Comparisons of in vitro ³¹P MRS data between treated and control animals</i>	174
4.5 Discussion	178
4.5.1 <i>Acute effects of chemotherapy/ saline</i>	179
4.5.2 Changes in PME and β-NTP.....	179
4.5.3 Phosphomonoesters (PME).....	182
4.5.4 <i>Significance of phosphoethanolamine and phosphocholine</i>	184
4.5.5 β-NTP.....	188

4.6 Summary and future directions.....	190
CONCLUSIONS AND POTENTIAL FUTURE STUDIES	191
APPENDIX	192
REFERENCE LIST.....	198

DECLARATION

I have been involved in the design and conduct of the study, analysis of data and writing of the thesis.

This includes submissions to ethics committee, consents of paediatric patients, tissue culture, growth of tumours in nude mice (subsequently maintained by Dr Yuen-Li Chung), preparation of animals for the experiments, processing of tumours after spectroscopic experiments including extracting the tumour, analysis of in vivo and in vitro MRS spectra and statistical analysis of data.

The following aspects of the study required expert assistance. I worked in collaboration with following colleagues:

1. Dr Yuen-Li Chung, (CRUK Biomedical Magnetic Resonance Research Group at the St. George's Medical School) assisted with technical aspects for in vivo and in vitro spectroscopy experiments in the animal model.
2. Dr Geoffrey Payne (CRUK Clinical Magnetic Resonance Research Group at the Institute of Cancer Research) assisted with technical aspects and analysis of the clinical study, and in vitro spectroscopy experiments.
3. Dr Alan Boddy and Julieann Sludden (Northern institute for Cancer Research, University of Newcastle upon Tyne) measured the ifosfamide metabolites by liquid chromatography –mass spectrometry.

ACKNOWLEDGEMENTS

There are many people without whom the studies performed in this thesis would not have been possible. I wish to acknowledge all the patients who participated in the clinical study.

I am particularly grateful to Professor Ross Pinkerton for giving me the opportunity to undertake this research with funding from the Children's fund at the Royal Marsden NHS Trust. He has been a constant source of inspiration during the planning and conducting the research and completion of this work would not have been possible without his supervision, advice and encouragement.

I wish to thank Dr Yuen-Li Chung for patiently and enthusiastically teaching me all the practical aspects of the study, guidance and supervision and assisting with the technical aspects of spectroscopy at the St. George's Medical school.

I wish to thank Dr Geoffrey Payne for his valuable supervision and support through out the research and thesis writing and for assisting with the clinical study and technical support for xenograft studies.

I am grateful to Dr Alan Boddy and Julieann Sludden for analysing the tissue extracts by high performance liquid chromatography-mass spectrometry at the Northern Institute of Cancer Research, University of Newcastle upon Tyne and also for their expert advice.

I wish to thank Professor Martin Leach (CRUK Clinical Magnetic Resonance Research Group at the Institute of Cancer Research) for his expert advice and support for this research.

I wish to thank Professor John Griffiths (CRUK Biomedical Magnetic Resonance Research Group at the St. George's Medical School) for expert advice and wish to acknowledge all the members of the department of Biochemistry at St. George's Medical school; particularly Helen Troy and Loretta Rodriguez.

I am very grateful to Dr. Kathy Pritchard Jones for encouragement and advice throughout the research and thesis preparation.

I wish to thank Suzie Little and Sandra Hing from Paediatric Oncology section of the Institute of Cancer Research for advice and help with tissue culture methodology.

I also wish to thank Jim Wallace, David Gregory, Alan Thornhill and Dr Andrez Jursac with assistance with personal licence and project licence.

I am very grateful to my colleagues at the Royal Marsden hospital for support for recruitment for the clinical study and research nurse Fiona Kennard for recruitment of adult patients.

I wish to acknowledge all the doctors and nurses in the children's department for assistance with the paediatric clinical study. I also wish to thank Dr Mary Taj, Dr Simon Meller, Dr Donna Lancaster, Dr Darren Hargrave, Dr Frank Saran, Dr Miguel Ortin, Dr Aurelia Norton and research nurses, Gina Dick, Tom Devine and Yvonne Wright. I also wish to thank Regan Barfoot and Patricia Boxall for their assistance.

I wish to thank my husband Jayant for his support, encouragement throughout the project and help in statistics and thesis writing. I wish to thank Dr and Mrs Lokare for encouragement and most importantly, I wish to thank my children Hrisheekesh and Uma for their everlasting love.

INDEX OF TABLES

Chapter 1:

1.1: Summary of clinical experiments relevant to MRS and tumour response in paediatric oncology.

Chapter 2:

2.1: Patient Characteristics.

Chapter 3:

3.1: Concentrations of ifosfamide and its metabolites in the liver extracts based on HPLC-MS measurements in nmol/g wet weight.

3.2: Concentrations of ifosfamide and its metabolites in tumour extracts based on HPLC-MS measurements in nmol/g wet weight.

3.3: Concentrations of ifosfamide and its metabolites in paired liver and tumour extracts in nmol/g wet weight.

3.4: Correlation of data obtained by in vivo MRS with ifosfamide concentrations as obtained by HPLC-MS in liver.

3.5: Correlation of data obtained by in vivo MRS with ifosfamide concentrations as obtained by HPLC-MS in tumour.

3.6: Summary of half-life measurements of ifosfamide obtained from clinical studies.

Chapter 4:

4.1: Summary of the in vivo ^{31}P MRS peak area ratios (mean \pm S.E.M) for which, there was a significant change on Day 1 or Day 8 of treatment compared with the pre-treatment value.

4.2: Summary of significant changes in the ratios following IFO treatment with changes in the ratios following saline treatment (Day 8-Day 1 comparison).

4.3: Comparison of in vitro ^1H MRS data between treated and control animals expressed as mean \pm S.E.M.

4.4: Comparison of in vitro ^{31}P MRS data between treated and control animals expressed as mean \pm S.E.M.

4.5: Comparison of concentration of metabolites obtained by in vitro ^1H MRS and ^{31}P MRS.

4.6: Summary of studies showing effects on PE/PC ratio.

INDEX OF FIGURES

Chapter 1:

- 1.1: Spinning nucleus
- 1.2: Magnetisation
- 1.3: Free induction decay of a single signal
- 1.4: Example of ^1H MRS of brain
- 1.5: Example of ^1H MRS of high grade glioma
- 1.6: Example of ^{31}P MRS of a tumour
- 1.7: PE, PC synthesis pathway
- 1.8: Structure of ifosfamide and cyclophosphamide
- 1.9: Metabolism of ifosfamide
- 1.10: Structures of ifosfamide metabolites

Chapter 2:

- 2.1: Example of a surface coil
- 2.2: Example of a spectrum of ifosfamide in liver
- 2.3: Relationship of quality of signal and depth of liver with total dose of drug (ifosfamide or cyclophosphamide) in mg and mg/m^2
- 2.4: Relationship of quality of signal and depth of liver with cyclophosphamide and ifosfamide dose of in mg/m^2
- 2.5: ^{31}P MRS of soft tissue sarcoma
- 2.6: Expansion of ifosfamide region

Chapter 3:

- 3.1: 4.7 T magnet
- 3.2: The heating blanket
- 3.3: A mouse tumour and the surface coil

- 3.4: An example of VARPRO analysed spectrum
- 3.5: Decay of ifosfamide signal intensity over time in a mouse liver
- 3.6: An example of a graph of ifosfamide signal intensity versus time in a mouse liver
- 3.7: Decay of ifosfamide signal intensity over time in a mouse tumour
- 3.8: Regression analysis of tumour volume Vs half-life (excluding 2 small tumours)
- 3.9: An example of a graph of ifosfamide signal intensity versus time in a RD tumour
- 3.10: Appearance of peak at $\cong 21$ ppm at 1.5 hours form IFO injection in a mouse liver
- 3.11: Peak at 11-12 ppm at 2.5 hours from ifosfamide injection in a tumour
- 3.12: In vitro ^{31}P MR spectrum obtained from a liver
- 3.13: Relationship of tumour volume with ifosfamide concentration as obtained by HPLC-MS
- 3.14: Relationship of half-life as obtained by in vivo ^{31}P PMRS with ifosfamide concentrations as obtained by HPLC-MS
- 3.15: Relationship of final amplitude of ifosfamide measured by in vivo ^{31}P PMRS with concentration as obtained by HPLC-MS

Chapter 4:

- 4.1: An example of the results of the analysis of ^{31}P MR spectra.
- 4.2: Tumour volumes in ifosfamide treated animals on Day 1 and Day 8
- 4.3: Tumour volumes in control animals on Day 1 and Day 8

- 4.4: β -NTP/Tot P ratios in IFO-treated animals on day 1 (before and after IFO)—Acute effects
- 4.5: β -NTP/Pi ratios in ifosfamide- treated animals on Day 1 and Day 8
- 4.6: β -NTP/Pi ratios in control animals on Day 1 and Day 8
- 4.7: PME/Pi ratios in IFO treated animals on Day 1 and Day 8
- 4.8: PME/Pi ratios in control animals on Day 1 and Day 8
- 4.9: ISIS localised spectrum of tumour treated with ifosfamide (Day 1 and Day 8)
- 4.10: ISIS localised spectrum of tumour treated with saline (Day 1 and Day 8)
- 4.11: In vitro ^1H MR spectrum of a tumour extract
- 4.12: In vitro ^{31}P MR spectrum obtained from ifosfamide-treated tumour on Day 8
- 4.13: In vivo ^{31}P MR spectrum obtained from control tumour on Day 8

LIST OF ABBREVIATIONS

ALDH	Aldehyde dehydrogenase
ALL	Acute lymphoblastic leukaemia
ATP	Adenosine triphosphate
AUC	Area under the concentration curve
ck	Choline kinase
ct	Cytidyltransferase
CDP-Cho	Cytidine diphosphocholine
CEA	Chloroethylamine
Cho	Choline containing compounds
C _{MAX}	Maximum concentration
CNS	Central nervous system
CSF	Cerebrospinal fluid
CSI	Chemical shift imaging
CYP	Cyclophosphamide
CXCP	Carboxycyclophosphamide
CXI	Carboxyifosfamide
2- DCI	2-Dechloroethylifosfamide
3-DCI	3-Dechloroethylifosfamide
DG	Diacylglycerol
DNA	Deoxyribonucleic acid
GC	Gas chromatography
Glc-IPM	Glucosyl ifosfamide mustard
GPC	Glycerophosphocholine

GPE	Glycerophosphoethanolamine
HPLC-MS	High performance liquid chromatography-Mass Spectrometry
IFO	Ifosfamide
ip	Intraperitoneal route
IPM	Ifosfamide mustard
ISIS	Image selected in vivo spectroscopy
iv	Intravenous route
FID	Free induction decay
FT	Fourier transformation
5-FU	5 -Fluorouracil
Keto	Keto-ifosfamide
MESNA	2-mercaptoethane sulphonate
MR	Magnetic resonance
MRI	Magnetic resonance imaging
MRS	Magnetic resonance spectroscopy
NAA	N-acetyl aspartate
NHL	Non-Hodgkin's lymphoma
NMR	Nuclear magnetic resonance
NTP	Nucleotide triphosphate
PC	Phosphocholine
PCA	Perchloric acid
PCr	Phosphocreatine
Pct	Phosphocholine transferase
PE	Phosphoethanolamine

PDE	Phosphodiester
pH _i	Intracellular pH
Pi	Inorganic phosphate
PL	Phospholipid
PME	Phosphomonoester
ppm	Parts per million
PtdCho	Phosphatidylcholine
PtdEtn	Phosphatidylethanolamine
RBCs	Red blood cells
RD	Rhabdomyosarcoma cell line
RF	Radio frequency
RMS	Rhabdomyosarcoma
S.E.M	Standard error of mean
SNR	Signal to noise ratio
TLC	Thin-layer chromatography
Tot P	Total Phosphorus
VARPRO	Variable projection

CHAPTER 1

INTRODUCTION AND LITERATURE REVIEW

1.1 Background

Magnetic Resonance Spectroscopy (MRS) can detect a range of biochemical metabolites in vivo, provided they contain an NMR nucleus (e.g. ^1H , ^{13}C , ^{19}F , ^{31}P etc) and are at a sufficiently high concentration. In particular, MRS has the potential to detect changes in tumour metabolism induced by chemotherapy. MRS may therefore demonstrate tumour response earlier than volume response and this may allow us to tailor therapies to individual patients.

Ifosfamide and cyclophosphamide are extensively used in cancer therapy. These are both pro-drugs, which produce active, inactive and toxic metabolites. There is considerable variation in the levels of metabolites of these pro-drugs in plasma and their clinical response rate.

Signals related to ifosfamide have been previously observed in rat liver (site of activation) and tumour in vivo [Rodrigues et al., 1997]. Therefore we planned a clinical study to ascertain whether this could be extended to clinical studies in children and adults (described in Chapter 2). We then planned studies in mouse liver and a paediatric tumour model to attempt to evaluate pharmacokinetics of ifosfamide in vivo and to assess if any additional information on the metabolites of ifosfamide could be obtained. The liver and tumour extracts were also analysed by high performance liquid chromatography -mass spectrometry (HPLC-MS). We also planned to study if any correlation could be obtained between magnetic resonance spectroscopy and concentration of metabolites as obtained by HPLC-MS (described in Chapter 3).

The role of MRS to assess chemotherapy response in a paediatric tumour model was also studied. In vivo and in vitro studies were done using ^{31}P MRS to evaluate effect of ifosfamide on phospholipid metabolism and high-energy phosphates (described in Chapter 4).

1.2 Magnetic resonance

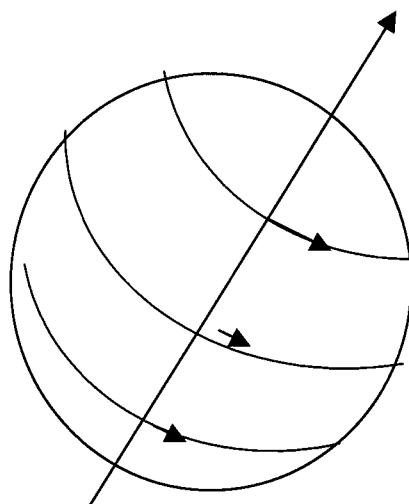
1.2.1 Historical perspectives

The application of magnetic resonance spectroscopy in medicine has been dependent on a vast amount of research on mammalian tissues in vitro and in vivo. The first successful nuclear magnetic resonance (NMR) experiments were performed in 1946 [Purcell EM et al., 1946;Block F et al., 1946]. The development of high-field superconducting magnets in the late 1960s together with technical advances allowed further developments. In the 1970s, NMR was applied to living systems including man in two distinct approaches. One application was production of images; magnetic resonance imaging (MRI) [Damadian, 1971;Lauterbur PC, 1973] and the other was the production of NMR spectra [Hoult et al., 1974;Moon RB and Richards JH, 1973]. Use of in-vivo magnetic resonance spectroscopy (MRS) in oncology has developed rapidly since the first animal experiment in 1981 and first in vivo human tumour experiment in 1983 [Griffiths et al., 1981;Griffiths et al., 1983].

1.2.2 Basis for the NMR phenomenon

Certain atomic nuclei, such as the hydrogen nucleus (^1H) or the phosphorus nucleus (^{31}P), possess a property known as spin. This can be visualised as a spinning motion of the nucleus about its own axis (Figure 1.1). These nuclei, in common with other spinning objects, possess the property of angular momentum and by virtue of their electrical charge have magnetic properties. The nuclear magnetism is analogous to the magnetism generated by an electric current circulating in a small loop of wire. Such a current loop behaves like a small bar magnet. Therefore, the nucleus can be regarded as a tiny bar magnet, rotating about its own axis [Gadian D.G, 1982a].

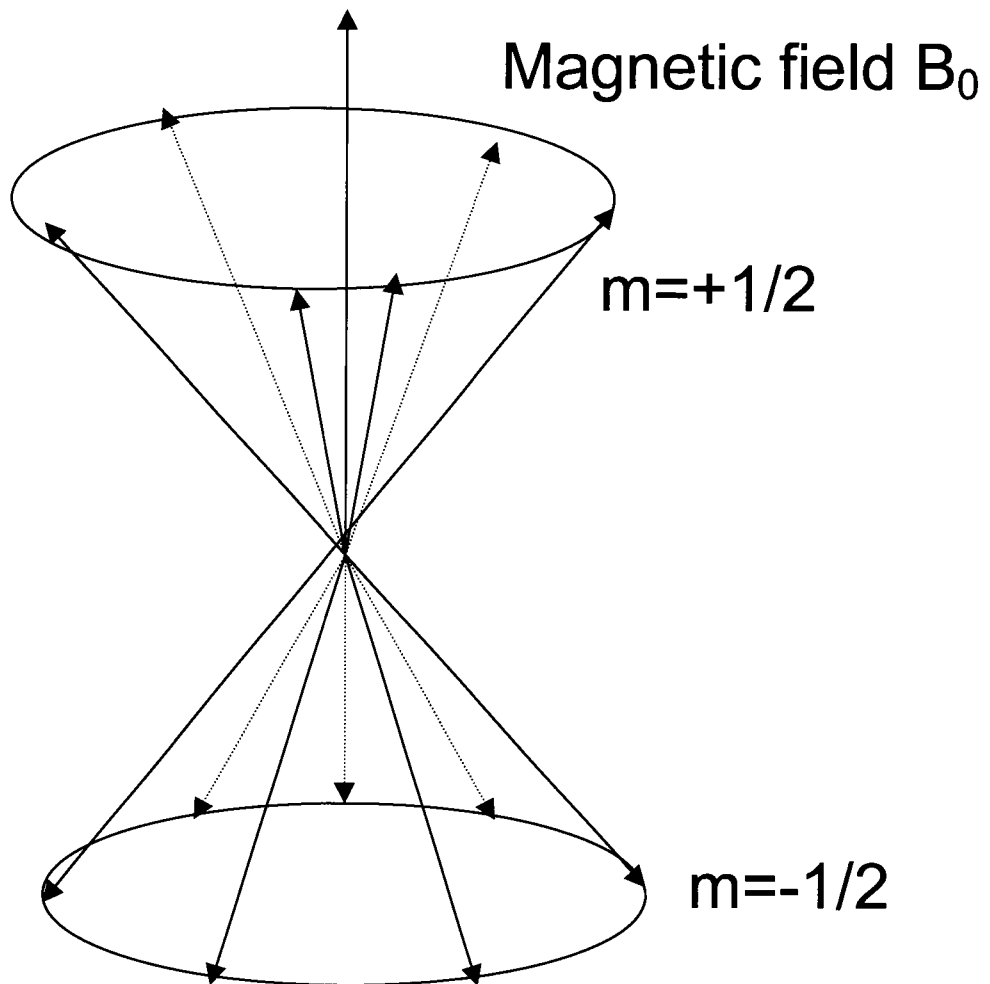
Figure 1.1: Spinning nucleus.



Quantum theory dictates that a nucleus possesses discrete values of angular momentum specified by the spin (quantum) number, I , which assumes integer or half-integer values depending on the numbers of protons and neutrons. An even mass number makes I , integral. Even numbers of both protons and neutrons makes I zero due to the tendency for both neutrons and protons to form pairs in such a way that the individual spins cancel out. I is half-integral for nuclei with odd mass numbers. The abundant isotopes of carbon and oxygen, ^{12}C and ^{16}O have zero spin and therefore do not produce NMR signals. The nuclei that possess the property of spin include ^1H , ^2H , ^{13}C , ^{14}N , ^{15}N , ^{19}F , ^{23}Na , ^{31}P , ^{35}Cl , ^{39}K . Protons (^1H) have been mostly used for magnetic resonance spectroscopy because of their high natural abundance in organic compounds and the high sensitivity of their NMR signal compared with those of other magnetic nuclei.

When a static field B_0 is applied, magnetic nuclei precess about the direction of B_0 with an angular frequency (rate of rotation usually quoted in MHz) known as the Larmor frequency. This is identical to the resonance frequency derived from quantum theory. At thermal equilibrium the net component of magnetisation in any direction within the XY-plane is zero and no signal is observed. Figure 1.2 shows the orientation that can be taken up in an applied field B_0 by the nucleus of spin $1/2$. The orientations are specified by the quantum number m and describe position on 2 cones.

Figure 1.2: Magnetisation

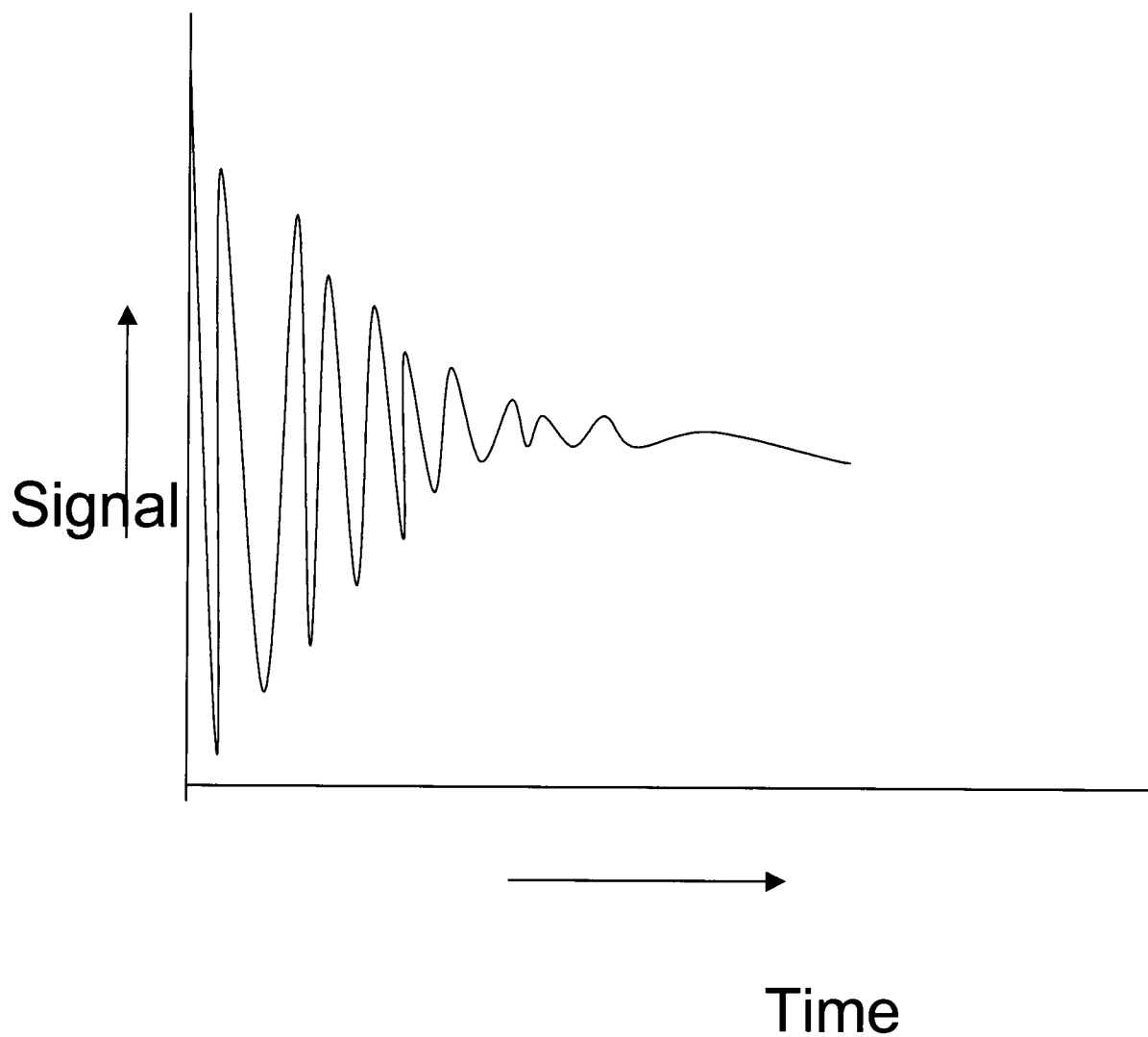


Possible orientations of single nucleus at the thermal equilibrium, net effect parallel to B_0 .

1.2.3 Manipulations required to produce an NMR signal

If an alternating field B_1 is also applied at or near the Larmor frequency, (usually along the x-axis or y-axis) this causes the nuclear magnetisation to rotate about B_1 . If this is applied for a certain time so that the nuclei rotate through an angle of 90° i.e. the nuclei receive a 90° radio frequency pulse that rotates them from the Z-axis to the X-axis, the spins now precess coherently for a time about B_1 , inducing a small signal in a receiver coil placed about it. When the pulse is turned off, the nuclei slowly relax to their original position along the Z-axis. The time it takes them to return to their original position along the Z-axis is governed by their longitudinal relaxation time (T_1). The XY components of the spin fan out, as some spins have slightly different precession frequencies. The rate at which they do this is determined by the transverse relaxation time (T_2). T_2 is never greater than T_1 and is usually a lot smaller. The receiving coil detects the voltage variations at many points in time during this period. The measured signal is termed the 'free induction decay (FID)'. It describes the decay of the induced signal arising from free precession of the nuclei in the field B_0 . This is usually displayed as signal versus time (Figure 1.3).

Figure 1.3: Free induction decay (FID) of a single signal



In order to obtain a conventional NMR spectrum, in which signal amplitude is plotted as a function of frequency, the response to radiofrequency pulse needs to be appropriately manipulated. This manipulation is performed by means of the mathematical device known as the Fourier transformation (FT) which enables a quantity that varies with time to be analysed in terms of the sum of frequency components [Gadian D.G, 1982b].

Accumulation of spectra: In an NMR experiment, the radiofrequency field is applied in short powerful pulses. As biological molecules are present at low concentrations, they produce weak signals, and the signal to noise ratio (SNR) of the spectral lines is improved by adding together a large number of responses. This accumulation of responses or 'scans' leads to an improvement of signal by a factor of N , whereas the noise, being random, increases by the square root of N . Therefore, in Fourier transform NMR, a radiofrequency pulse is applied, the response is observed, and the process is repeated a number of times at intervals (TR-repetition time). Processes such as 'saturation' and 'relaxation' affect the choice of time interval between consecutive radiofrequency pulses. Fourier transformation of this information yields information in the frequency domain, namely a plot of peaks at different Larmor frequencies. The responses are automatically added in a computer until the required signal to noise ratio is obtained or for the time allocated, and then Fourier Transformation of the data is performed using the computer to produce the final spectrum.

1.2.4 Chemical shift

Chemical shift is the separation of resonance frequencies from an arbitrarily chosen reference frequency. It is usually expressed in the terms of the dimensionless units of parts per million (ppm). The resonance frequency of a given nucleus is modified slightly (typically by a few parts per million) by its molecular environment, due to the screening effect of the electron cloud. This allows identification of different molecules containing the given nucleus. Frequency separation of resonances is proportion to B_0 . Therefore an increase in B_0 improves spectral resolution. Spectra are plotted with decreasing frequency to the right.

The parameters that characterise each peak include its resonance frequency, its height, and its width at half-height. The height (maximum peak intensity) or the area under the peak may be calculated and yields an indication of the concentration of nuclei.

In in vivo ^{31}P MRS, phosphocreatine (PCr) is generally used as a reference frequency. In vitro experiments dictate that an external reference be added. This reference should preferably consist of a single resonance that occurs well away from the sample resonances. It should be chemically inert and its resonance frequency should be independent of the nature of the sample. It should contain a large number of chemically equivalent nuclei, to enable a small concentration to give an intense signal. As common solvents contain protons, for NMR experiments deuterated solvents are used.

1.2.5 Localisation

The initial development of MR spectroscopy was separate to that of MR imaging, with early in vivo spectrometers having no imaging capabilities. This was rapidly seen to be a drawback for tumour studies, where identifying target tissue within patient, based on morphological data i.e. defining volume of interest by MR imaging was essential. Most localisation strategies use imaging techniques and modern equipment allows imaging and spectroscopy studies to be integrated. As imaging speed and techniques have improved, it has become possible to combine imaging and spectroscopic studies, providing complementary imaging, physiological and metabolic information. This remains challenging but the benefits of integrating such information are showing promise. In a typical MRS exam, MRI images are first acquired for identification of tumour location. Without moving the subject, a process called shimming is then performed to optimise the uniformity of the magnetic field, and ensures that signals are narrow. Spectral data is then acquired. A range of strategies exists for localisation of MRS signals to the region of interest (ROI). One method of localisation makes use of a type of radiofrequency coil called surface coil [Ackerman et al., 1980]. [Gadian D.G, 1982c] When this coil is placed adjacent to any object, it will detect signals from an approximately disc shaped region of the object immediately in front of the coil, of radius and thickness approximately equal to the radius of the coil. Single- voxel methods make use of the intersection of three (usually orthogonal) slices to localise to a cuboid. The position of this is usually specified using the MRI images previously acquired in the same session. The most popular single voxel methods are Stimulated Echo acquisition mode

(STEAM) [Frahm et al., 1989;Frahm et al., 1987] and Point Resolved Spectroscopy (PRESS) [Bottomley, 1987] for ^1H studies and Image selected in vivo spectroscopy (ISIS) [Ordidge R et al., 1986] for ^{31}P studies. ISIS provides localisation by performing a series of eight measurements, each with a different permutation of inversion of the three orthogonal slices. A suitable addition/ subtraction scheme yields a central voxel signal with no loss in signal to noise ratio. In contrast, so- called Chemical Shift Imaging (CSI) [Brown et al., 1982], also known as Spectroscopic Imaging, acquires signals from a matrix of voxels, either within a selected slice (2D-CSI) or [Brown, 1992] in three dimensions (3D-CSI).

1.2.6 Interpretation of data

Spectral data is easily visualised in the absorption mode. But the data obtained is a mixture of spectra in absorption and dispersion mode. Phase correction is necessary to ensure that all the signals in the real part of the transformed spectrum are in the absorption mode. The areas of NMR signals are commonly measured by integration using the computer. Alternatively they can be estimated by plotting the spectra on graph paper and counting the squares underneath the peak [Gadian D.G, 1982d] .The results are generally expressed as metabolite ratios. Whilst these avoid the need for absolute quantification, for some metabolites there are difficulties in determining biochemically appropriate ratios [Leach, 1992]. To obtain absolute concentration of a compound, the signal intensity is compared with that of a known quantity of reference compound.

1.2.7 ³¹P Magnetic Resonance Spectroscopy

Although the sensitivity of ³¹P MRS is only one-fifteenth of that of ¹H NMR, it is nevertheless one of the most sensitive biologically useful nucleus. As it is the naturally occurring isotope of phosphorus, no isotopic enrichment is necessary. Narrow resonances can be obtained and they occupy a fairly wide range of chemical shifts (about 30 ppm for biological phosphates). The spectra are simple and more easily interpretable than ¹H MR spectra. Moon and Richards (1973) first demonstrated the measurement of ³¹P spectra in intact blood cells, followed by application to progressively larger organisms, using specialised equipment [Moon RB and Richards JH, 1973]. Since then, ³¹P MR spectroscopy has been used clinically to study changes in high-energy metabolism in a number of pathological processes.

Several important phosphorus containing compounds such as Adenosine triphosphate (ATP), phosphocreatine (PCr) and inorganic phosphate (Pi) are involved in bioenergetics and occur in the living systems at concentrations high enough to be detectable by ³¹P MRS. Lipid metabolism can be studied via detection of phosphomonoesters (PME), a group of compounds which includes phosphocholine (PC) and phosphoethanolamine (PE) and phosphodiester (PDE), such as Glycerophosphocholine (GPC) and Glycerophosphoethanolamine (GPE) and to some extent of membrane bi-layer phospholipids.

Metabolic studies by MRS in living systems have the advantage of being non-invasive and therefore the reaction time course can be followed in a single experiment. This is the basis of studying pharmacokinetics of drugs,

which have nuclei with spin properties. Components of the intra-cellular environment such as pH and binding of Mg^{2+} ions to ATP can also be studied. MRS is non-specific i.e. resonances are obtained from all mobile compounds that are present in sufficiently high concentrations. Therefore, the simultaneous observation of all of these compounds, rather than just those selected for chemical analysis, could help identify metabolites of drugs. The main disadvantage is sensitivity and only those metabolites that are in sufficient large concentration can be identified.

Phosphocreatine signal is present in the ^{31}P MR spectra of many intact tissues and provides a suitable and very convenient chemical shift reference. This is because PCr has a pK_a value of about 4.6, and its resonance frequency is relatively insensitive to pH changes within the normal physiological range. It is, therefore, assigned a value of 0 ppm and other signals are expressed relative to PCr.

^{31}P NMR spectra of adenosine triphosphate show signals from three chemically distinct phosphorus nuclei. The signals have been assigned to the γ -, α - and β - positions on the triphosphate groups at -2.5 , -7.5 and -16 ppm. The resonance of inorganic phosphate (Pi) is sensitive to pH and this property is utilised in measurement of intracellular pH.

1.2.8 Coupling and decoupling

Interaction between adjacent nuclear spins within a molecule is called J-coupling. In a ^{31}P MR spectrum, interactions between the P and proton nuclei can produce a broad spectrum. Proton decoupling can improve spectral resolution substantially, resulting in better resolved resonances and more reliable quantitative information [Luyten et al., 1989; Freeman and Kupce, 1997] .

1.2.9 High-resolution Magnetic resonance spectroscopy

It is essential that samples produce signals that are intense enough to distinguish from noise and narrow enough to be distinguishable from each other. To the MR spectroscopist, these are the familiar problems of sensitivity and resolution. High-resolution MRS experiments are those in which experiments are done at higher field strengths, usually in over 3T magnets. Signals of different frequencies can be resolved from each other. Narrow signals are usually only obtained from molecules that are fairly mobile, and therefore most high-resolution MRS studies are performed on solutions. Many of the metabolites in biological tissue are freely mobile and, therefore, intact living systems can give rise to high-resolution spectra. The signal to noise ratio depends on several parameters such as the nucleus that is studied, volume of sample, concentration of the nuclei under investigation, magnetic field strength, design of spectrometer and time for which spectra are accumulated.

For in vitro experiments, the tissue is often freeze clamped under liquid nitrogen. MRS of samples following freeze clamping, measure total amounts of metabolites whereas in vivo MRS generally measures only the mobile components. Therefore, the values obtained by the two methods could differ. In addition, for many tissues there are unavoidable breakdown of high-energy phosphates during the process of freeze clamping and subsequent extraction [Gadian D.G, 1982e].

1.2.10 Magic angle sample spinning

This was the first technique suggested to obtain high-resolution spectra from solids [Roberts J.E and Griffin R.G, 1987]. In solids, NMR shifts can have an angular dependence, which depends on the relative orientation of crystal axes and the direction of the applied magnetic field. For powder samples, all possible orientations are sampled and a broad "powder pattern" results. If the sample is spun rapidly about the magic angle (54.7356 degrees) from each of the axes, most of the orientational dependence averages out leaving a narrow NMR signal.

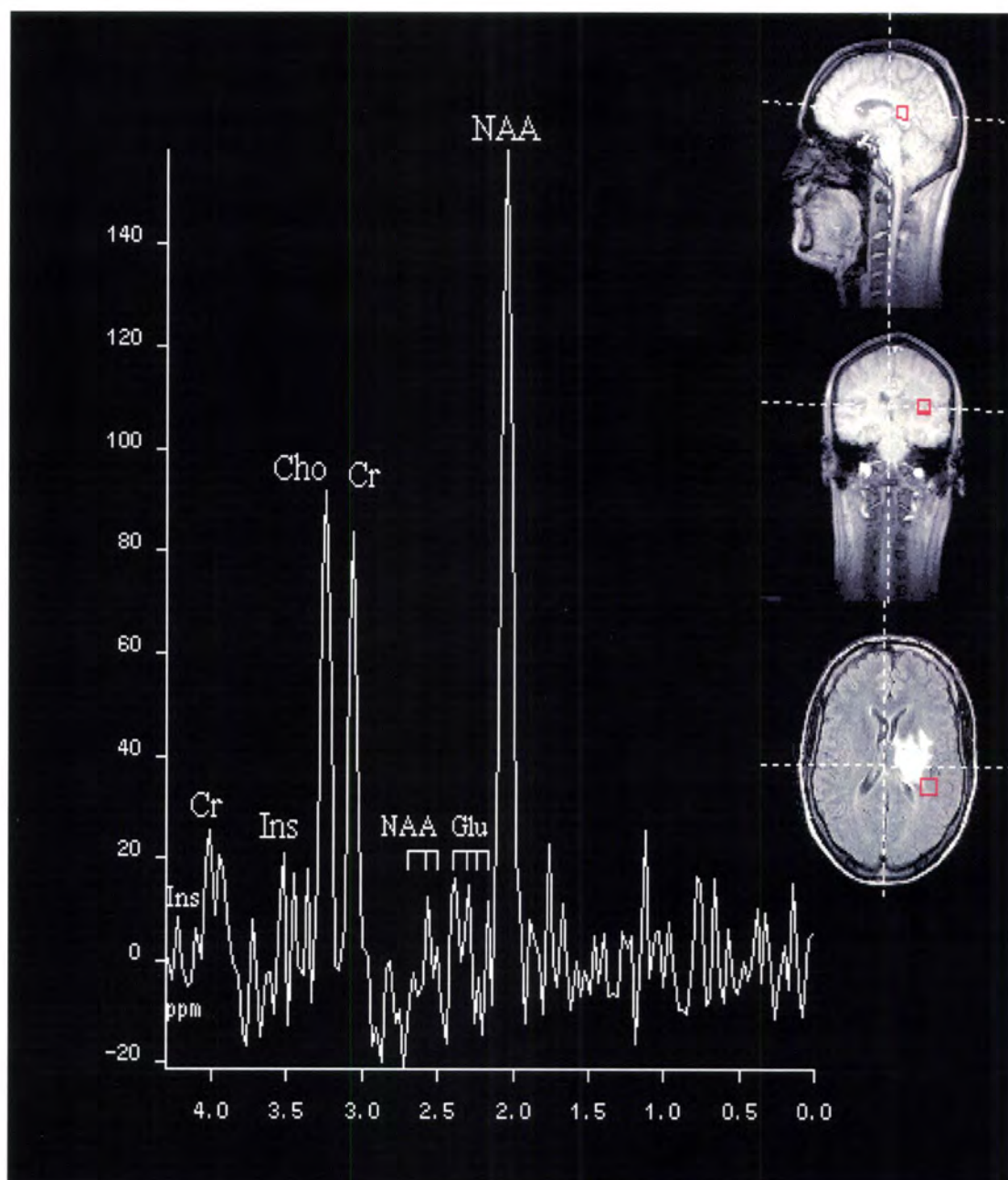
For typical solids, the spinning rate should be 1 kHz or higher. The procedure consists of placing the sample in a gas-driven rotor tilted at the 'magic angle' with respect to B_0 . The sample may experience temperature degradation and it is important to have a tight temperature control.

1.3 Applications of MRS to cancer

MRS is a non-invasive tool that is being increasingly evaluated in several clinical contexts to distinguish benign from malignant lesions, [Negendank et al., 1989;Castillo et al., 1996;Lee and Gonzalez, 2000;Narayan et al., 1991;Koutcher et al., 1990;Lean et al., 1993;Lin et al., 1999] characterise histology, [Preul et al., 1996;Meyerand et al., 1999;Dillon and Nelson, 1999;Hanaoka et al., 1993;Hwang et al., 1998], grade tumours [Poptani et al., 1995] and distinguish scar tissue and radiation necrosis from tumour recurrence [Taylor et al., 1996;Kamada et al., 1997]. MRS could also aid in selecting sites for biopsy in brain tumours [Kwock, 2001;Martin et al., 2001;Dowling et al., 2001;Burtscher et al., 1997]. Changes in the bioenergetics of cancer cells following treatment could potentially identify responders and non-responders to therapy. The role of MRS to study pharmacokinetics of drugs is also being studied.

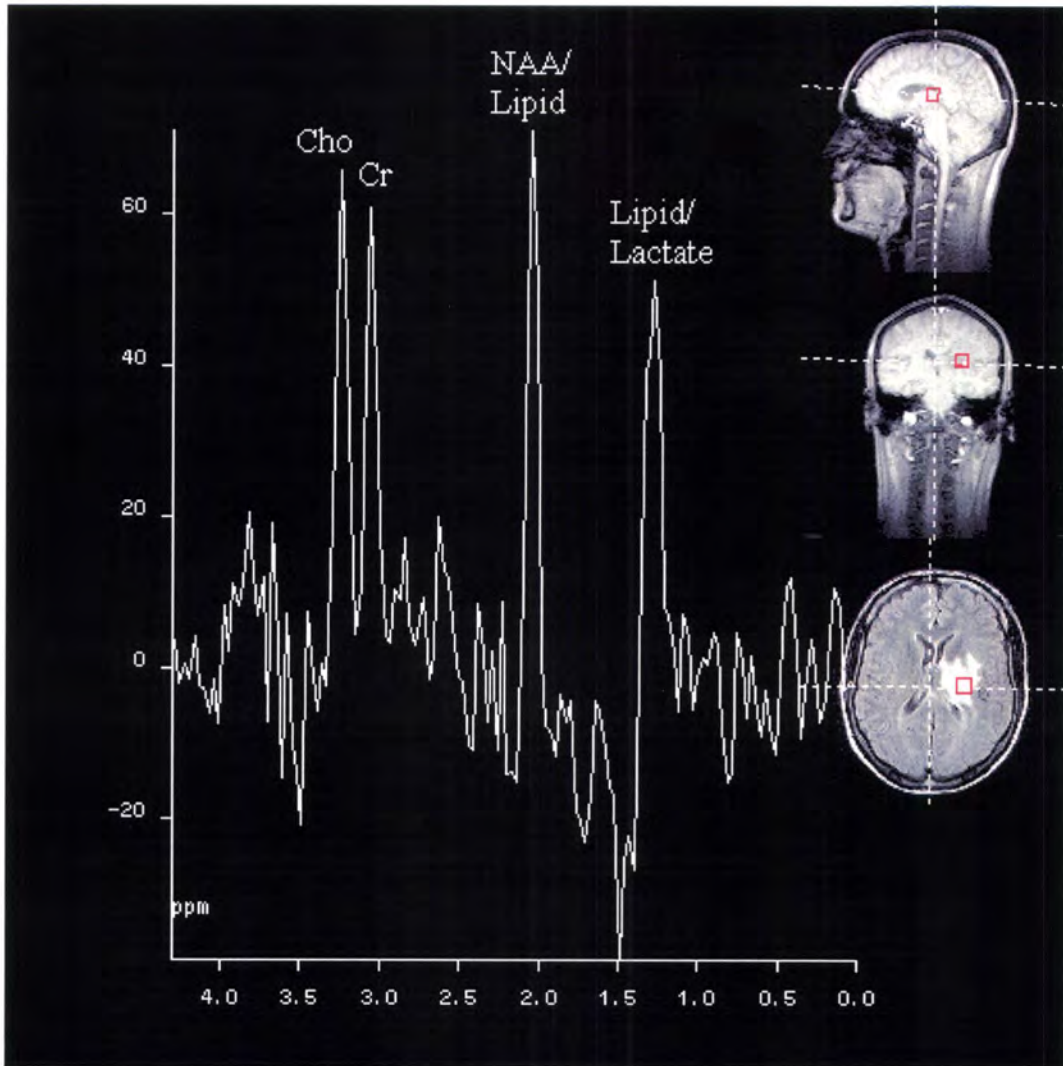
1.3.1 MRS of tumours

Proton MRS has the advantage that the hydrogen nucleus is the most sensitive nucleus and most compounds in the body contain hydrogen atoms. ^1H MRS can quantify the relative concentrations of several ^1H containing metabolites from specified tissue regions. This normally requires suppression of the much larger signals from water and lipids although when adequately localised, lipid signals may also provide valuable information. ^1H MRS has been studied in all types of tumours, but is particularly important for brain tumours where ^{31}P MRS may not be very sensitive. The principal metabolite signals that can be measured by ^1H MRS are N-acetyl aspartate (NAA) (in the CNS), creatine plus phosphocreatine (Cr), and choline containing compounds (Cho). Signals from a range of saturated and unsaturated lipids can also be measured. NAA is present in normal functioning neurons and its signal can be used as a neuronal marker. Creatine and phosphocreatine are important in energy metabolism and vary little in normal brain tissue. Creatine is often absent from tumours. Choline containing compounds are involved in synthesis and metabolism of cell membranes. Tumours often exhibit high levels of choline compared with normal. Lactate, a marker of anaerobic metabolism, is not usually detected in normal brain but may be present in brain tumours or areas of ischemic injury. The presence of lipid in tumours may indicate higher grade. Several other metabolites such as inositol, myoinositol, glutamate, glutamine, acetate, alanine have also been characterised. Figure 1.4 shows an example of ^1H MRS of brain. Figure 1.5 shows an example of ^1H MRS of high grade glioma.



Both voxels (Fig 1.4 and 1.5) are from the same CSI study from a high grade glioma patient; SE sequence, TE=135ms, TR=800ms, 4 acquisitions, voxel size 13mmx13mmx13mm (FOV= 208ms, 16x16grid). Identical postprocessing parameters were used for both voxels.

Figure 1. 4: Example of ¹H MRS of normal brain NAA: N-acetyl aspartate;
Cr: Creatine; Cho: choline, Glu: Glutamine and glutamate, Ins: Inositol.



Both voxels (Fig 1.4 and 1.5) are from the same CSI study from a high grade glioma patient; SE sequence, TE=135ms, TR=800ms, 4 acquisitions, voxel size 13mmx13mmx13mm (FOV= 208ms, 16x16grid). Identical postprocessing parameters were used for both voxels.

Figure 1. 5: Example of ^1H MRS of high grade glioma NAA: N-acetyl aspartate; Cr: Creatine; Cho: choline, Glu: Glutamine and glutamate, Ins: Inositol.

With ^{31}P MRS, signals can be seen from low energy phosphates i.e. phosphomonoesters (PMEs), inorganic phosphate (Pi), phosphodiester (PDEs), and from high-energy phosphates i.e. phosphocreatine (PCr) and nucleotide triphosphate (γ -, α - and β -NTP). Many studies using ^{31}P MRS show that human cancers, with the exception of glioma, have typical metabolic characteristics that include prominent PME and PDE, low PCr and a pH slightly more alkaline than that of normal cells [Negendank, 1992] (Figure 1.6).

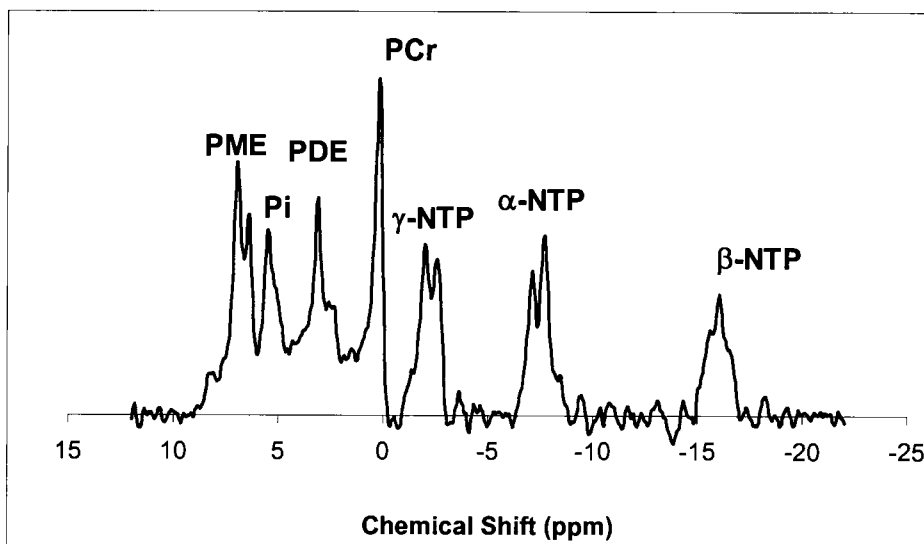


Figure 1.6: Example of ^{31}P MRS of a tumour (gastro-intestinal stromal tumour). The measurement was performed using ^1H -decoupled Chemical shift imaging (CSI) with a voxel size of 5x5x5cm at 1.5T. The tumour shows the various peaks. PME: Phosphomonoesters; Pi: Inorganic phosphate; PDE: Phosphodiester; PCr: Phosphocreatine; NTP: Nucleotide triphosphate. In this figure, PME can be further resolved into PE and PC.

1.3.2 Biological implications of ³¹P MRS

Phospholipid (PL) components have established roles both as 'passive' structural building blocks of cell structure and 'active' regulators of cell function [Podo, 1999]. Combined NMR and chromatographic analysis of aqueous extracts of rat tumours has unequivocally demonstrated that the PME resonance mainly comprises signals from phospholipid metabolites, particularly phosphoethanolamine (PE) and phosphocholine (PC) rather than sugar phosphates [Evanochko et al., 1984]. Phosphomonoesters such as sugar phosphates and 2,3 -diphosphoglycerate, only provide minor contributions to the PME resonance band in tumours although they are more important in liver. Phosphoethanolamine and phosphocholine are precursors of the most abundant phospholipid classes in eukaryotic cells, phosphatidylcholine (PtdCho) and phosphatidylethanolamine (PtdEtn). If the magnetic field is homogeneous and if ¹H decoupling is used PME can be further resolved into PE and PC [Freeman and Hurd, 1997]. [Luyten et al., 1989]. PME levels are interesting spectral and biochemical parameters, in view of their possible role as 'fingerprints' of altered phospholipid turnover and cell proliferation in tumour cells [Leach et al., 1992]. An increase in PME has been associated with rapid tissue growth or rapid membrane synthesis.

PDEs include phosphodiester resonance resulting from contributions from glycerophosphocholine and glycerophosphoethanolamine [Evanochko et al., 1984]. Additional contributions to the PDE spectral profile could arise from broad, field dependent signals of mobile phospholipid headgroups [Murphy et al., 1989; Bates et al., 1989]. Glycerophosphocholine and

glycerophosphoethanolamine are produced by membrane catabolism. GPC levels may undergo significant reduction during cell maturation, suggesting that this metabolite may be a marker for cell differentiation.

1.3.2.i. Choline cycle

Phosphatidylcholine is the major phospholipid component of eukaryotic cells and is involved in membrane structure, signal transduction mechanisms and lipoprotein metabolism. The *de novo* synthesis of membrane phosphatidylcholine occurs on the cytosolic side of the endoplasmic reticulum membrane through a cascade of three enzymatic steps (Kennedy pathway) consisting of (1) Phosphorylation of choline by choline kinase (ck) to produce phosphocholine (PC). (2) Conversion of PC to cytidine diphosphocholine (CDPCho) by cytidyltransferase (ct). (3) Phosphocholine transferase (pct) mediates phosphatidylcholine condensation from CDPCho and diacylglycerols (DG) [de Certaines et al., 1993; Podo, 1999]. The rate-limiting step is thought to be the step catalysed by cytidyltransferase. Figure 1.7 shows schematic description of biosynthesis of PME and PDE. Specific translocators transfer phosphatidylcholine from the cytosolic side of endoplasmic reticulum to cell membranes. Phosphatidylcholine can also be formed by base exchange with other existing phospholipids as well as by methylation of phosphatidylethanolamine. Conversion of phosphatidylethanolamine to phosphatidylcholine is important in the liver where it accounts for 20%-40% of phosphatidylcholine synthesis. Several agents affect the activation of these enzymes. Phosphatidylcholine hydrolysis

is mainly mediated by phospholipases and these could provide substrates for re-synthesis of PtdCho. Phospholipase C converts PtdCho to PC and diacylglycerol (which could act as a second messenger). Phospholipase D converts PtdCho to choline and phosphatidate (a potent mitogen). The third mechanism involves phospholipase A2 which converts PtdCho by deacylation pathway to release free fatty acids (including arachidonic acid- a second messenger) and glycerophosphocholine.

1.3.2.ii. Ethanolamine cycle

Phosphatidylethanolamine synthesis occurs by three pathways. (1) By a pathway similar to PtdCho synthesis using ethanolamine kinase enzyme, (2) Decarboxylation of phosphatidylserine in the mitochondria. (3) From pre-existing phosphatidylserine or phosphatidylcholine by base exchange in the endoplasmic reticulum. Degradation of PtdEtn occurs by a series of enzymes. It is now apparent that the anabolic and catabolic pathways are cross-linked and various factors could affect them.

High-energy phosphates such as NTP tend to decrease as tumours increase in size, probably because of increased hypoxia. However, due to difficulty in quantitative analysis of peak areas, the MRS data are generally expressed as ratios of metabolites [Leach et al., 1992].

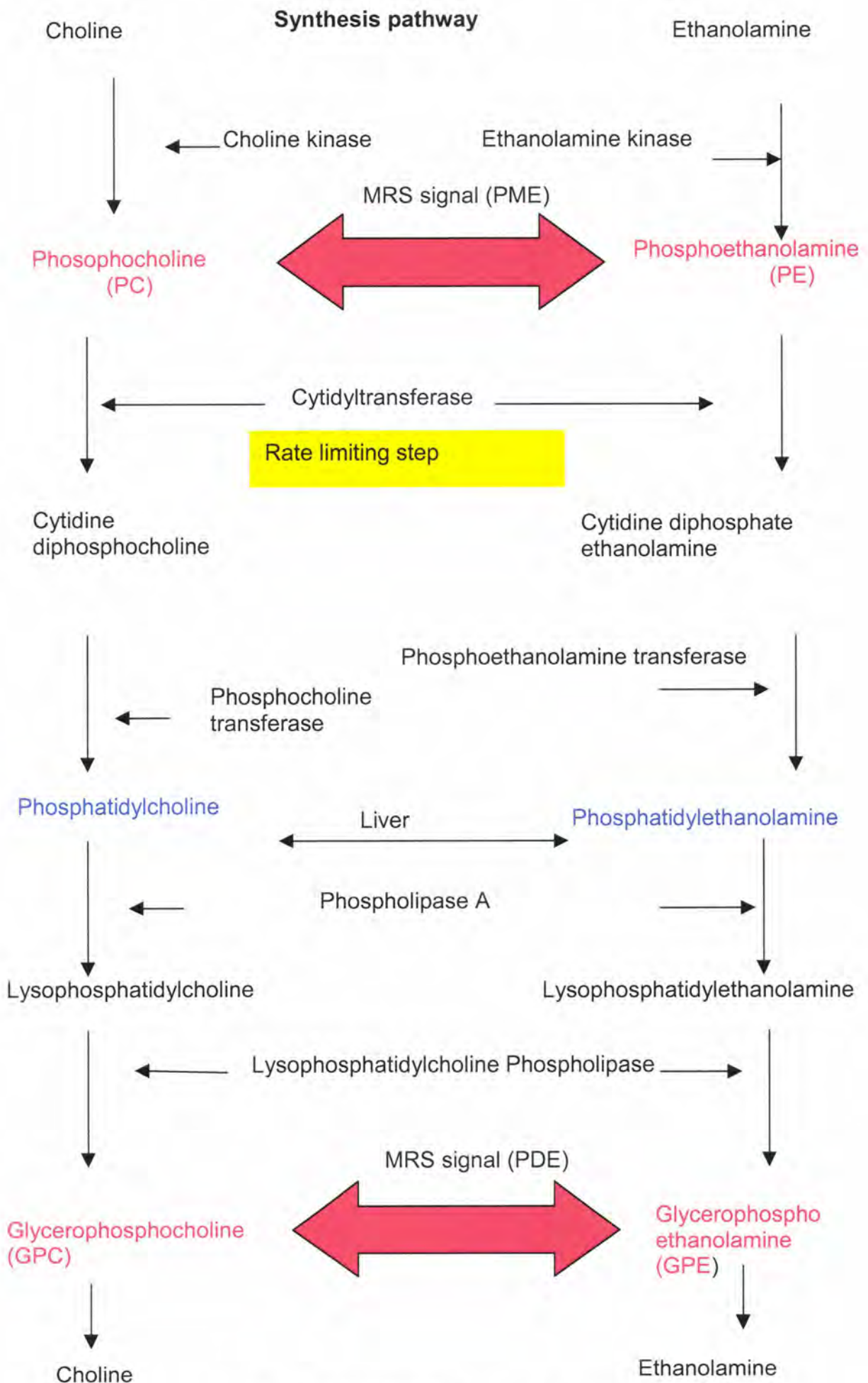


Figure 1.7: PE, PC synthesis pathway

1.3.3. Study of tumour physiology

Magnetic resonance techniques can be applied to study tumour physiology [Stubbs, 1999]. One parameter, which could potentially influence cancer therapeutics, is pH. MRS offers the unique possibility of non-invasively measuring intracellular and extra-cellular pH, based upon pH dependent changes in chemical shift of some compounds. Endogenous metabolites with this property include Pi, the chemical shift of which, when compared with that of PCr or α -NTP gives a measure of pH. Since PCr (often absent in tumours) and NTP are exclusively intracellular and much of the Pi signal comes from the intracellular compartment, this method measures intracellular pH. The extra-cellular pH can be measured by introducing an exogenous probe [Gillies et al., 1994a; Ojugo et al., 1999]. Intracellular pH is tightly controlled and maintained at neutral or slightly alkaline levels [Griffiths, 1991]. Extracellular pH in tumours is often acidic. The pH gradient across the tumour cell plasma membrane is the reverse of that found in normal tissue. This pH gradient could have implications for cancer therapy and uptake of drug [Ojugo et al., 1998; Evelhoch et al., 2000].

MRS can also play a role in evaluating specific cellular pathways following targeted therapies [Ronen et al., 2001]. For example, effects of drugs, which inhibit ras signalling, were studied in cell lines using MRS. Members of the ras oncogene family are mutated in a high proportion of cancers leading to constitutive ras activation. NIH 3T3-mouse fibroblast line and a mutant ras-transfected counterpart cell line were studied. Ras-signalling was increased

in the transfected cell line, which also showed significantly higher phosphocholine content. Treatment with 3 different inhibitors of ras pathway was associated with partial reversal of phosphocholine increase in ras transfected cells.

1.3.4. Potential role of MRS in assessment of tumour response in paediatric oncology

[Vaidya et al., 2003]

1.3.4.i. Introduction

X-rays, ultrasonography, computerised tomography and magnetic resonance imaging are conventionally used to evaluate response in solid tumours. With these tools, tumour anatomy, site and size are obtained. Decreasing volume of tumour is generally documented as a sign of response. It may be difficult to ascertain whether the tumour is composed of viable or dead cells and volume change may not occur very rapidly during therapy. Absence of volume response may present assessment difficulties in new cytostatic therapies targeted for example on proliferation or cell cycle control. An early non-invasive indicator of tumour response to therapy would therefore provide useful information regarding the effectiveness of therapy. This might be a relevant prognostic factor in new patients and in phase II studies could facilitate recommendations at an early stage as to whether to continue treatment.

1.3.4.ii. Examples of pre-clinical studies relevant to tumour response

The first in vivo ^{31}P MRS experiment in an animal tumour model was performed in 1981 [Griffiths et al., 1981]. Since then, many studies have been done both in cell lines and xenograft models to evaluate the energy status of tumours [Jackel et al., 2000; Street et al., 1995; Tausch-Treml et al., 1991]. Pre-clinical data have suggested that ^{31}P MRS could be used to

provide markers for cell growth, cell kill, response to therapy and to determine resistance to treatment [Tausch-Treml et al., 1991; de Certaines et al., 1992]. PME's have been suggested as markers for cellular proliferation and sensitive markers of both tumour regression and regrowth [de Certaines et al., 1993].

The effect of cyclophosphamide (CYP) on the metabolic profile of implanted mammary carcinoma has been studied using ^{31}P MRS, both in vivo and in perchloric acid extracts [Street et al., 1995]. Phosphoethanolamine /phosphocholine (PE/PC) ratio increased rapidly during the first 48 hours after treatment reflecting a decrease in the PC component. This effect was qualitatively similar to that previously observed following radiation treatment [Koutcher et al., 1992]. It appears that the PE/PC ratio is a good indicator of response to both radiation and chemotherapeutic drugs and is a marker of cell kill or cessation of cellular proliferation.

Changes in phosphorus metabolism in a xenografted pharyngeal carcinoma that was sensitive to cisplatin have been compared with those occurring in two tumour sub-lines characterised by moderate to high resistance to cisplatin. Prior to cisplatin therapy, no difference in phosphorus metabolism was noted between cell lines but after cisplatin, alterations in the tumour spectra were related to the degree of tumour response. The earliest and most sensitive marker of tumour regression was a decrease in the PME/PDE ratio, paralleled by a gradual increase in PCr/Pi ratio. This suggested that changes detected by ^{31}P MRS following chemotherapy with cisplatin are response specific [Tausch-Treml et al., 1991].

In xenografted human pharyngeal carcinoma, radiation was associated with alterations in phosphorus metabolism that were correlated with growth delay, histological appearance and mitotic activity of the treated tumour [Jackel et al., 2000]. Within 48 hours of 30 Gy radiation, there was an increase in the PDE levels, tumour pH and a decrease in PME levels. These changes preceded measurable tumour response and were accompanied by extensive histological changes and marked depression of mitotic indices. Pre-treatment levels of tumour phospholipids were found to be indicative of radiosensitivity.

Changes in phosphate metabolism correlate with tumour growth rate. Normal growth of bladder carcinoma was associated with an increase of inorganic phosphate and phosphomonoesters and a decrease of phosphocreatine [de Certaines et al., 1992]. Rapidly growing tumours and early stage of re-growth after treatment with cisplatin showed a high phosphocreatine/ β -NTP ratio.

1.3.4.iii. Examples of clinical studies

Many studies using ^{31}P MRS show that human cancers, with the exception of glioma, have typical metabolic characteristics that include prominent PME and PDE, low PCr and a pH slightly more alkaline than that of normal cells [Negendank, 1992]. Ideally, one would like to compare cancer spectra with normal cell counterparts from which the cancer arises, but this is only possible in a very few tumour types. Some examples of studies in sarcoma, lymphoma, neuroblastoma and glioma are considered below and summarised in Table 1.

1.3.4.iii.a Soft tissue sarcoma

The potential prognostic significance of ^{31}P MRS has been studied in sarcomas of the extremity [Koutcher et al., 1990]. The aims were to determine if pre-treatment spectra might be useful in defining good risk versus poor risk or predicting responsive versus resistant tumours and also whether subsequent changes that occur early during the course of chemotherapy can be used as a predictor of tumour response. Twenty-two patients with suspected soft tissue sarcoma were studied prior to any treatment. Six patients subsequently received chemotherapy. The pre-treatment spectra of the three chemotherapy responsive sarcoma patients were characterised by relatively lower PDE/PME ratio compared to the spectra of the three non-responsive tumours. Response was defined conventionally on the basis of pathological examination and tumour volume. Response was found to be associated with a large increase in the PDE/PME ratio during the initial cycle of chemotherapy. In contrast, a decrease or minimal increase was noted in two of the three non-responding tumours and an oscillating pattern was seen in the third.

Twenty-eight patients with musculoskeletal tumours were studied at presentation with MRS and elevated levels of PME & PDE were observed relative to normal muscle [Redmond et al., 1992]. There was some overlap between the spectral characteristics of different tumour histologies but no association was observed with tumour extent or grade. Fifteen patients were studied post chemotherapy of which eleven showed a reduction in PME, and increase in Pi. The post-chemotherapy MRS was compared to histology. In

eight patients who had surgery, reductions in PDE levels of >20% were associated with a high level of necrosis (>90%) at surgery. An increase in PDE level was associated with a poor histological response.

In a similar patient group, age 9-75 years, ^{31}P MRS spectroscopy was studied before starting chemotherapy (32 cases) and serially thereafter during the preoperative chemotherapy [Moller et al., 1996]. The spectroscopic features were correlated with the percentage of tumour necrosis after surgical resection in 28 patients. Tumours with less than 10% viable cells on histology were defined as responders. 21 cases were treated on co-operative study protocol, of which 8 were responders. In the 13 non-responders, PME, Pi and PDE increased whereas energy rich phosphates decreased. In 2 responders, the energy rich phosphates increased whereas the others showed an initial increase in Pi and decrease in PCr followed by increase in high-energy phosphates (biphasic pattern).

1.3.4.iii.b Neuroblastoma

In an innovative study in 1985, spectral characteristics of an infant with stage IV-s disease were compared with an infant with stage IV disease [Maris et al., 1985]. NMR spectra from the liver regions in both the infants and primary tumour in the infant with stage IV disease showed substantially elevated PME/ β -NTP ratios as compared to a spectrum from normal control. ^{31}P NMR spectra from the rapidly enlarging liver (stage IV) and the spontaneously regressing liver (stage IV-s) were quantitatively different. The ^{31}P NMR spectrum of neuroblastoma also changed as a function of time and with

clinical behaviour. The PME/ β -NTP ratio increased during periods of rapid progression and persisted until treatment became effective. In this study, however, no field localisation techniques were used and the observed spectra had contributions from overlying tissue.

1.3.4.iii.c Non-Hodgkin's lymphoma (NHL)

A large prospective multi-centre National Cancer Institute funded study is currently documenting treatment-related changes in ^{31}P MRS spectra of adult NHL [Arias-Mendoza et al., 1999; Arias-Mendoza et al., 2000; Arias-Mendoza et al., 2001]. Spectral changes have been previously described during and after therapy in NHL patients [Bizzi et al., 1995; Bryant et al., 1988; Negendank et al., 1995]. For example, treatment response was studied in eight newly diagnosed NHL patients using image guided ^{31}P MRS [Smith et al., 1990]. Pre-treatment spectral characteristics were different in high and low grade NHL. High-grade tumours had a larger Pi peak relative to PME or β -NTP. The PME/Pi ratio produced the best separation between low and high-grade lymphomas. All patients had serial studies performed after commencing treatment and changes in tumour metabolites were seen prior to reductions in tumour size. In low-grade lymphomas treated with oral alkylating agents, there was a relative increase in Pi peak area and decrease in β -NTP, followed by increase in the phosphodiesteres. This was detected between days 10 and 27 of commencing treatment. For patients with high-grade NHL similar metabolic changes were detected much earlier (day 3).

1.3.4.iii.d Central Nervous System (CNS) tumours

With currently available techniques, ^{31}P MRS of brain tumours can not differentiate between different histological types or correlate with malignancy. However, ^1H MRS has been extensively used to study brain tumours. N-acetyl aspartate (NAA) signal is reduced in areas of tumour as compared with normal cerebral hemispheres [Heesters et al., 1993]. A co-operative in vivo study carried out in 15 clinical research centres confirmed that the 'Chol' resonance was higher in glial tumours than in non-involved brain tissues [Negendank et al., 1996]. Attempts have been made to predict histology and grade and to differentiate tumour from scar tissue or radiation necrosis as well as to evaluate response [Wang et al., 1995; Tedeschi et al., 1997; Taylor et al., 1996; Hwang et al., 1998; Lin et al., 1999; Preul et al., 1996].

For example, a study of 27 children with recurrent brain tumours demonstrated the prognostic significance of Cho/NAA ratio in tumour [Warren et al., 2000]. Diagnoses included high-grade glioma (10), brain stem glioma (7), medulloblastoma/peripheral neuroectodermal tumour (6), ependymoma (3) and pineal germinoma (1). The concentrations of Cho and NAA in the tumour and normal brain were quantified and maximum Cho/NAA ratio was determined for each patient's tumour. The maximum Cho/NAA ratio ranged from 1.1 to 13.2 (median 4.5). The ratio in apparently normal brain tissue was less than 1. Children with maximum Cho/NAA ratio of less than or equal to 4.5 had a projected survival of more than 50% at 63 weeks and those with ratio of greater than 4.5 had a median survival of 22 weeks, and all 13 children were dead by 63 weeks.

The role of ^1H -MRS in monitoring response of histologically proven glioma to adjuvant chemotherapy or radiotherapy was studied in 10 children [Lazareff et al., 1999]. Thirty-eight ^1H -MRS scans were done. The follow up period ranged from 6 months to 40 months. The ratio of tumour Cho to brain Cho correlated with tumour volume and clinical response. In 4 patients whose tumour progressed after treatment, the tumour choline to brain choline ratio increased and in 6 patients who had a stable or decreased tumour volume, the ratio decreased.

The resonance profiles of five metabolites measured on ^1H MRS (choline containing compounds, creatine and phosphocreatine, N-acetyl groups, lactate and lipids) were studied in sixteen adults with recurrent glioma before and during treatment with tamoxifen. MRS imaging metabolite ratios relative to contralateral creatine were studied at 2 weeks and 4 weeks from starting tamoxifen. 7 patients responded to tamoxifen. Responders and the non-responder group differed significantly in the mean intensities of the five metabolites, both at pre-treatment evaluation and at very early treatment stages (2 and 4 weeks) [Preul et al., 2000].

Peak areas of NAA, Cho, creatine and phosphocreatine were assessed in 14 young people (average 10 years) with newly diagnosed cerebral hemispheric tumours. There were three glioblastomas, 4 gangliogliomas and one each of Primitive neuroectodermal tumour, ganglio-glioblastoma, ependymoma, anaplastic ependymoma, rhabdoid teratoid tumour, pilocytic astrocytoma and gliomatosis cerebri. Four patients died and 10 survived. The NAA/Cho and creatine/choline ratios were low in patients who died and high in the survivors [Girard et al., 1998].

1.3.4.iv. Conclusion of literature review of MRS and tumour response

^1H and ^{31}P MRS measurements detect in vivo biochemical changes following treatment in normal tissue and tumour in a range of tumour types. However, there is a lack of consistency in the descriptive measures used. Many studies include a range of histological types that may mask effects specific to each class. In addition, the range of treatments, variability in defining response and use of different localisation strategies make interpretation difficult. There is therefore, a need for standardised methodology to allow comparison between studies and to understand the basis of changes observed. This needs large disease specific multi-centre trials to be performed with standardised methodology. It is evident from the review of literature that several markers and ratios are emerging as potential prognostic markers of tumour response. For example, a decrease in PME could suggest a responsive or non-responsive tumour and help to tailor treatment. With non-responsive tumours, second line treatment could be initiated at an earlier stage and in phase two studies, MRS changes could have implications for early evaluation of efficacy.

Table 1: Summary of clinical experiments relevant to MRS and tumour response in paediatric oncology

Reference	Diagnosis	No. patients	Observations
[Koutcher et al., 1990]	Soft tissue sarcoma	22	Pre-treatment: Lower PDE/PME ratio in responders During chemotherapy: ↑PDE/PME in responders
[Redmond et al., 1992]	Musculo-skeletal tumour	28	↓PDE, ↓PDE/NTP, ↓PDE/PCr, ↓PDE/Pi in responders
[Moller et al., 1996]	Musculo-skeletal tumour	28	Pre-treatment: PCr+Pi/total phosphate ≥ 0.35 , PCr/ α NTP ≥ 1.5 , rapid initial ↑ in (PME+PDE)/(PCr+Pi+NTP) & long term decrease in responders. In non-responders: PME, Pi and PDE↑
[Maris et al., 1985]	Neuroblastoma	2	↑PME/ β -NTP in progression
[Smith et al., 1990]	NHL	8	Relative ↑in Pi peak, ↑PDE, ↓ β -ATP in responders
[Warren et al., 2000]	CNS	27	In recurrent tumours, Cho/NAA ratio ≤ 4.5 -- better survival
[Lazareff et al., 1999]	CNS (glioma)	10	Tumour Cho/Brain Cho increased with progression
[Girard et al., 1998]	CNS	10	Pre-treatment NAA/Cho high in survivors

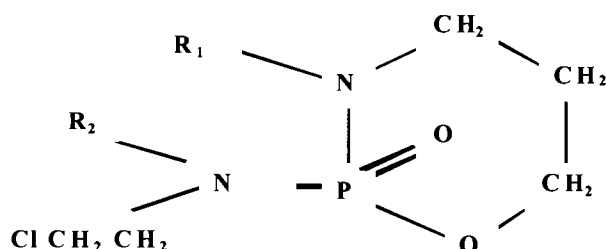
1.4 Pharmacokinetic study of ifosfamide

1.4.1. History of oxazaphosphorines

The development of drugs with more selective antitumour actions and a wider margin of safety have contributed significantly towards advances in cancer chemotherapy. It was known that the biological efficacy of nitrogen mustard compounds is closely linked with the reactivity of the functional 2-chlorethylamino groups, which is in turn linked to the basicity of the corresponding nitrogen atoms. The substitution of electrophilic groups at the amino nitrogen reduces the basicity and thus reduces the reactivity of the functional groups. Based on this principle, a phosphoryl group was chosen as the electrophilic group and coupling of a mustard group to phosphoric acid resulted in oxazaphosphorines. Out of over 1000 compounds synthesised, four compounds were found to possess particularly favourable properties i.e. retained chemotherapeutic activity but reduced reactivity and toxicity when compared to nitrogen mustard. These were cyclophosphamide (CYP), introduced in 1958, trofosfamide introduced in 1972, ifosfamide (IFO), introduced in 1977 and sulfosfamide [Brock, 1983]. Of these, cyclophosphamide and ifosfamide are extensively used in paediatric and adult oncology.

1.4.2. Structures of ifosfamide and cyclophosphamide

Ifosfamide and cyclophosphamide have the same molecular weight (261.09) and the same chemical formula ($C_7H_{15}Cl_2N_2O_2P$). However, IFO differs from CYP by the translocation of one of the side chain chloroethyl groups to the ring nitrogen. Transferring the chloroethyl group to the ring nitrogen created a compound different in properties from both nitrogen mustard and cyclophosphamide, both of which have two chloroethyl groups attached to an exocyclic nitrogen [Loehrer, Sr., 1992]. Figure 1.8 shows the structures of IFO and CYP.



Structure of Ifosfamide and Cyclophosphamide

Ifosfamide: $R_1 = ClCH_2CH_2$ $R_2 = H$.

Cyclophosphamide: $R_1 = H$; $R_2 = ClCH_2CH_2$.

Figure 1.8

1.4.3 Mechanism of action of ifosfamide

After intracellular activation, both 2-chloroethyl groups of IPM are converted to reactive electrophilic alkyl group ($R-CH_2^+$), which in turn reacts with the nucleophilic moieties of the bases in the deoxyribonucleic acid (DNA), such as N⁷- guanine. Because of its bifunctional character, IPM forms two reactive alkyl groups. Attachment of these alkyl groups to two bases result in an intra-strand link, if the two bases are in the same DNA strand, or in an interstrand cross-link if the two bases are on different DNA strands. Interstrand cross-linkage impairs DNA replication by inhibition of double strand separation prior to cell division [Kerbusch et al., 2001a]. This causes 'S' phase arrest of cells [Schwartz and Waxman, 2001]. The final pathway leading to cell death is thought to be apoptosis [Becker et al., 2002;Schwartz and Waxman, 2001].

1.4.4. Metabolism of ifosfamide

[Kerbusch et al., 2001a; Nowrousian MR et al., 1993; Kaijser et al., 1994; Boddy and Yule, 2000]

Both ifosfamide and cyclophosphamide are inactive drugs in vitro and are mainly metabolised in the liver [Allen et al., 1976]. IFO is hydroxylated at the C4 position by hepatic cytochrome P450 enzymes, mainly CYP3A4, to produce 4-hydroxyifosfamide [Walker et al., 1994]. 4-hydroxyifosfamide equilibrates with its tautomer aldo-ifosfamide. 4-hydroxyifosfamide can decompose to give ifosforamide mustard (IPM), the primary alkylating agent, and acrolein [Connors et al., 1974; Low et al., 1983]. This process seems to be catalysed by 3', 5'-exonucleases [Kaijser et al., 1993]. Acrolein is responsible for the urotoxic effects of IFO, mainly haemorrhagic cystitis [Brock et al., 1979; Brock et al., 1981a]. This can be prevented by concomitant use of sodium 2-mercaptoethane sulphonate (MESNA) [Brock and Pohl, 1986; Brock and Pohl, 1983; Brock et al., 1982; Brock et al., 1981b]. 4-hydroxyifosfamide is also metabolised to the inactive metabolites 4-ketoifosfamide and 4-thioifosfamide.

Aldo-ifosfamide can be oxidised by aldehyde dehydrogenase (ALDH) to give inactive carboxyifosfamide (CXI) and alcoifosfamide. Because of the decreased level of these enzymes in tumour cells in comparison with normal cells, only limited deactivation can take place in the tumour cell, being one of the causes of the selective cytotoxic action on tumours [Kaijser et al., 1993]. Resistant tumour cell lines seem to have increased ALDH activity [Brock, 1989].

IFO is also subject to deactivation routes that involve removal of the chloroethyl group from either the exo or endocyclic nitrogen atom to form non toxic 2-dechloroethylifosfamide (2-DCI) and 3-dechloroethylifosfamide (3-DCI) respectively. Dechloroethylation is achieved by side-chain oxidation, releasing an equimolar amount of irritant chloroacetaldehyde. This pathway of metabolism is particularly important for ifosfamide because as much as 50% of IFO is metabolised by this pathway compared with only 10% of cyclophosphamide [Kamen et al., 1995]. This is probably because of lower affinity of the 4-hydroxylating enzymes to IFO and, therefore, more dechloroethyl ifosfamide and chloroacetaldehyde are produced [Norpoth, 1976;Norpoth et al., 1976;Kaijser et al., 1993]. Possibly, the close proximity of the 'bulky' chloroethyl groups to the C4 position plays a crucial role [Nowrousian MR et al., 1993]. Due to this difference in metabolism, three-fold higher doses of ifosfamide are generally administered to achieve equipotent alkylating activity compared to cyclophosphamide [Sarosy, 1989]. This results in higher amounts of metabolites of dechloroethylation pathway.

Chloroacetaldehyde is believed to be responsible for the nephrotoxicity and neurotoxicity associated with IFO [Skinner et al., 1993;Springate, 1997;Dubourg et al., 2001]. It has also been suggested to contribute to anti-tumour activity [Borner et al., 2000]. In vitro studies have demonstrated that kidney microsomes are capable of biotransforming ifosfamide to 2-DCI and 3-DCI and hence local production of chloroacetaldehyde [Woodland et al., 2000]. Human kidney tubules also metabolise chloroacetaldehyde at high rate producing a less toxic chloracetate [Dubourg et al., 2001]. Two other

IPM metabolites, chloroethylamine (CEA) and the 1,3-oxazolidin -2-one (OXAZ) have been also identified [Highley et al., 1995].

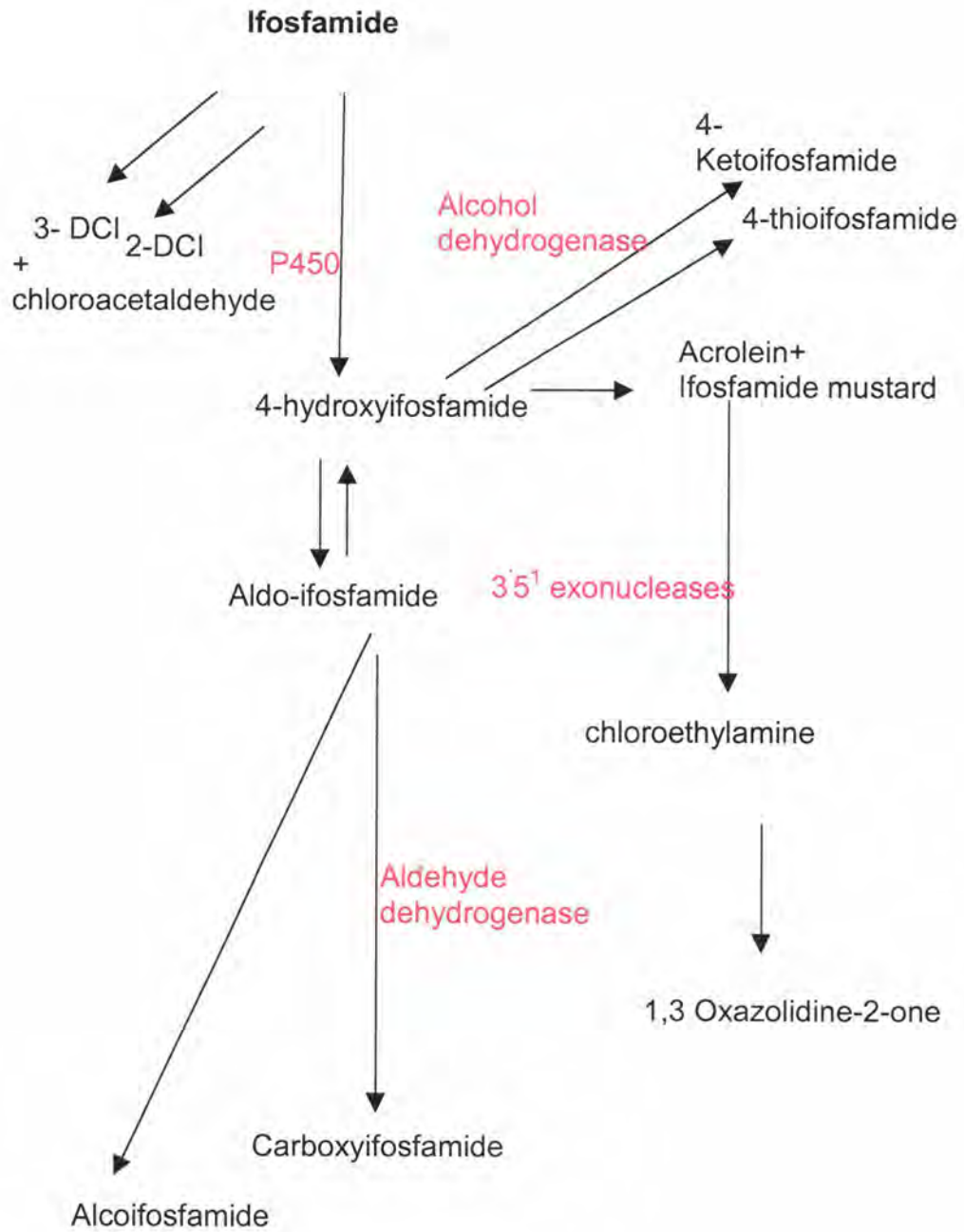


Figure 1.9: Metabolism of ifosfamide

3-DCI: 3-dechloroethylifosfamide, 2-DCI: 2-dechloroethylifosfamide

1.4.5. Metabolic distribution of ifosfamide

Both ifosfamide and cyclophosphamide are rapidly absorbed after oral administration. Within a few minutes, alkylating compounds can be detected in the plasma. Radioactively labelled IFO and CYP are detectable in organs and tissue within a few minutes of intravenous injections. The highest concentrations are found in the liver, small intestines and kidneys, followed by the lungs, spleen, muscle, tumour, large intestine, skin, brain and bones. Excretion is mainly renal [Nowrousian MR et al., 1993]. Oral administration of IFO causes unacceptable levels of encephalopathy, probably as a result of a metabolic shift towards increased dechloroethylation pathway [Lind et al., 1989a]. Therefore, this route is not favoured in clinical practice. Concomitant oral methylene blue could possibly prevent encephalopathy [Aeschlimann et al., 1998].

Earlier studies suggested that ifosfamide mustard is membrane impermeable and has to be formed intracellularly for its cytotoxic actions [Engle et al., 1979]. There is debate about the transport form of the drug. Red blood cells (RBCs) have been proposed to be transporters of activated IFO and CYP but it is still not clear whether 4-hydroxyifosfamide or IPM is the main transport form [Highley et al., 1997; Momerency et al., 1996]. One group has suggested that IFO is bioactivated in the liver to IPM and then IPM is loaded onto or in the RBCs. The RBC transports IPM to the target tissue where it interacts with the capillary endothelium and releases IPM [Highley et al., 1997]. In a study on 5 patients treated with IFO, RBCs contained as much as 77% of the total

whole blood concentration of IPM, resulting in an erythrocyte: plasma ratio of area under the concentration time curve (AUC) of 2.7 [Highley et al., 1997].

The 4-hydroxy metabolite may be trapped intracellularly and act as the transport form of activated cyclophosphamide with low plasma concentrations of the metabolite [Wagner et al., 1977]. Extracellular 4-hydroxy compound exerts more cytotoxic effect compared to extracellular phosphoramidate mustard due to the higher ability of the former to penetrate the tumour cell membranes [Sladek, 1988].

The distribution of IFO, cyclophosphamide and their metabolites was studied in cerebrospinal fluid (CSF) of children. Twenty-five patients were studied, 21 of these received cyclophosphamide. CSF: plasma ratio was higher for IFO when compared to cyclophosphamide. The CSF: plasma ratio for IPM was higher than that of the parent drug and concomitant dexamethasone reduced the ability of the drugs to cross the blood brain barrier [Yule et al., 1997]. In another study, plasma: CSF ratio of ifosfamide ranged from 0.5-1.7 whereas 2 and 3 dechloroethylifosfamide concentrations in CSF were very low [Kaijser et al., 1998].

1.4.6 Pharmacokinetic variations and factors affecting metabolism

The metabolism of ifosfamide has been studied using different doses and schedules. Children clear the drug more quickly than adults do [Boddy et al., 1993]. A decrease in the parent compound, with a concomitant increase in dechloroethylated products, has been observed during continuous 3 days infusion of ifosfamide [Boddy et al., 1993]. A study in children comparing continuous infusion of ifosfamide over 3 days with bolus infusions for 3 days showed that there was 70% less of the dechloroethylated metabolites in the plasma following bolus administration compared to continuous infusion but no change in other metabolites [Boddy et al., 1995a]. A similar study in adults showed no difference in the concentrations of any metabolite in plasma or urine, thereby indicating that there is no identifiable pharmacokinetic basis for recommending either bolus or infusional methods for IFO administration [Singer et al., 1998]. Another study compared 3 schedules of administration; short (1-4 hours), medium (24-72 hours) and long (96-240 hours). During a long infusion duration the dose corrected AUC was significantly decreased for IFO and increased for 3-dechloroethylifosfamide compared with short infusion durations [Kerbusch et al., 2001b].

Saturable metabolism of continuous infusion of high-dose IFO has been described. In 32 patients with advanced soft tissue sarcoma who received a five-day continuous infusion at a total IFO dose of 12-18 g/m², the AUC for IFO increased linearly with dose while the AUCs of the metabolites did not change. This was true of ifosfamide mustard and carboxyifosfamide as well as for the dechloroethylation pathway. The authors concluded that IFO doses

greater than 14-16 g/m² per course appeared to result in a relative decrease of the active metabolites [Cerny et al., 1999].

Both ifosfamide and cyclophosphamide are metabolised in the liver by the cytochrome P450 enzyme. Drugs affecting the activity of this enzyme could induce or inhibit their metabolism. Fluconazole inhibits cytochrome P-450 and therefore could reduce the therapeutic effects of cyclophosphamide [Yule et al., 1999]. The same enzyme CYP3A4 has role in both activation and N-dechloroethylation pathways of ifosfamide metabolism and this prohibits selective inhibition of the N-dechloroethylation pathway [Walker et al., 1994]. A more recent study has shown that CYP3A4 catalyses over 95% of dechloroethylation of cyclophosphamide but only approximately 70% of dechloroethylation of IFO. CYP2B6 is responsible for the rest of the IFO dechloroethylation. Selective inhibition of hepatic CYP2B6 activity could minimise production of dechloroethylated products [Huang et al., 2000]. Studies have also been done in animal models to evaluate effects of different drugs on P-450 modulation [Yu et al., 1999;Brain et al., 1998].

A double randomised crossover clinical study of 16 patients receiving ifosfamide either alone or with ketoconazole or rifampicin showed that rifampicin increased the metabolism of IFO without specifically favouring activation or deactivation route and ketoconazole decreased activation to 4-hydroxyifosfamide. Ketoconazole is a potent inhibitor of CYP3A4 and rifampicin is an inducer [Kerbusch et al., 2001c]. Although the CYP3A4 enzymes are predominantly expressed in the liver, they may also be expressed in tumour [Murray et al., 1993;Murray et al., 1998], leading to the

speculation that the intra-tumoral activation may also contribute to ifosfamide activity.

Marked intra-subject variations have been noted in both ifosfamide and cyclophosphamide in different courses of chemotherapy [Boddy et al., 1992;Yule et al., 1996;Boddy et al., 1993;Boddy et al., 1995b;Boddy et al., 1996a;Yule et al., 1995]. Factors such as age and liver function as reflected by plasma bilirubin have been shown to affect half-life of IFO [Boddy et al., 1996a]. This could reflect variability in the levels of enzymes necessary for its metabolism.

Metabolism of IFO is an auto-inducible enzymatic process, resulting in increased clearance over time. This has been studied in both adults and children and has been observed within 24 hours after the start of treatment [Boddy et al., 1995c;Kaijser et al., 1996]. In the case of ifosfamide autoinduction leads to an increase in either the formation of dechloroethylated metabolites [Boddy et al., 1993;Lind et al., 1990a] or both dechloroethylation and 4-hydroxylation [Kurowski and Wagner, 1993]. Increased ifosfamide clearance is sustained between treatment cycles and is reproducible in subsequent cycles. Increased metabolism of IFO occurs at least in two consecutive cycles of 5 day-fractionated therapy to approximately the same magnitude in each cycle. The increased IFO metabolism is transient and not demonstrable 21 days after discontinuing IFO [Lewis, 1996]. The exact physiological mechanism for the auto-induction for IFO is not clear. For most other drugs autoinduction results from de novo synthesis of enzymes performing the metabolic breakdown. However, IFO reduces

protein synthesis and could have a similar effect on enzymes responsible for CYP3A4 degradation/ inactivation thereby increasing IFO clearance [Kerbusch et al., 2000;Kerbusch et al., 2001a].

1.4.7. Pharmacogenetics

Pharmacogenetics is the study of how genetic inheritance influences response to drugs [Watters and McLeod, 2003]. This would help identify the genetic reasons of toxicity or lack of tumour response and reduce unpredictability of cancer treatment [Innocenti and Ratain, 2002;Iyer and Ratain, 1998].

Ifosfamide and cyclophosphamide are metabolised by enzymes from cytochrome p450 family and aldehyde dehydrogenase family. A phenotypic deficiency in the excretion of carboxyphosphamide arising from aldehyde dehydrogenase polymorphism has been suggested [Boddy et al., 1992]. Variability in the excretion of carboxyphosphamide was observed and patients were termed low carboxylators and high carboxylators [Hadidi et al., 1988]. Overexpression of the enzyme has been observed in cells resistant to the cytotoxic effects of cyclophosphamide [Colvin et al., 1988;Hilton, 1984] . The aldehyde dehydrogenase family is made up of several members and genetic polymorphism has been described with ALDH2 which is involved with metabolism of alcohol [Iyer and Ratain, 1998]. There is however no report on cyclophosphamide/ifosfamide metabolism and gene encoding for aldehyde dehydrogenase enzyme.

Cytochrome p450 enzymes are important for metabolism of ifosfamide. A group of these enzymes is responsible for metabolising many endogenous and exogenous substances, including 40% to 50% of all medications. A large number of single nucleotide polymorphisms for CYP3A have now been

identified [Kim, 2002] but a clear relationship between genetic polymorphism and metabolism of ifosfamide or cyclophosphamide is yet to be established. A marked inter-individual variation has been observed in the metabolism of oxazaphosphorines and it is possible that in the future pharmacogenetics would play an important role in the use of these drugs.

1.4.8. Relationship between Ifosfamide metabolism and efficacy & toxicity

The recent development of analytic methods for assessment of DNA cross-links [Hartley et al., 1999] has confirmed that in breast cancer patients, systemic DNA damage is related to the active metabolite [Johnstone et al., 2000].

Few studies have investigated the effect of variable metabolism on efficacy and toxicity of IFO. In a study on 15 patients with breast cancer, a marked negative correlation was found between both disease free survival and overall survival and the AUCs of the products of IFO activation (IPM and CXI). In addition, recovery of IPM in urine was higher in patients who experienced partial response compared with those with progressive or stable disease. In this study, clearance, volume of distribution and half-life were studied after a 24 hour infusion [Boddy et al., 1995b].

Cellular levels of aldehyde dehydrogenases are considered to be predictors of therapeutic responses to cyclophosphamide based chemotherapy in breast cancer [Sladek et al., 2002]. A retrospective study on 171 breast tumours showed that the cellular levels of ALDH1A1 were significantly higher in metastatic tumours that had survived exposure to CYP than those that had not been exposed to the drug. The levels were also found to be higher in metastatic tumours that did not respond to CYP.

The relationship between nephrotoxicity (both acute and chronic) and ifosfamide metabolism was studied in 15 children. In 8 children, the IFO metabolism was investigated during one early course (1-3) and one late

course (>8) to study the magnitude of changes following repeated administration. Acute measures of renal toxicity did not correlate with any of the IFO pharmacokinetic or metabolic parameters. AUC of dechloroethylated metabolites declined with repeated courses. Chronic renal toxicity determined at 1 month or 6 months after treatment did not correlate with any of the IFO metabolic parameters. However, a negative correlation was found between change in AUCs of dechloroethylated metabolites of IFO and the overall nephrotoxicity at 1 month and 6 months implying that patients in whom metabolism via dechloroethylation decreases are at a greater risk of chronic toxicity. These data contradict the hypothesis that the systemic production of chloroacetaldehyde is responsible for IFO nephrotoxicity [Boddy et al., 1996b].

1.4.9. Ifosfamide and magnetic resonance spectroscopy

1.4.9.i Introduction

During the last decade, validated assays have been developed enabling quantitative determination of IFO and its metabolites. Thin-layer chromatography (TLC) with various detection methods is easy to apply but hampered by cross-selectivity and low sensitivity. High performance liquid chromatography (HPLC) is a more established technique but due to its indiscriminating detection at lower wavelengths, a labour intensive sample preparation is required to separate the analyses from interfering plasma components. Gas chromatography (GC) quantifies volatile analytes and can be selective and sensitive, but the analytes need to be thermally stable, which excludes 4 hydroxyifosfamide and IPM [Kerbusch et al., 2001a]. Drug uptake and distribution has also been studied using radio labelled drugs. This exposes the patient to radioactivity and its potential adverse effects [Moretti et al., 1979].

1.4.9.ii ³¹P MRS

The principle that certain drugs contain magnetic nuclei is utilised to study pharmacokinetics-using MRS. Almost all the metabolites of IFO contain ³¹P. Figure 1.10 shows structures of IFO metabolites.

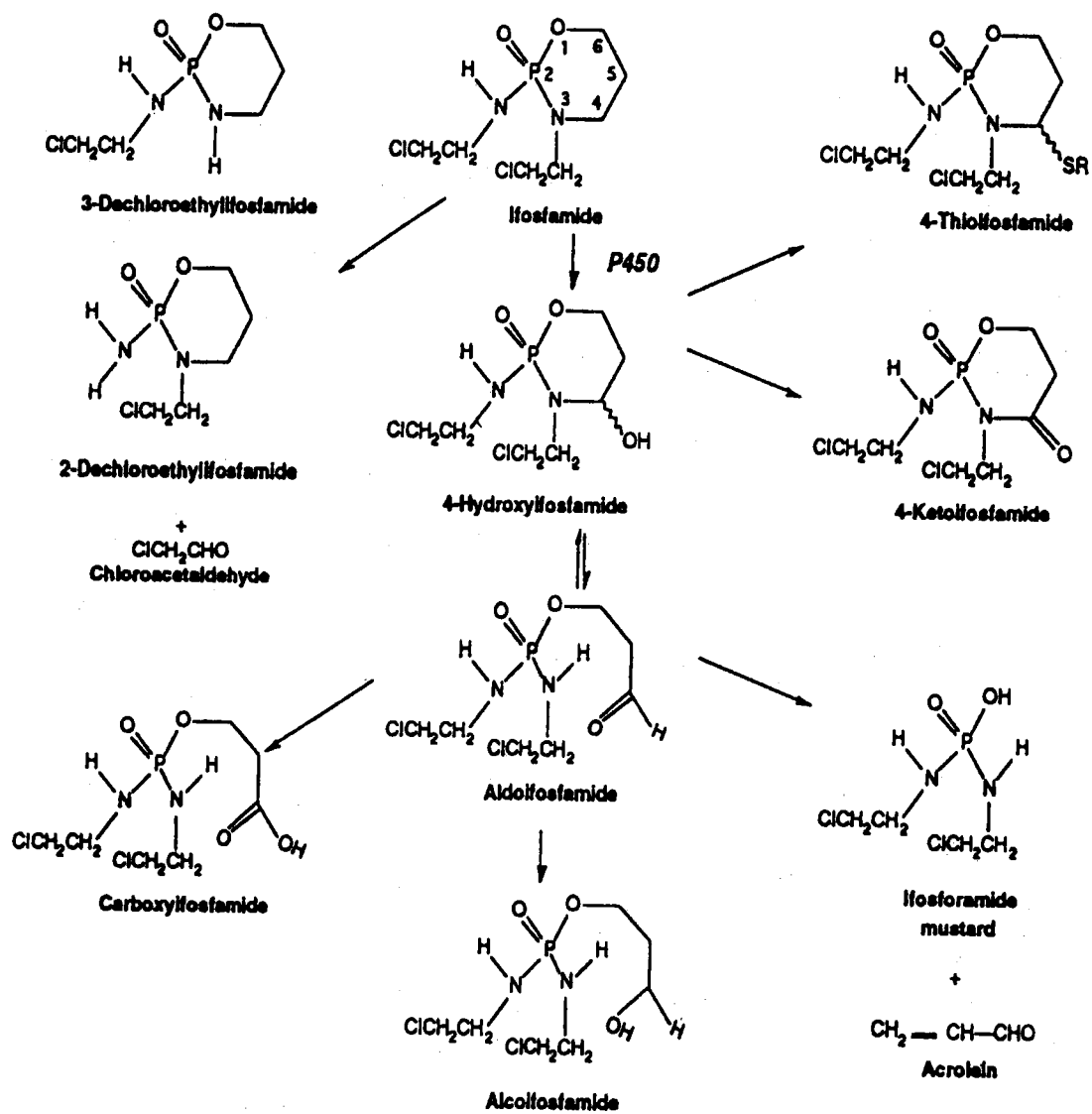


Figure 1.10: Structure of ifosfamide metabolites [Kajiser et al., 1998]

Several studies have emphasised the role of MRS to study IFO metabolites in urine and other body fluids [Gilard et al., 1993; Martino et al., 1992]. MRS has the advantage that the body fluids do not need any extraction or chemical derivatization and therefore can be directly studied. No radiolabelled drug is required, as the probe, the ^{31}P nucleus, is an inherent part of the parent drug and its metabolites. The disadvantage is that MRS is a relatively insensitive technique and it can take a long time (12-15 hours) to obtain a spectrum with a good signal to noise ratio.

In 1983, Misiura et al were the first to use ^{31}P MRS to study the urinary excretion of IFO and its phosphorylated metabolites, namely keto-ifosfamide and the metabolites of dechloroethylation pathway [Misiura et al., 1983].

In 1992, urine and blood samples of 7 patients with metastatic soft tissue sarcoma and cerebrospinal fluid (CSF) and blood of a patient with non-Hodgkin's lymphoma were collected following IFO infusions [Martino et al., 1992]. Concentrated samples of urine were used to shorten the time of experiments. Control samples of IFO, cyclophosphamide, carboxyifosfamide, ketoifosfamide, IPM, 2-Dechloroifosfamide, 3-Dechloroifosfamide, 4-hydroxyifosfamide and 2,3 Dechloroethylifosfamide were used for comparison. Chemical shifts were reported relative to the resonance peak of 85% H_3PO_4 as an external chemical shift reference. IFO was detected at 15.89 ppm, carboxyifosfamide at 19.09 ppm, 2-DCI at 17.71 ppm, 3-DCI at 15.80 ppm, IPM at 13.95 ppm. In few samples ketoifosfamide was detected at 11.27 ppm. Neither hydroxyifosfamide nor aldo-ifosfamide was detected. Urine was collected over 8-hour time intervals for 24 hours after the

beginning of infusion in 3 patients. Although there was considerable inter-individual variability, over a 24-hour period, the total excretion for the three patients was relatively similar. Cumulative urinary excretion of IFO and its metabolites was 44% of the injected dose. Unmetabolised ifosfamide was the major compound in 0 to 8 hour and 8 to 16 hour fractions. 2-DCI and 3-DCI were the main metabolites detected in each 8 hour fractions of urine. The proportion of IFO decreased over time, whereas the proportion of its metabolites increased. Comparison between a CSF sample and a plasma sample collected 16 hours from the end of a 3 hour infusion of IFO identified unmetabolised IFO and 3-DCI in the CSF sample and none in plasma indicating that these compounds persist longer in the CSF [Martino et al., 1992].

In 1993, the same French group identified 4 unknown phosphorylated compounds in the urine of patients treated with IFO as well as quantifying the urinary excretion of IFO and its metabolites in 9 patients [Gilard et al., 1993]. A signal at 19.21 ppm was attributed to Alco-ifosfamide. 2, 3 Dechloroethylifosfamide was never seen but two of its degradation products were seen at 10.88 ppm and 6.50 ppm. A compound at 10.91 ppm was attributed to a degradation product of 2-DCI. The total urinary excretion of IFO and its phosphorylated metabolites as recovered from urine over a 24 hour period was $50.6 \pm 10.6\%$ (range, 38.6%-72.3%). A mean of $17.9 \pm 4.7\%$ (range 11.4%-28.5%) of the delivered dose was excreted unmetabolised. The most abundant urinary metabolites were the dechloroethylated compounds. Urinary excretion of the metabolites of the activation pathway i.e. carboxyifosfamide, IPM and Alco-ifosfamide were 3 times lower than the

metabolites of the dechloroethylation pathway. The excretion of IFO and its metabolites were nearly equal in the 0 to 8 hour and 8-16 hour collection, but was lower in the 16-24 hour. About 11% of the injected dose were recovered in the 24 to 48 hour urine samples obtained from 2 people.

In 1997, ³¹P MRS was used to evaluate the stability of carboxyifosfamide (CXI) and carboxycyclophosphamide (CXCP) in urine at different pH and temperatures. CXCP was more stable than CXI at either pH (7.0 and 5.5) and at all temperatures. To obtain true estimates, urine had to be frozen and stored at -80°C within a few hours of micturation. CXCP and CXI assay should be carried out within 2 months and 1 month of storage respectively [Joqueviel et al., 1997].

The first in vivo study in rat livers and tumours was published in 1997. The aims of this study were to assess the pharmacokinetics of the drug in rat livers and tumours (GH3 prolactinoma) and assess the effect of carbogen (95% oxygen, 5% carbon dioxide) breathing on uptake and metabolism of IFO. At +18 ppm from PCr, IFO peak was seen. The time course showed a rapid uptake followed by elimination of the drug over 6 hours. No drug was detected at 24 hours. Carbogen breathing by rats bearing GH3 prolactinomas markedly increased IFO uptake compared with controls breathing air. There was also a significant increase in the AUC. However, there was not significant change in the half-life for elimination. In the rat liver, the half-life for elimination was 59±10min. Carbogen breathing did not significantly affect the pharmacokinetics in the liver [Rodrigues et al., 1997].

A year later, in 1998, ^{31}P MRS was used to investigate glucosylifosfamide mustard (Glc-IPM) transport and uptake in rats with prostate adenocarcinoma. This was compared with uptake of IFO. The chemical shift position for Glc-IPM was approximately 20 ppm relative to PCr. The signal to noise ratio of IFO was remarkably lower than Glc-IPM. This study once again confirmed that pharmacokinetics of ^{31}P containing drug could be studied in vivo using MRS [Haberkorn et al., 1998].

A recent study has compared uptake of IFO by tumours and normal tissues using different hypercapnic hyperoxic gases. All gases caused an increased uptake compared to normal air, with carbogen inducing the largest increase. The increased uptake was selective to tumour tissue with no significant increase in any of the normal tissues studied [Rodrigues et al., 2002].

1.4.10. Therapeutic drug monitoring

Therapeutic drug monitoring can contribute to improvements of anticancer treatment. Classically, the main conditions for therapeutic drug monitoring are a wide interindividual pharmacokinetic variability, well-defined relationships between systemic exposure and response (both toxicity and efficacy), and a narrow therapeutic window [Rousseau and Marquet, 2002]. Doses for conventional chemotherapy are generally calculated using formulae based on body surface area. However, patients suffering from the same disease and receiving the same dose intensity based on body surface area can have different toxicity and efficacy. In a large randomised trial, children with acute lymphoblastic leukaemia (ALL) received either standard fixed dose or dose individually adjusted to reach a target steady-state plasma concentration of 3 drugs, cytarabine, teniposide and methotrexate. Significantly better outcome was observed in children with B-lineage leukaemia receiving individualised dosing. No difference was seen in T-lineage ALL [Evans et al., 1998]. In another study in childhood ALL, receiving 6-Mercaptopurine, risk of relapse has been correlated with mercaptopurine metabolism [Lilleyman and Lennard, 1994]. There are also pharmacokinetic and pharmacodynamic studies of 5-Fluorouracil (5-FU) using ^{19}F MRS. In patients with liver metastases from colorectal cancers studied using MRS, those with visible 5-FU signals were likely to respond to treatment [Findlay et al., 1993]. In another study, the half-life of 5-FU equal or greater than 20 minutes was defined as trapping of 5-FU. Close relationship between ability of tumour to accumulate 5-FU and cytotoxic effect of the drug was observed.

Longer half-life resulted in trapping of the drug in the tumour and was associated with favourable response [Wolf et al., 1998;Presant et al., 1994;Presant et al., 1990].

Methods used for individual dose adjustments can be classified into three categories:

- (1) The 'a priori' methods that use no concentration data, but only patient factors known to influence the concentration profile such as body weight, age, gender, serum creatinine level, glomerular filtration rate. The design of such a formula requires a close relationship between an estimated parameter and a pre-treatment factor. Carboplatin clearance is known to be related to renal function and therefore Calvert's formula [Calvert et al., 1989] is widely used to calculate carboplatin dose.
- (2) The 'test dose method', this requires concentration data obtained after administration of a low or a moderate dose. This method is often used for methotrexate. However this method can be only used when the pharmacokinetics are linear, thus excluding high dose methotrexate and this method is associated with a delay in administering the treatment dose.
- (3) The 'a posteriori methods', are convenient for repetitive administration or long continuous infusions and require concentration data and other known patient factors. These are complicated and have been developed using nomograms, multilinear regression or Bayesian estimation. This method has been used to predict 5-FU doses [Rousseau and Marquet, 2002].

The interest in IFO metabolism stems from the fact that it is an inactive drug, which is activated in the body, and variability in metabolism could affect anti-tumour activity and toxicity. Thus host metabolism may be an important determinant of treatment outcome [Sladek, 1988].

1.4.11 : Overall aims

The studies in this thesis are described in 3 chapters.

Chapter 2 describes a clinical study to detect ifosfamide and cyclophosphamide in liver and tumours of patients and has following aims:

- i) To investigate whether IFO and CYP can be detected by ^{31}P MRS in liver and tumour of patients receiving chemotherapy.
- ii) To study factors affecting identification of IFO and CYP signals in liver and tumour.
- iii) To assess if metabolites of the drugs could be detected in vivo.

Chapter 3 describes a pre-clinical study to evaluate pharmacokinetics of ifosfamide in an animal model and has following aims.

- i) To study ifosfamide metabolism in vivo in liver and tumours in an animal model using ^{31}P MRS.
- ii) To evaluate short-term kinetics of the drug in mouse liver and tumour using ^{31}P MRS.
- iii) To attempt to identify ifosfamide and its metabolites by in vivo MRS and high resolution in vitro MRS.
- iv) To obtain in vitro data on ifosfamide and its metabolites in liver and tumours using High Performance Liquid Chromatography-Mass Spectrometry (HPLC-MS).
- v) To correlate the ^{31}P MRS data with HPLC-MS data on extracts.

Chapter 4 describes a pre-clinical study to evaluate response to chemotherapy in a paediatric embryonal rhabdomyosarcoma model using MRS. The aims of this study are as follows:

- i) To investigate the role of MRS to define early markers of tumour response in vivo using a paediatric tumour model.
- ii) To evaluate the metabolic changes in ifosfamide- and vehicle-treated tumours using in vivo ^{31}P MRS.
- iii) To complement in vivo findings with in vitro high-resolution ^1H and ^{31}P MRS on tumour extracts.

CHAPTER 2

CLINICAL STUDY TO DETECT IFOSFAMIDE AND CYCLOPHOSPHAMIDE IN LIVER AND TUMOURS OF PATIENTS.

2.1 Introduction

Ifosfamide (IFO) and cyclophosphamide (CYP) are structurally similar alkylating agents. Both are pro-drugs requiring activation in the liver to the active metabolite. Marked intra-subject variability has been observed in their metabolism in both adults and children and metabolism patterns differ between the two compounds [Boddy et al., 1992; Boddy et al., 1996a; Yule et al., 1995]. For example, there is an increase in the metabolites of the dechloroethylation pathway after continuous infusions of IFO over 3 days compared with bolus administration, which is not observed with cyclophosphamide [Boddy et al., 1993; Boddy et al., 1995a; Yule et al., 2001]. In breast cancer, drug metabolism may influence survival [Boddy et al., 1995b]. It has been shown that for other drugs e.g., 5-Fluorouracil (5-FU), half-life correlates with disease outcome [Presant et al., 1990; Presant et al., 1994]. This suggests that measurements of pharmacokinetics of IFO and CYP in vivo might help predict tumour response and outcome and optimise scheduling. Most paediatric chemotherapy schedules administer IFO as short infusions for 2-5 days and monitoring pharmacokinetics on day 1 non-invasively could help dose adjustments on subsequent days.

2.2 Aims and objectives

The aims of this study were:

- 1) To investigate whether IFO and CYP can be detected by ^{31}P MRS in liver and tumour of patients receiving chemotherapy.
- 2) To study factors affecting identification of IFO and CYP signals in liver and tumour.
- 3) To assess if metabolites of the drugs could be detected in vivo.

The liver was included as a target tissue for the following reasons:

- 1) Uptake in the liver is important for drug activation.
- 2) Microsomal metabolism in the liver determines rate of availability of active compounds to the tumour.
- 3) The liver is a large organ, which can be within range of MRS surface coils, and therefore suitable for this technique.

2.3 Materials and methods

The study was conducted as per the ethical guidelines under study 355 and 1580 of the Royal Marsden NHS Trust and the Institute of Cancer Research.

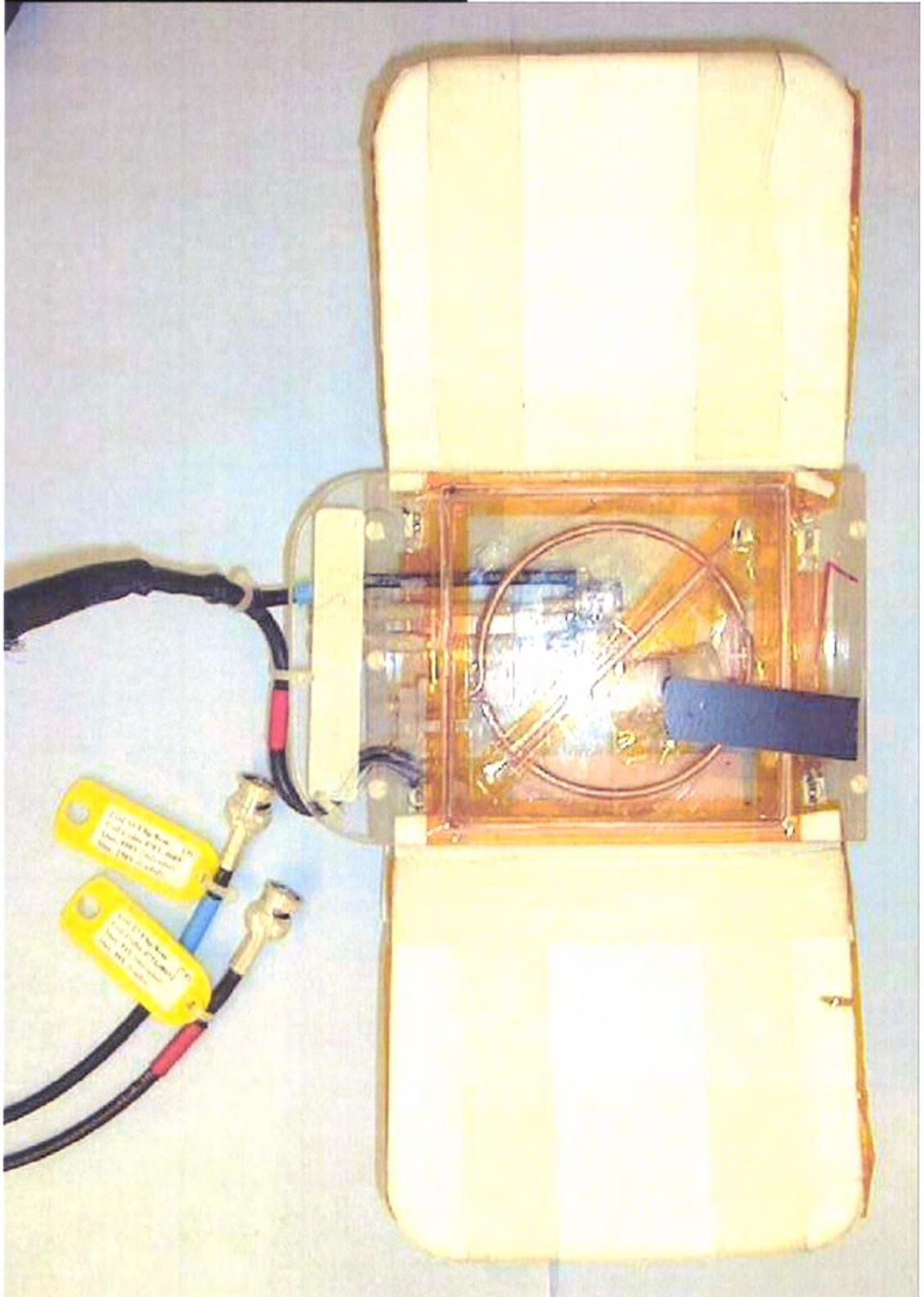
Patients receiving ifosfamide or cyclophosphamide were included in the study. All patients receiving IFO or CYP doses more than 1000 mg/m² were given additional hydration and 2-mercaptoethane sulphonate (MESNA) for uro-protection. The drugs were administered as short infusions (1 hour-3 hour). At the end of the infusion, a bolus dose of MESNA was given. The drip was disconnected and the patient was transferred to the Magnetic Resonance (MR) department. Dr Geoffrey Payne performed studies using a 1.5T Siemens 'Vision' whole-body MR system. The data was acquired by placing a ¹H/³¹P dual resonant surface coil over the liver or tumour with no further localisation. The diameters of the surface coils used were 5cm (1 study), 8cm (25 studies) and 12cm (5 studies). Figure 2.1 shows the 8cm surface coil. Initially 5.12ms 45° BIR4 adiabatic RF excitation pulses were used to achieve uniform 45° excitation of the spins throughout the region of the coil. Later studies used shorter 1.28ms 90° tanh pulses.

Thirty-one experiments were performed in 27 patients. Liver was studied in 29 experiments and tumour in 2. IFO was studied in 13 and CYP in 18. Eighteen studies were in children and 13 in adults. Age ranged from 4.6 years -61.8 years. The dose of IFO ranged from 1000-3000 mg/m²/dose and dose of CYP ranged from 600 mg-2000 mg/m²/dose. A single observer graded the signals as good, small, possible and none, based on the height of peak. Patient characteristics are shown in table 2.1

Table 2.1: Patient Characteristics

No	Age	Diagnosis	IFO /CYP	Dose(mg)	Dose/m2	Coil (cm)
1	14	Osteogenic sarcoma	IFO	3250	2.5	8
2	17	Ewing's sarcoma	IFO	4200	2.1	8
3	5	Rhabdomyosarcoma	IFO	2220	3	8
4	19	Osteogenic sarcoma	IFO	5000	3	8
5	9	Hodgkin's disease	IFO	1200	1	8
5	9	Hodgkin's disease	IFO	1200	1	8
6	28	Breast Cancer	CYP	1140	0.6	8
7	17	Osteogenic sarcoma	IFO	5700	3	8
7	17	Osteogenic sarcoma	IFO	5700	3	8
8	55	Leiomyosarcoma	IFO	4200	2	8
9	16	Rhabdomyosarcoma	CYP	2400	1.5	8
10	15	Ewing's sarcoma	CYP	2100	1.2	8
11	53	Breast Cancer	CYP	1140	0.6	8
12	41	Breast Cancer	CYP	900	0.6	8
13	62	Breast Cancer	CYP	900	0.6	8
14	38	Breast Cancer	CYP	1200	0.6	8
15	54	Breast Cancer	CYP	1200	0.6	12
16	51	Breast Cancer	CYP	1200	0.6	12
17	52	Breast Cancer	CYP	1200	0.6	12
18	49	Breast Cancer	CYP	960	0.6	12
19	32	Rhabdomyosarcoma	IFO	4500	3	12
20	52	Non Hodgkin's lymphoma	CYP	1575	0.75	8
21	13	Rhabdomyosarcoma	CYP	2600	2	8
21	13	Rhabdomyosarcoma	CYP	2600	2	8
22	10	Neuroblastoma	CYP	1900	2	8
23	16	Intracranial Germ cell tumour	IFO	2700	1.5	8
24	18	Rhabdomyosarcoma	IFO	4200	3	8
25	14	Medulloblastoma	CYP	3400	2	8
25	14	Medulloblastoma	CYP	3400	2	8
26	15	Rhabdomyosarcoma	CYP	2100	1	5
27	43	Sarcoma	IFO	4200	2	8

Figure 2.1: Example of a surface coil.



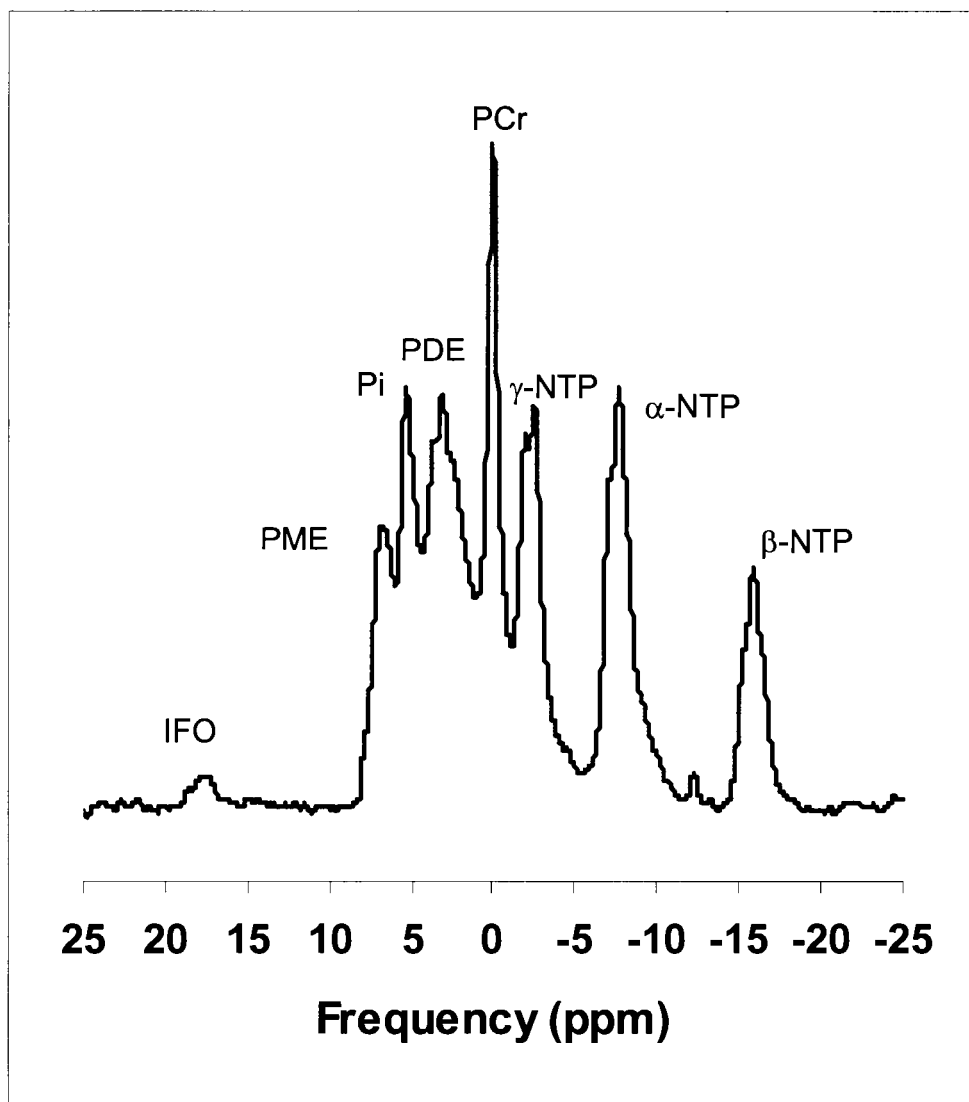
2.4 Results

2.4.1 Liver measurements

All spectra showed peaks due to phosphomonoesters (PME), inorganic phosphate (Pi), phosphodiester (PDE), phosphocreatine (PCr) and adenosine triphosphate (α -, β -, γ - ATP). The liver lacks PCr and therefore the peak arises from overlying muscle. The muscle also contributes to Pi and ATP peaks whereas the PME, PDE, Pi and ATP arise from liver. A small broad peak at 18.4 ppm downfield of PCr was attributed to IFO or CYP and was seen in 15/31 studies. Figure 2.2 shows an example of a spectrum of IFO in the liver.

Out of 18 studies using CYP, signals were seen in 6. Signals were seen in all the paediatric patients (5) who received CYP dose of 2000 mg/m² (1900 mg-3400 mg). Absence of signal was associated with relatively low doses (<1200 mg) and deep livers. Out of 13 IFO studies, signals in the region of IFO were seen in 9. In the 4 studies where no signal was seen, 2 had received dose of 1000 mg/m² and in 1, the liver was deep-seated (55mm from the surface). In 1 child it was not possible to acquire data due to a portacath over the liver producing susceptibility artefacts (line broadening). Figure 2.3 shows the relationship of the quality of the signal and depth of the liver with total dose of the drug in mg and mg/m². Figure 2.4 shows the quality of signals due to CYP and IFO in dose/m².

Figure 2.2: Example of a spectrum of ifosfamide in liver



PME: Phosphomonoester; Pi: Inorganic phosphate; PDE: Phosphodiester;
PCr: Phosphocreatine; NTP: Nucleotide triphosphate; IFO: ifosfamide

Figure 2.3: Relationship of quality of signal and depth of liver with total dose of drug (ifosfamide or cyclophosphamide) in mg and mg/m².

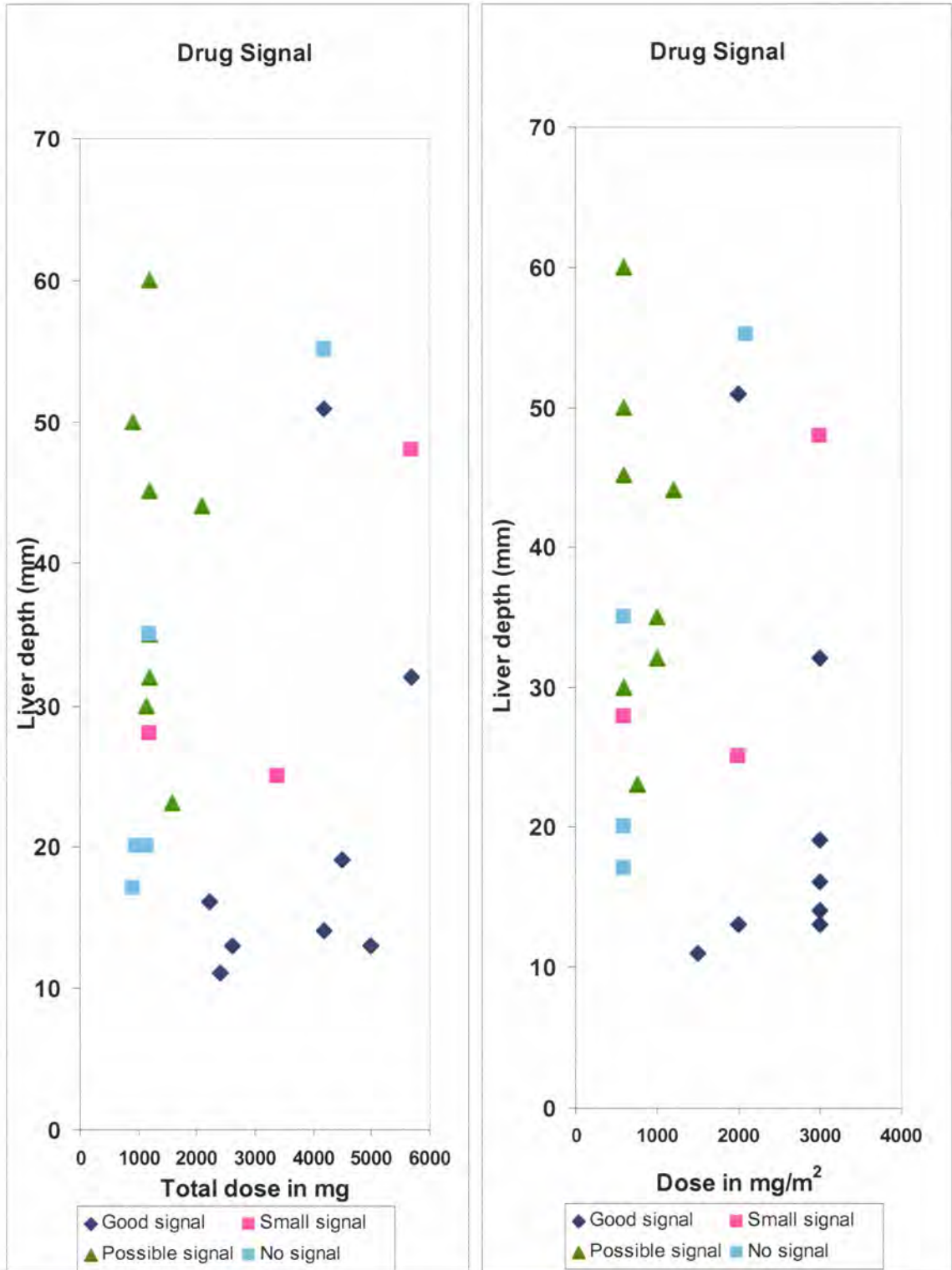
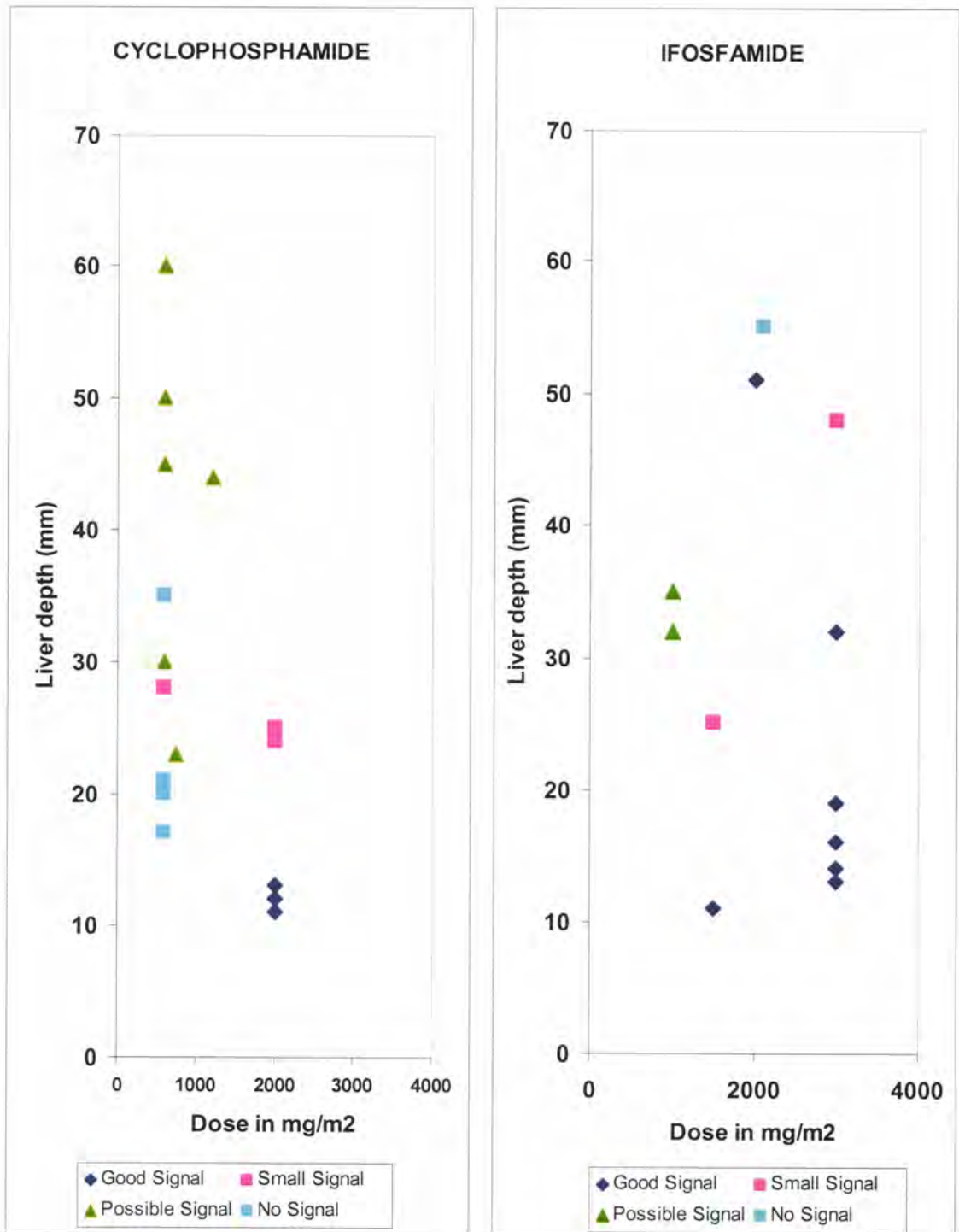


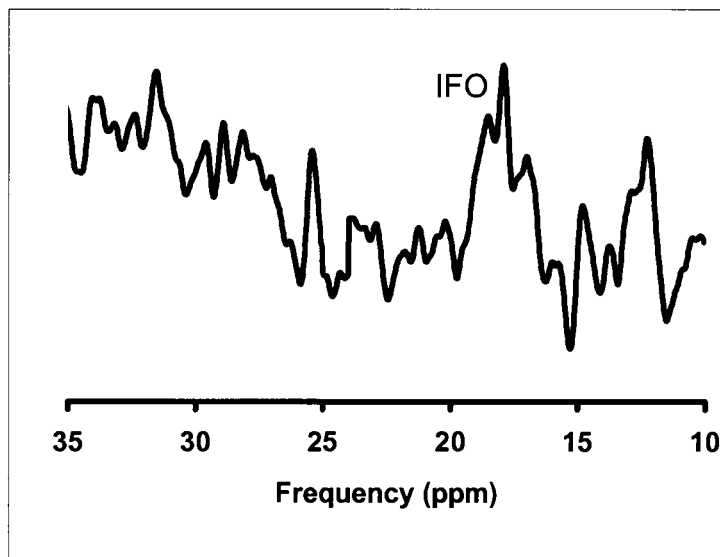
Figure 2.4: Relationship of quality of signal and depth of liver with cyclophosphamide and ifosfamide dose of in mg/m²



2.4.2 Tumour measurements

Only two patients had superficial tumours suitable for scanning. One patient had a soft tissue sarcoma of the thigh and was given 4200 mg (2000 mg/m²) of IFO. A small broad signal at 16.9-18.4 ppm was seen with a possibility of another small signal at 12.2 ppm (Figure 2.5). In this figure the phase is correct and the signal is at appropriate frequency and therefore likely to be related to IFO rather than noise alone. The sensitivity is much lower than that seen in the liver. This probably reflects the lower concentrations of mobile species in this tissue as well as smaller tissue volume. The other experiment was in a patient with rhabdomyosarcoma of the hand who received CYP 2100 mg (1000 mg/m²). No CYP related signal was seen. This could be attributable to the low dose.

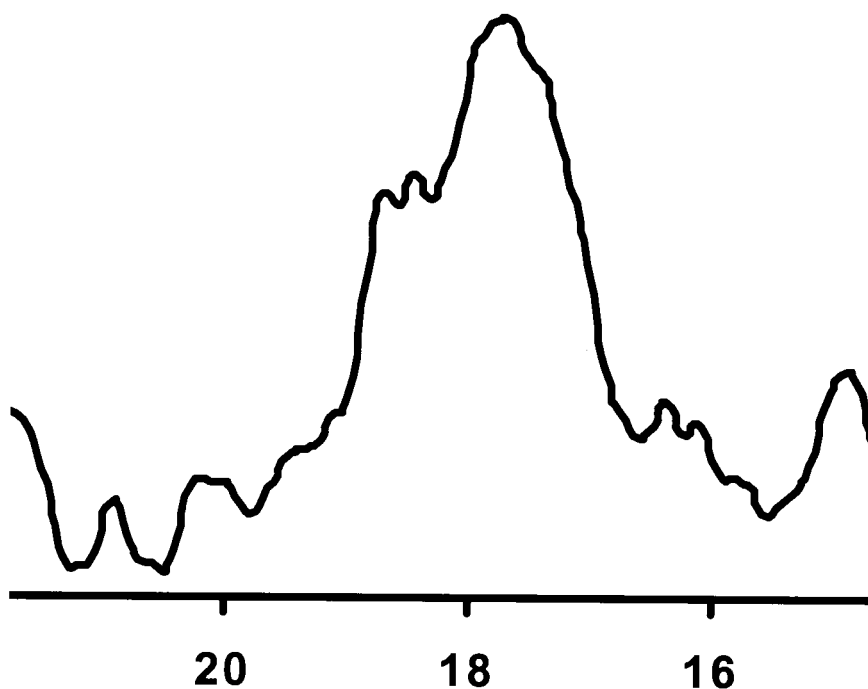
Figure 2.5: ³¹P MRS of soft tissue sarcoma



2.4.3 Composition of the 'Ifosfamide' peak

Figure 2.6 shows an example of an expansion of IFO region from one patient's liver. The broadness of the peak is unlikely to be entirely due to magnetic field inhomogeneity as the other spectral peaks are narrower (not shown in this figure). In the subsequent results and discussion, the term 'ifosfamide peak' is used. This is likely to be a composite of parent drug and metabolite.

Figure 2.6: Expansion of ifosfamide region



Possible peaks related to other IFO/CYP metabolites: In one spectrum, a small peak at the expected frequency of the metabolite carboxy-ifosfamide was seen.

2.5 Discussion

These data confirm that it is possible to detect good signals from IFO and CYP in livers of patients by in vivo ^{31}P MRS. Two main factors influencing the detection of these signals are 1) the dose of the drug administered and 2) the depth of the liver from the surface. A higher proportion of signals observed after IFO are possibly due to higher doses of IFO that are generally used. Higher doses of IFO are used in clinical practice because of the difference in the metabolism of the 2 drugs. Other factors, which influenced acquisition of adequate signal in some patients were presence of portacath over the liver, breast between the coil and the liver, and gut in the region of the coil.

To our knowledge this is the first in vivo study in children and adults where MRS has been used to study IFO and CYP in livers and tumour. The technical aspect of the study in liver has previously been published [Payne et al., 2000]. Further data must be obtained from tumours. Soft tissue and bone sarcoma would be appropriate in view of their accessibility. Once the threshold for detection is confirmed in such tumours, it would be interesting to study the pharmacokinetics of the drug in vivo and obtain an objective short-term measure of uptake and metabolism. This could then be used to assess the effects of different methods of administration, or study use of treatment modifiers such as carbogen breathing to affect drug delivery. It could also be correlated with clinical response. It would be useful to obtain a better analysis of the composition of the observed 'ifosfamide peak' and for this purpose a mouse model was used, as described in Chapter 3.

CHAPTER 3

PRE-CLINICAL STUDY TO EVALUATE

PHARMACOKINETICS OF IFOSFAMIDE IN AN

ANIMAL MODEL

3.1 Introduction

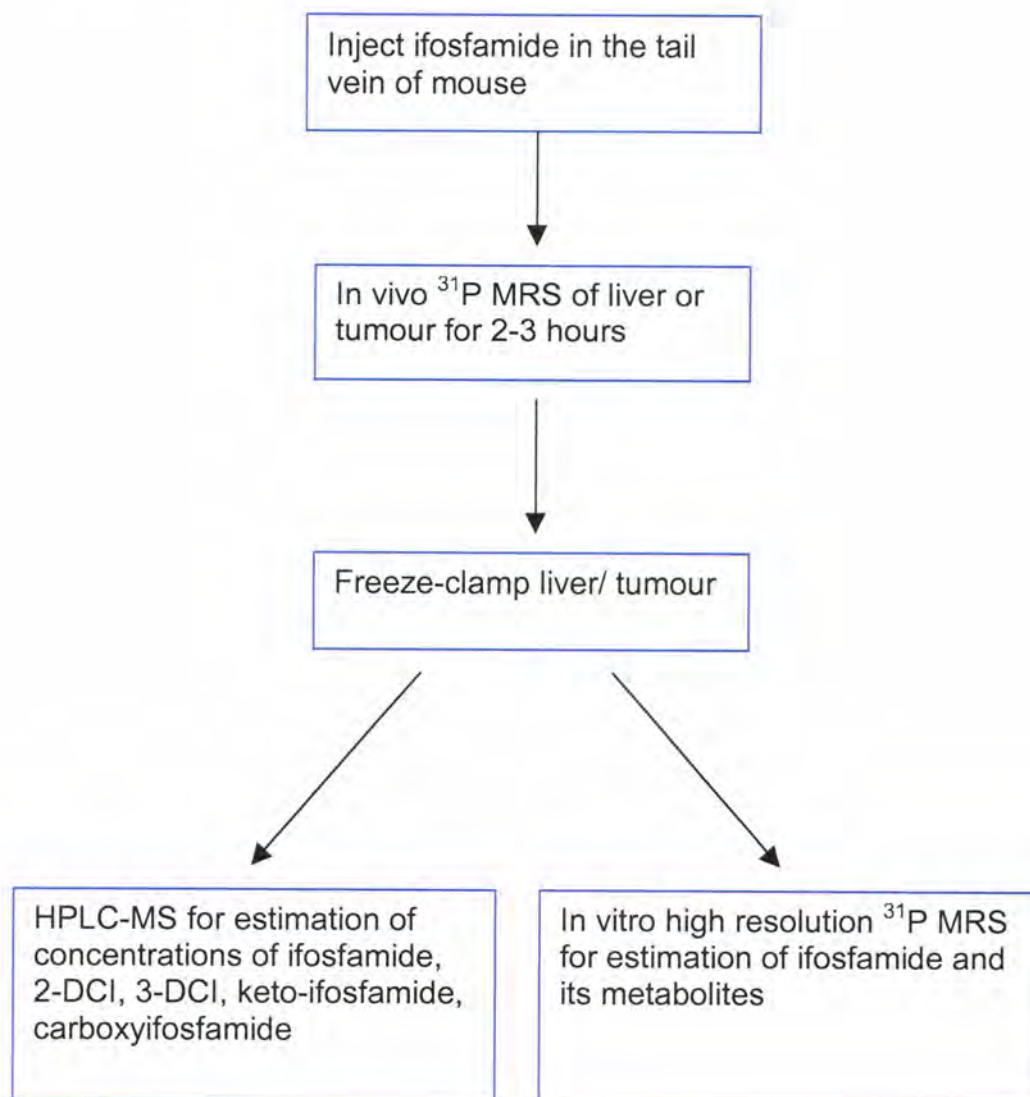
Conventional pharmacokinetic studies need frequent blood tests to assess the drug metabolism and may not give an indication of the drug in the target organs. In vivo metabolism has been studied using radiolabelled drugs [Moretti et al., 1979] but this exposes the subject to undesirable radioactivity. MRS has the potential to study pharmacokinetics of drugs non-invasively [Griffiths and Glickson, 2000] and this was first studied in 1984 using 5-Fluorouracil (5-FU) and a rat tumour [Stevens et al., 1984]. 5-FU is the drug most extensively studied using ^{19}F MRS [Findlay et al., 1993; Findlay and Leach, 1994; Glaholm et al., 1990; Presant et al., 1990; Presant et al., 1994; Wolf et al., 1998; Wolf et al., 2000]. Pharmacokinetics of temozolamide have been studied using ^{13}C MRS [Artemov et al., 1995]. The role of ^{31}P MRS to study ifosfamide metabolism has been described in Chapter 1.

The athymic nude mouse will accept human tumour and is a valid experimental model for pre-clinical studies can be established [Sharkey and Fogh, 1984]. It is an economical and effective model for pharmacokinetic and pharmacodynamic studies [Budach et al., 1987].

3.2 Aims and objectives

- 1) To study ifosfamide metabolism in vivo in liver and tumours in an animal model using ^{31}P MRS.
- 2) To evaluate short-term kinetics of the drug in mouse liver and tumour using ^{31}P MRS.
- 3) To attempt to identify ifosfamide and its metabolites by in vivo MRS and high resolution in vitro MRS.
- 4) To obtain in vitro data on ifosfamide and its metabolites in liver and tumours using High Performance Liquid Chromatography-Mass Spectrometry (HPLC-MS).
- 5) To correlate the ^{31}P MRS data with HPLC-MS data on extracts.

3.3 Study design



3.4 Materials and methods

The study was conducted under the project licence 70/4495 of the Cancer Research UK Biomedical Magnetic Resonance Research group, St George's Hospital Medical School. The ethical approval was also obtained from the Institute of Cancer Research. Tissue culture was done in the laboratories of department of Paediatric Oncology at the Institute of Cancer Research. Tumours were grown and in vivo ^{31}P MR studies were performed at St George's Hospital Medical School and the high-resolution in vitro studies were performed at Cancer Research UK Clinical Magnetic Resonance Research Group at the Institute of Cancer Research. HPLC-MS estimations of ifosfamide and metabolites were performed at the Northern Institute of Cancer Research, University of Newcastle upon Tyne.

3.4.1 Tissue culture

A frozen ampoule of RD cell line (human embryonal rhabdomyosarcoma) cell line was obtained from European Collection of Cell Culture (LOT 001/B/037). The culture medium was prepared using RPMI 1640 + glutamine +10% foetal calf serum. The frozen cells were defrosted and added to 10ml of the medium in a 25cm³ flask. The flask was kept in an incubator at 37°C with 5% CO₂. The medium was pipetted out the next day and replaced. Subsequent passaging of cells in larger flasks was done by pipetting out the medium, rinsing with versene and adding trypsin. The cells were ready for injecting into nude mice on Day 22 from the start of tissue culture.

3.4.2 Growth of the tumour in nude mice

Human embryonal rhabdomyosarcoma xenografts were established by injecting 5×10^6 freshly trypsinised cells into the flanks of anaesthetised nude mice. Inhalation anaesthesia (halothene) was used. Eight weeks later 2mm^3 biopsy fragments were implanted subcutaneously in the flanks of anaesthetised nude mice. The animals were housed in a caging system situated in a sterile environment and they were inspected regularly for size of the tumour and any focus of necrosis, bleeding, ulceration or scabbing. The tumours were used for spectroscopy experiments after the second solid to solid passage. Tumours were not allowed to grow beyond 1500 mg. On average, the tumours grew in 8 out of 10 mice.

3.4.3 Preparation of animal prior to experiments

3.4.3.i Anaesthesia

The animal was anaesthetised using a mixture of fentanyl/ fluanisone (hypnorm, Janssen Pharmaceuticals), midazolam (hypnovel, Roche) and water (1:1:2). The dose of 0.9ml/100g (0.27ml/30g) was given intraperitoneally.

3.4.3.ii Ifosfamide preparation

Vials of ifosfamide (Asta Zeneca) were obtained from the pharmacy of the Royal Marsden Hospital. A concentration of 100 mg/ml was prepared with saline. Unused solution was kept at 4°C for 1 month as per manufacturer's instructions.

3.4.3.iii Tumour volume measurement

The animal was weighed. Vernier Callipers was used to measure the size of the tumour. Three-dimensional measurements were used to calculate tumour volume by using the following formula for volume of an ellipsoid.

Tumour volume (mm³) = $\frac{\pi}{6}$ x length x width x depth.

3.4.3.iv Ifosfamide injection

The tail vein of the mouse was cannulated using a 27G-butterfly cannula and 400 mg/kg of ifosfamide was injected slowly over 2-5 minutes before the animal was placed in the magnet.

3.4.4 *In vivo* animal experiments

^{31}P MR spectra were performed using a 4.7Tesla SISCO 200 spectrometer (Figure 3.1) with a 12mm two turn surface coil. The anaesthetised animal was kept warm in the magnet with a heating blanket (Figure 3.2).

Figure 3.3 shows a mouse tumour and the surface coil.

The procedure for optimising the magnetic field homogeneity, i.e. shimming, was achieved using ^1H signal from the water within the sample. This ensured that the signal was as narrow as possible.

For the liver experiments, gradient echo images were used to confirm that the scanned tissue was predominantly liver. For tumour experiments, the superficial tumour was placed on the surface coil. Non-localised spectra of liver /tumour were obtained using an adiabatic sincos pulse, a TR of 2.2seconds and in sets of 256 acquisitions (7.5 minutes). For evaluation and improving signal to noise ratio, 1024 acquisitions; (4 spectra of 256 acquisitions each) were added together. Spectra were obtained for 3 hours. For the liver experiments, data collection started at 30 minutes after ifosfamide injections, as about 30 minutes were necessary for imaging, shimming and confirmation of liver position relative to the surface coil. Therefore, the first data point for liver experiments is from 30 minutes to 60 minutes. For tumour experiments, it was possible to obtain spectra within 5-10 minutes from injection of ifosfamide and the first data point for half-life calculation is 0-30 minutes.

Figure 3.1: 4.7 T Magnet

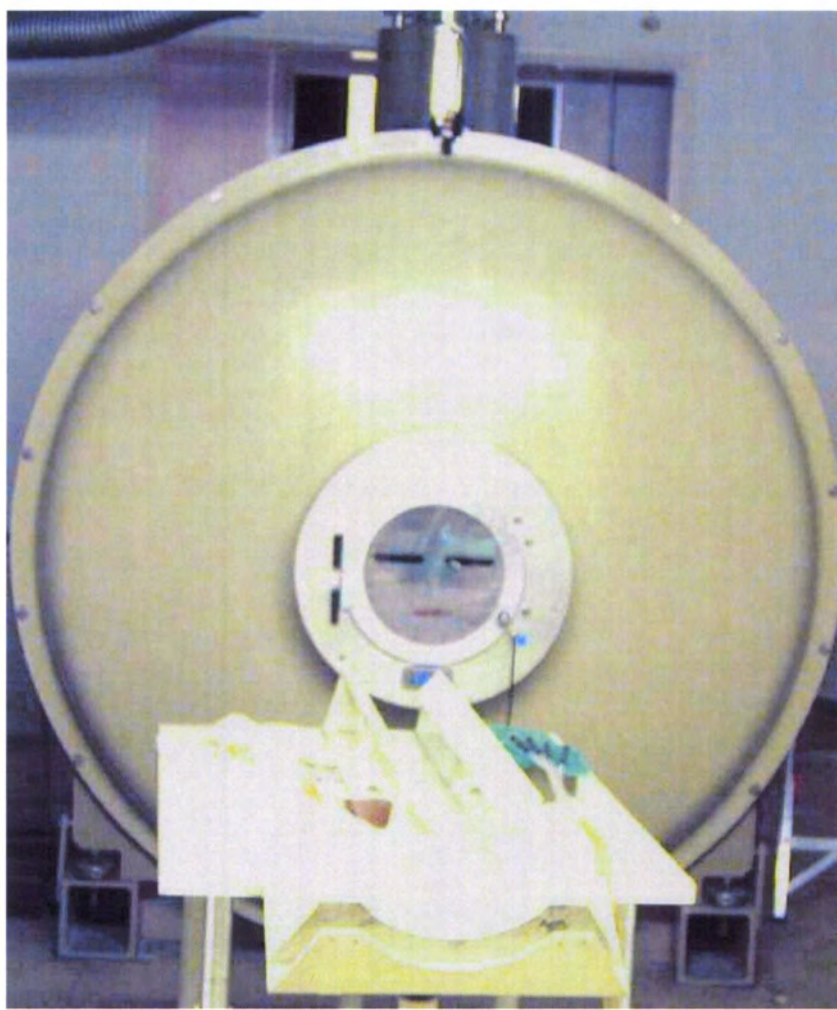


Figure 3.2: The heating blanket

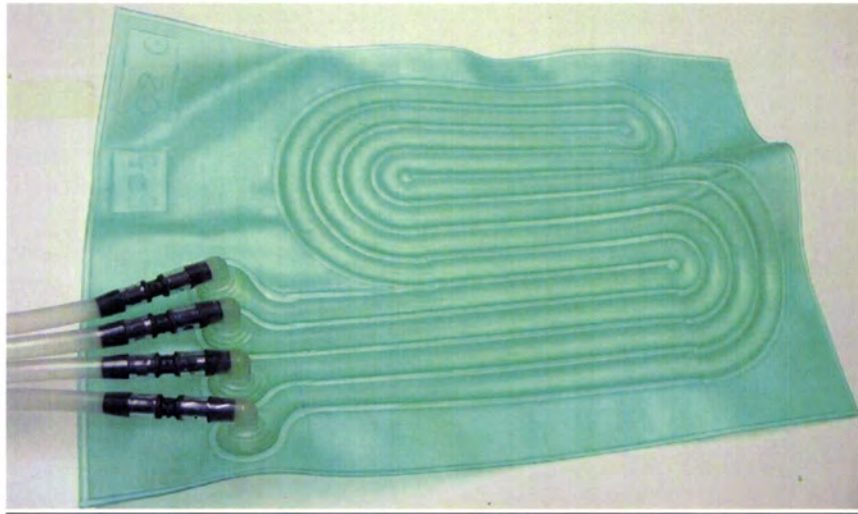
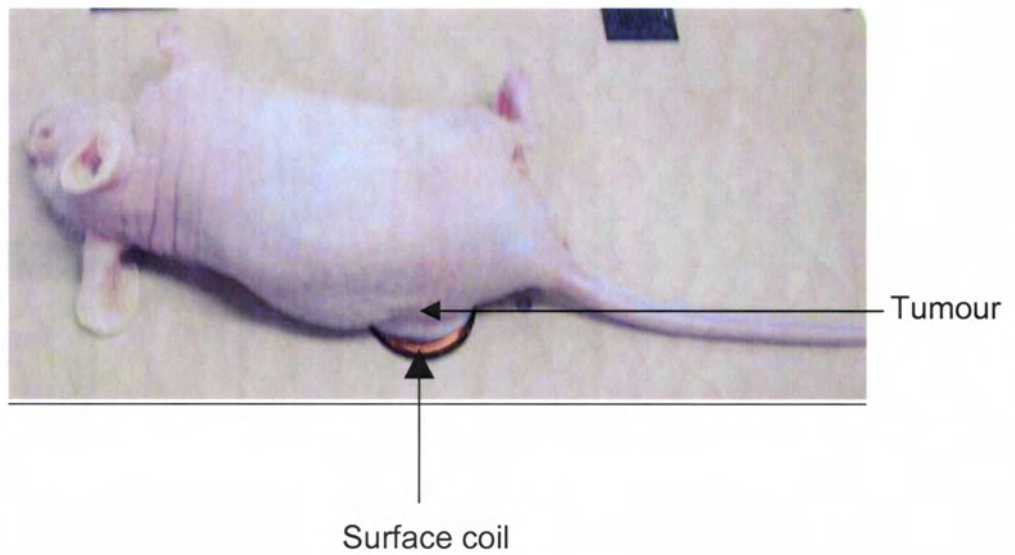


Figure 3.3: A mouse tumour and the surface coil



3.4.5 Processing of tumours after spectroscopy experiments

The animal was killed by cervical dislocation and the tumour was excised within 1-2 minutes. One half of the tumour was freeze clamped while the other half was freshly frozen. Both the samples were stored under liquid nitrogen.

Procedure for extraction of the tumour metabolites prior to high resolution

MRS

The freeze-clamped samples were taken out of big canister of liquid nitrogen and immediately transported to the laboratory in a smaller canister. Perchloric acid was stored at 4⁰ C and transported to the laboratory in a thermacol box filled with ice. This ensured that it was cold. The freeze clamped samples were weighed and homogenised under liquid nitrogen. A volume of cold 6% perchloric acid equal to 4 times the weight of the tissue was added to the homogenised sample and allowed to stand on ice for 20 minutes. The sample was centrifuged at 2000 revolutions per minute for 10 minutes at 4⁰C and the supernatant was separated and neutralised to a pH of 7 using varying concentrations of potassium hydroxide and perchloric acid. The neutralised sample was again centrifuged and the supernatant was freeze-dried.

3.4.6 *In vitro* ^1H and ^{31}P MRS experiments

1ml of D_2O was added to the freeze-dried sample and centrifuged at 10,000 rpm for 5 minutes. 0.5ml was transferred to a 5mm NMR tube and 50 μl of 5 mM TSP (3-trimethylsilyl-2-2,3,3-tetradeutero propionate) was added as a chemical shift reference for quantification in ^1H MRS. 25 μl of 10 mM MNPA (methylene diphosphoric acid) was added as reference for ^{31}P MRS. The experiments were performed using a Bruker 11.74T magnet.

3.4.7 HPLC-MS analysis of tissue extract

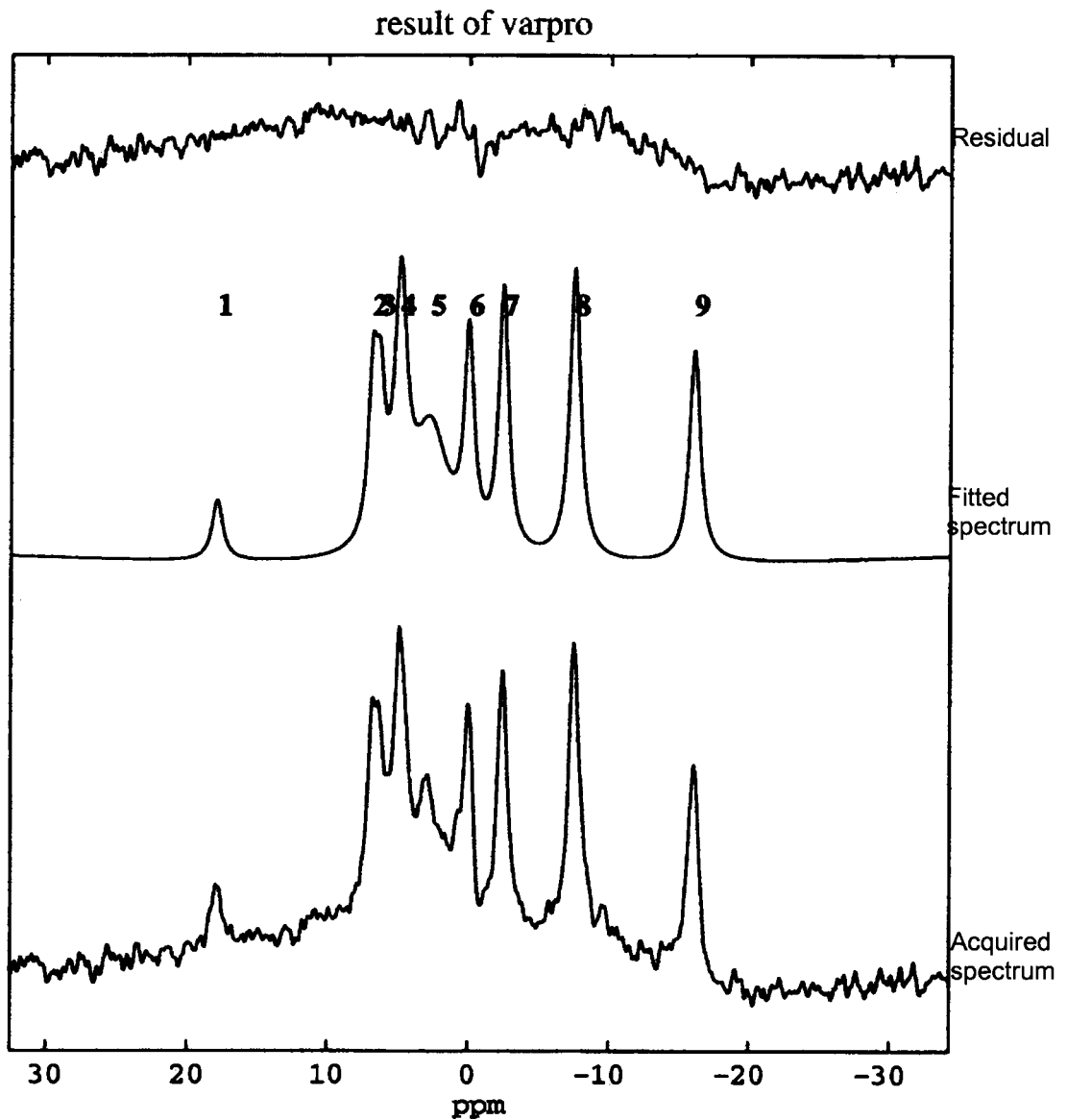
Previously freeze-clamped tissue was homogenised and sent to Dr Alan Boddy at the Northern Institute of Cancer Research, University of Newcastle upon Tyne. The samples were analysed by Dr Julieann Sludden using an HPLC-MS technique. Tissue extraction was performed using ethyl acetate. Levels of Ifosfamide, 2-dechloroethylifosfamide (2-DCI), 3-dechloroethylifosfamide (3-DCI), carboxyifosfamide (CXI) and keto ifosfamide (Keto) were measured in liver and tumour samples. Standard operative procedure for analysis is given in Appendix 3.1

3.4.8 Data analysis

3.4.8.i Analysis of spectra

The spectral data was analysed using the VARPRO (VARiable PROjection) algorithm from within MRUI along with algorithm called AMARES (advanced method for accurate, robust, and efficient spectral fitting) [Vanhamme et al., 1997]. The PCr peak was used as reference. Prior knowledge of linewidth being equal for PE and PC component of PME was used. Linewidth of ifosfamide was not fixed. Figure 3.4 shows an example of data after Varpro analysis.

Figure 3.4: An example of VARPRO analysed spectrum



- 1: Ifosfamide peak
- 2,3: PME (PE+PC)
- 4: Pi
- 5: PDE
- 6: PCr
- 7: γ -NTP
- 8: α -NTP
- 9: β -NTP

3.4.8.ii Calculation of half-life

Signal at around 18 ppm downfield to PCr was attributed to be related to ifosfamide as this peak appeared after ifosfamide administration and did not exist prior to IFO administration [Rodrigues et al., 1997]. The signal intensities of each peak in the summed spectra (4x256 acquisitions) were calculated. The time from ifosfamide injection to achieve maximum signal intensity (C_{MAX}) was noted (T_{MAX}). The natural logs of ifosfamide signal intensity after C_{MAX} were plotted against time and the exponential decay 'k' was obtained by the formula:

$$\text{Slope } y/x = -k,$$

where y and x represent the two axes.

Half-life (T_{1/2}) was calculated using the following formula.

$$T_{1/2} = \ln 2 / k = 0.693 / k$$

(Ln2: Log to the base 2)

3.5 Results

3.5.1 Liver experiments

Non-localised ^{31}P MR spectral data from liver was obtained from 5 mice for 3-3.5 hours after injection of ifosfamide. Figure 3.5 shows example spectra illustrating the decay of IFO peak in liver over 3 hours. In 4 animals the drug was detected in the first summed spectrum (30-60 minutes from IFO injection). In 1 animal the drug was first visualised between 60 minutes to 90 minutes from injection. The maximum concentration of ifosfamide was seen in livers at 30- 60 minutes in 2 mice, 60-90 minutes in 1 mouse and 90-120 minutes in 2 mice. The mean half-life of ifosfamide in liver was 109 min (range, 46 minutes-169 minutes). Figure 3.6 shows an example of a graph of the ifosfamide signal intensity in liver versus time. For purpose of graph, spectrum obtained from 30 minutes- 60 minutes is averaged as 45 minutes and so on.

It was possible to identify various other peaks in the ^{31}P MR spectra. PME could be partially resolved into PE and PC in the majority of the experiments. The other visible peaks were Pi, PCr, PDE and the 3 NTP (α -, β - and γ -) peaks.

Figure 3.5: Decay of ifosfamide signal intensity over time in a mouse liver

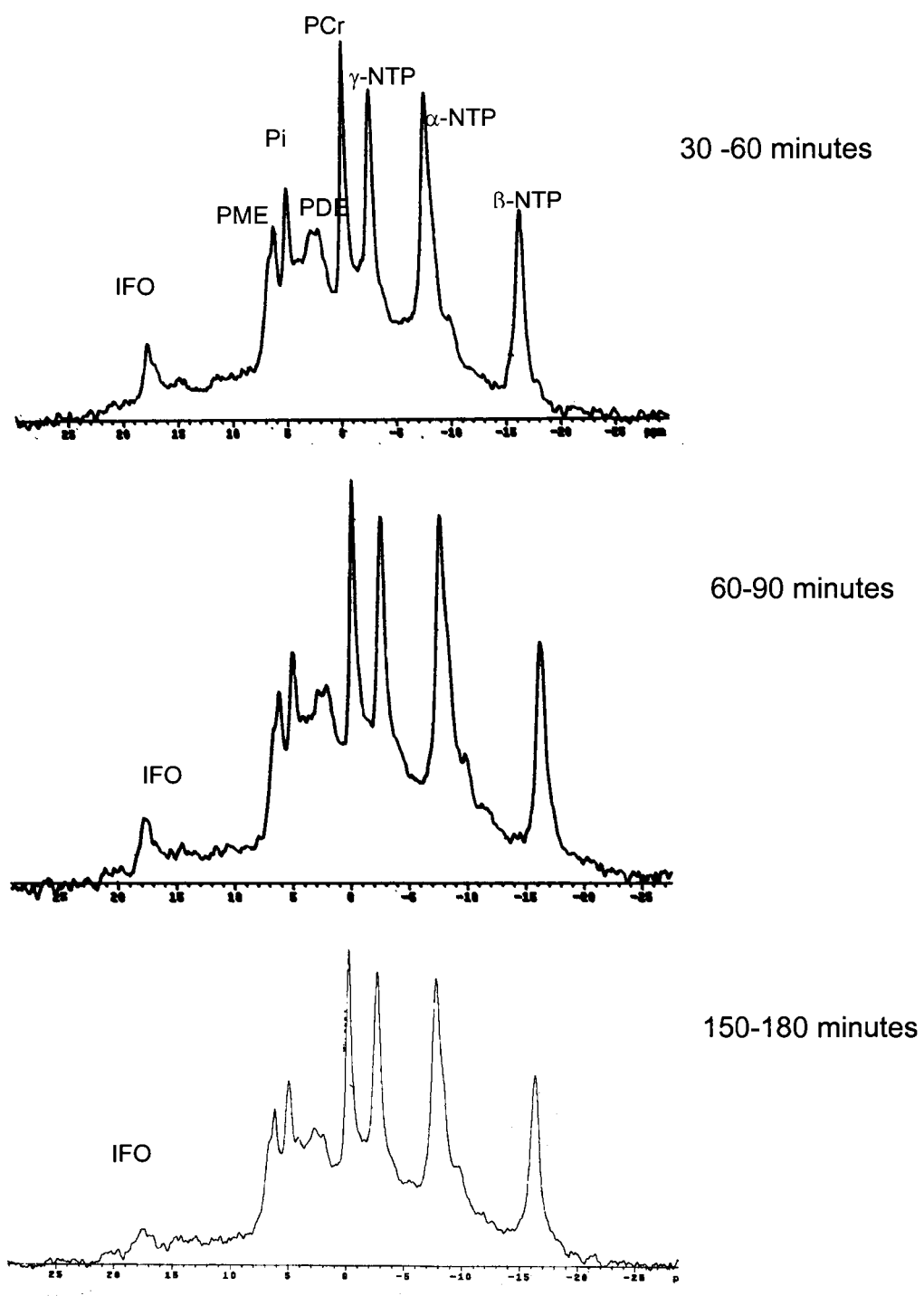
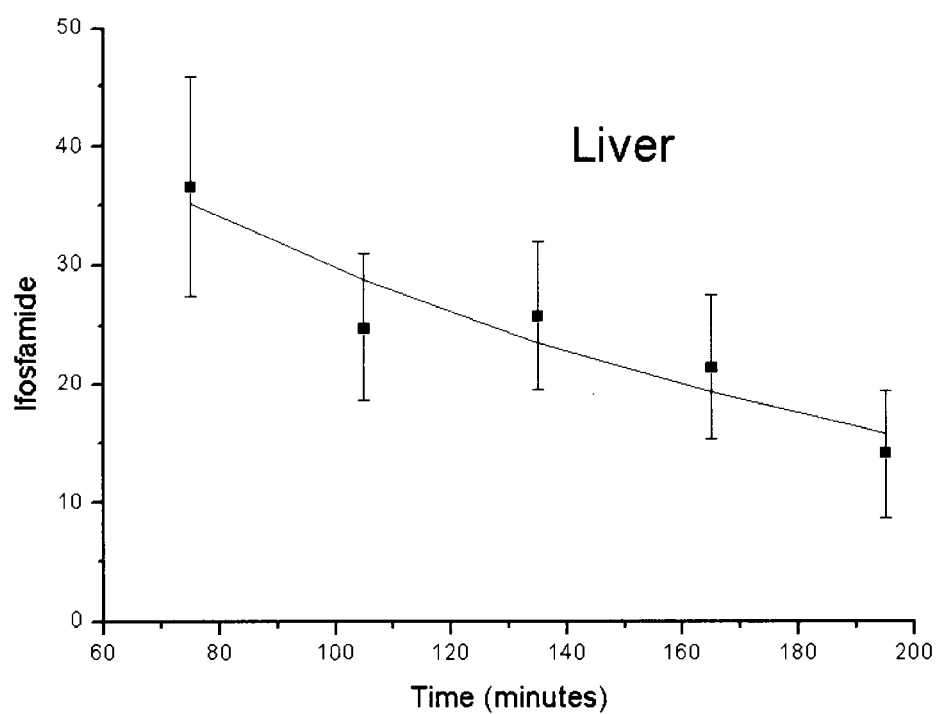


Figure 3.6: An example of a graph of ifosfamide signal intensity versus time in a mouse liver.



Mean half-life \pm standard deviation for ifosfamide in liver is 109 ± 46 minutes

3.5.2 Tumour experiments

Nine tumour-bearing mice were studied. The average tumour volume was $613 \pm 87 \text{mm}^3$. IFO was visible in seven animals within 30 minutes of administration. It was first detected between 30 minutes and 60 minutes in the remaining two animals. In one case this was for technical reasons as data were not obtainable in the first 30 minutes. In six animals, the maximum IFO signal intensity was obtained in the tumour within 30 minutes from injection of the drug. In one animal (for technical reasons) the maximum ifosfamide signal was observed at 30-60 minutes from the injection. In two animals the signal intensity was maximal at 60-90 minutes from injection. Figure 3.7 shows example spectra illustrating the decay of IFO in tumour over 2.5 hours. The median half-life was 205 minutes; the mean was 225 minutes (range, 50-405 minutes). In two small tumours (volumes 296mm^3 , 307mm^3) a rebound increase in ifosfamide was seen at 90 minutes and 120 minutes from injection, thereby increasing the half-life to 385 minutes and 238 minutes respectively. In two animals for no obvious technical reasons, ifosfamide was undetectable in the tumour in 1-summed spectrum and reappeared in the subsequent spectra. This phenomenon was observed in the largest tumour (1124mm^3) and one small tumour (307mm^3). The total phosphorus content in the summed spectrum was not different.

The half-life varied from 50 minutes to 205 minutes in tumours ranging in size from 488mm^3 to 676mm^3 . In large tumours and very small tumours the half-life was prolonged. Regression analysis of tumour volume versus half-life showed that when the two very small tumours were excluded, (It is possible that accurate data was not obtained from these small tumours ($<400 \text{mm}^3$))

there was a positive correlation between tumour size and half-life ($R^2=0.76$, $P=0.01$) (Figure 3.8).

Half-life calculations in the liver and tumour were done in different experimental animals. There was no statistically significant difference between means of half-life in liver and tumour ($p=0.08$).

Figure 3.7: Decay of ifosfamide signal intensity over time in a mouse tumour

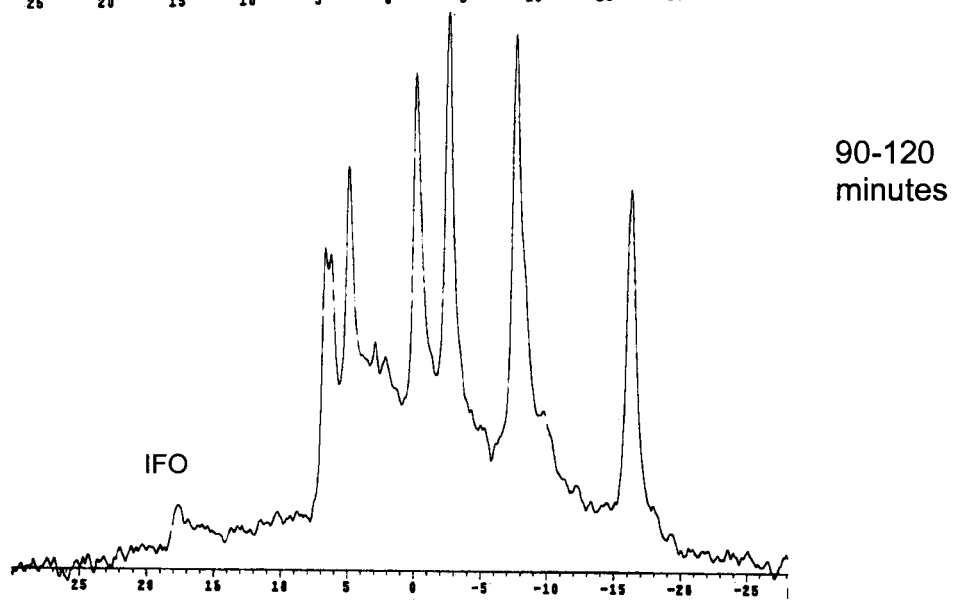
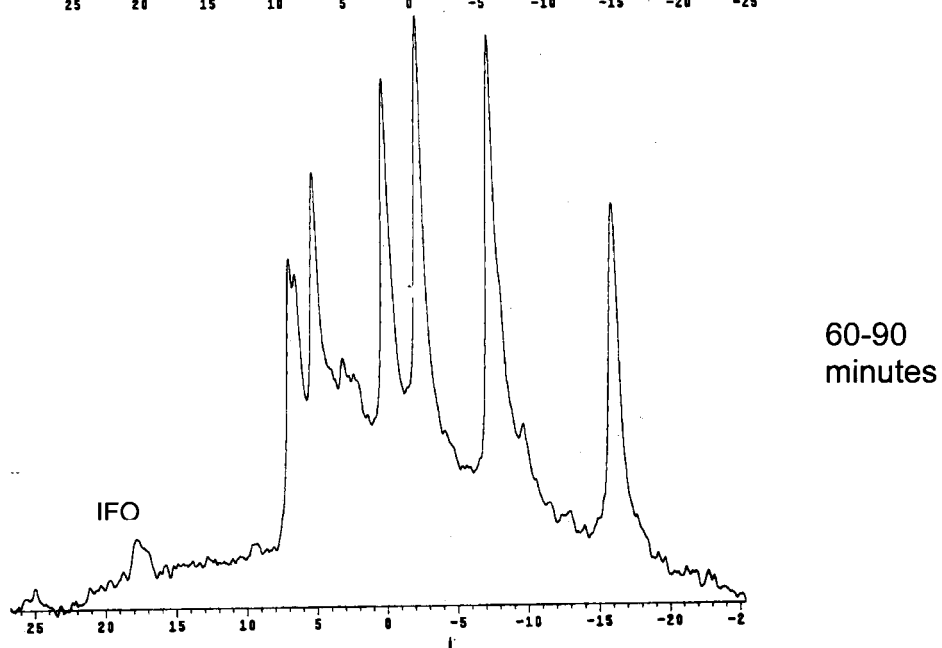
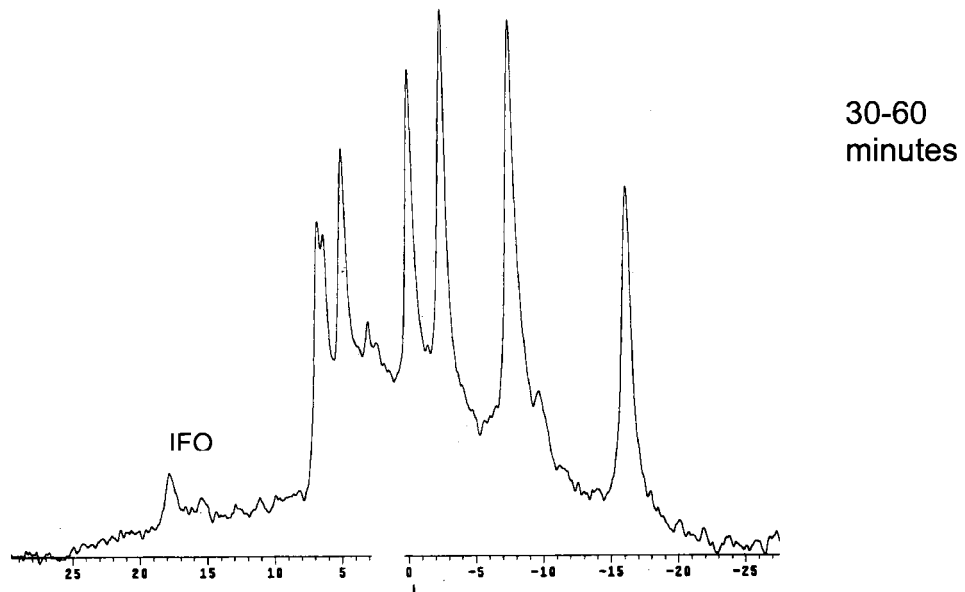


Figure 3.8 : Regression analysis of tumour volume Versus half-life (Excluding 2 small tumours)

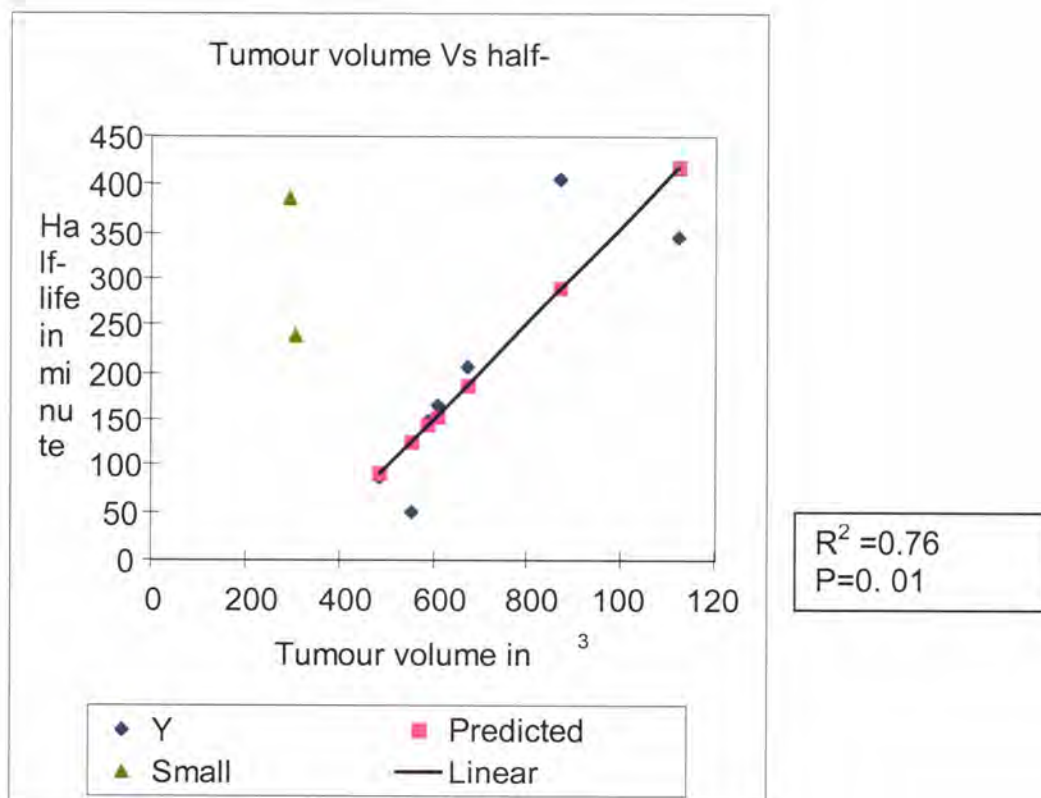
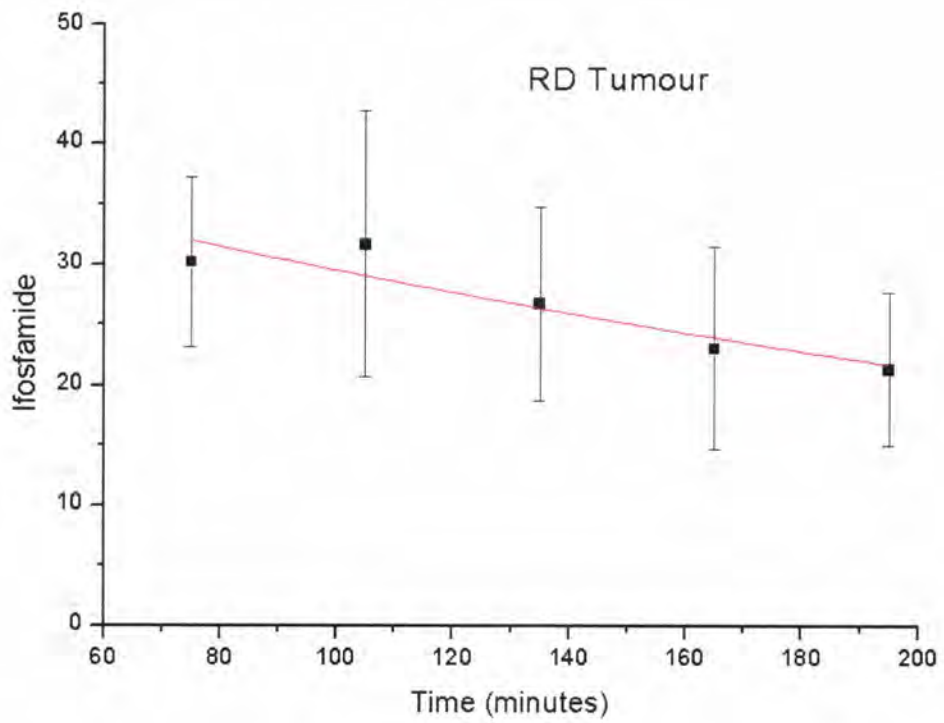


Figure 3.9: An example of a graph of ifosfamide signal intensity versus time in a RD tumour.



Mean half-life \pm standard deviation for ifosfamide in tumour is 225 ± 109 minutes

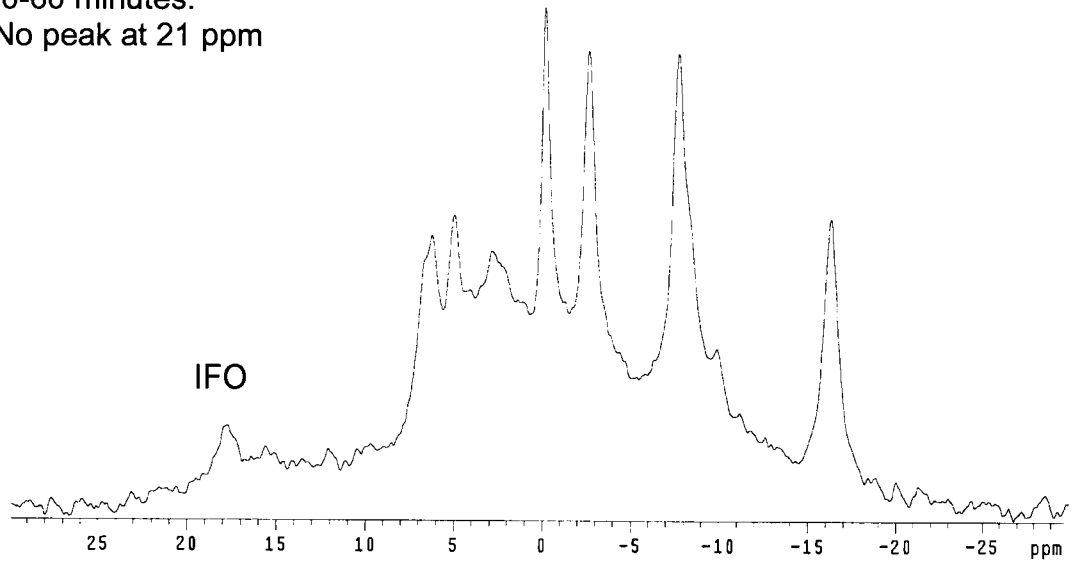
3.5.3 Ifosfamide metabolites

3.5.3.i Liver

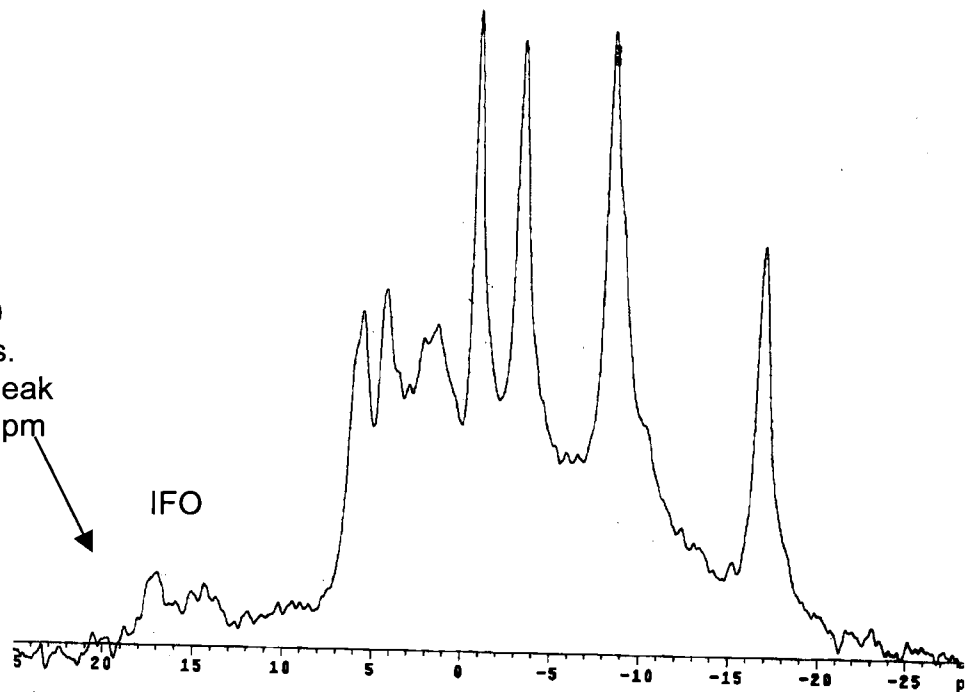
In two animals, extra peaks were seen at frequency of 20.9 ppm relative to PCr in the liver at 1.5-2.5 hours from injection of ifosfamide. These were peaks, which were not present in the first spectrum of the liver. Figure 3.10 shows the position of the peak and time of appearance. This peak is probably related to carboxyifosfamide because in the urine experiments described by Martino et al, a peak approximately 3 ppm downfield from ifosfamide was attributed to this metabolite [Martino et al., 1992].

3.10: Appearance of peak at $\cong 21$ ppm at 1.5 hours after IFO injection in a mouse liver

30-60 minutes.
No peak at 21 ppm



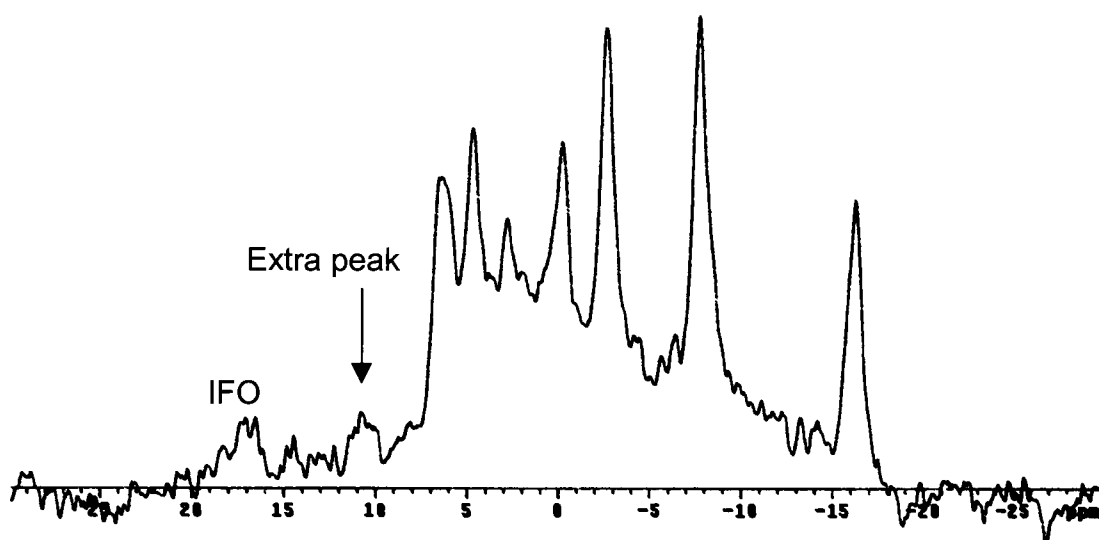
90-120
minues.
extra peak
at 21 ppm



3.5.3.ii Tumour

In 1 mouse tumour, a signal was seen at 21 ppm at 1.5 hours after IFO injection. This is again possibly due to carboxyifosfamide. In 3 other mice tumours, signals were seen between 11 and 12 ppm relative to PCr at 2.5 hours from ifosfamide injection (Figure 3.11). Although it is difficult to be certain about the origin of this signal, it could be due to keto-ifosfamide as Martino et al have attributed a signal approximately 5 ppm upfield from ifosfamide to be due to this compound [Martino et al., 1992]. There are no in vivo studies to compare this peak and extracts were not done at specific time points.

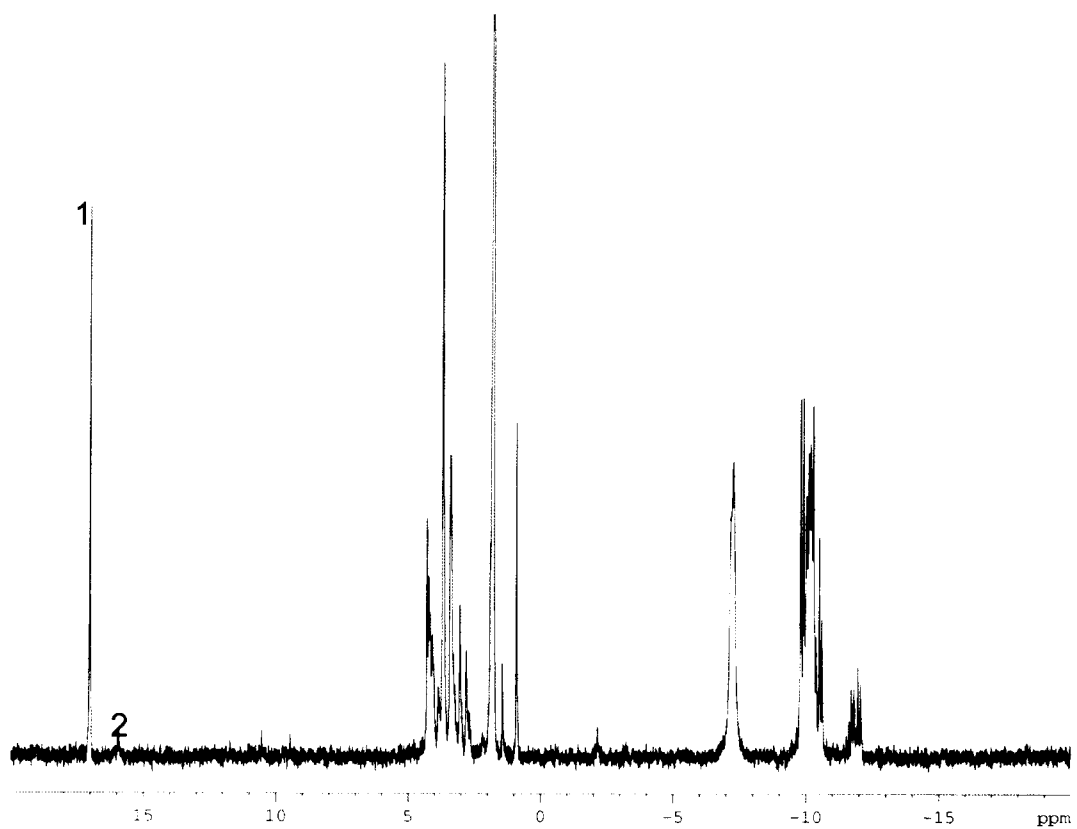
Figure 3.11: Peak at 11-12 ppm at 2.5 hour from IFO injection in a tumour



3.5.4 ³¹P high resolution spectra

³¹P MRS was performed on 2 liver extracts and 2 tumour extracts obtained following the in vivo study i.e. at 2 -3 hours after ifosfamide administration. Apart from a small peak at 18 ppm relative to PCr, i.e. at the frequency of ifosfamide, no other ifosfamide related peaks were detected and therefore we did not perform any further experiments (Figure 3.12). This could be possibly explained based on the relative concentrations of ifosfamide and metabolites present in tumours as shown in Table 3.2. The concentration of parent ifosfamide in tumours as measured by HPLC-MS has been significantly higher than that of the other metabolites. Using the currently available extraction technique and high-resolution spectroscopic method, it was not possible to obtain adequate signals from ifosfamide metabolites.

Figure 3.12: In vitro ^{31}P MR spectrum obtained from a liver



1: MNPA (reference); 2: signal possibly related to IFO.
This extract is at low pH and correct assignment to other peaks is difficult.

3.5.5 HPLC-MS data

Data were obtained from 17 liver extracts and 10 tumour extracts. Concentrations of ifosfamide, 2-DCI, 3-DCI, keto ifosfamide and carboxyifosfamide were estimated. The mean concentration of ifosfamide in liver was 1131 ± 120 nmol/g and in tumour was 910 ± 86 nmol/g. The mean concentration of 2-DCI in liver was 150 ± 43 nmol/g and in the tumour was 93 ± 14 nmol/g. The mean concentration of 3-DCI in liver was 237 ± 88 nmol/g and in the tumour was 137 ± 36 nmol/g. The mean concentration of carboxyifosfamide in liver was 244 ± 33 nmol/g and in the tumour was 33 ± 9 nmol/g. The mean concentration of keto ifosfamide in liver was 19 ± 2 nmol/g and in tumour was 48 ± 25 nmol/g. Table 3.1 and Table 3.2 show the concentrations of the various metabolites in the liver and tumour extracts respectively.

The effect of tumour volume on concentration of ifosfamide as estimated by HPLC-MS was tested using regression analysis. A positive correlation was obtained between tumour size and ifosfamide concentration ($R^2 = 0.59$, $P = 0.01$) (Figure 3.13).

Table 3.1: Concentrations of ifosfamide and its metabolites in the liver extracts based on HPLC-MS measurements in nmol/g wet weight.

Liver of animal no.	Time from injection (min)	2-DCI	3-DCI	Ifosfamide	Keto	CXI
1	180	110	122	1120	18	185
2	240	195	223	1352	26	289
3	190	132	135	1268	ND	260
4	190	44	64	716	8	224
5	190	98	175	289	16	208
6	190	181	442	1292	38	368
7	150	141	138	1320	16	228
8	225	780	288	1560	34	374
9	240	137	162	1640	17	179
10	200	37	38	744	ND	45
11	180	105	123	1528	14	262
12	195	145	1576	1400	10	192
13	135	106	124	1124	25	172
14	190	4	4	311	12	16
15	230	162	159	1243	35	287
16	190	Not done	239	2000	14	628
17	190	18	18	318	4	230
Mean± S.E.M	195±7	150±43	237±88	1131±120	19±2	244±33

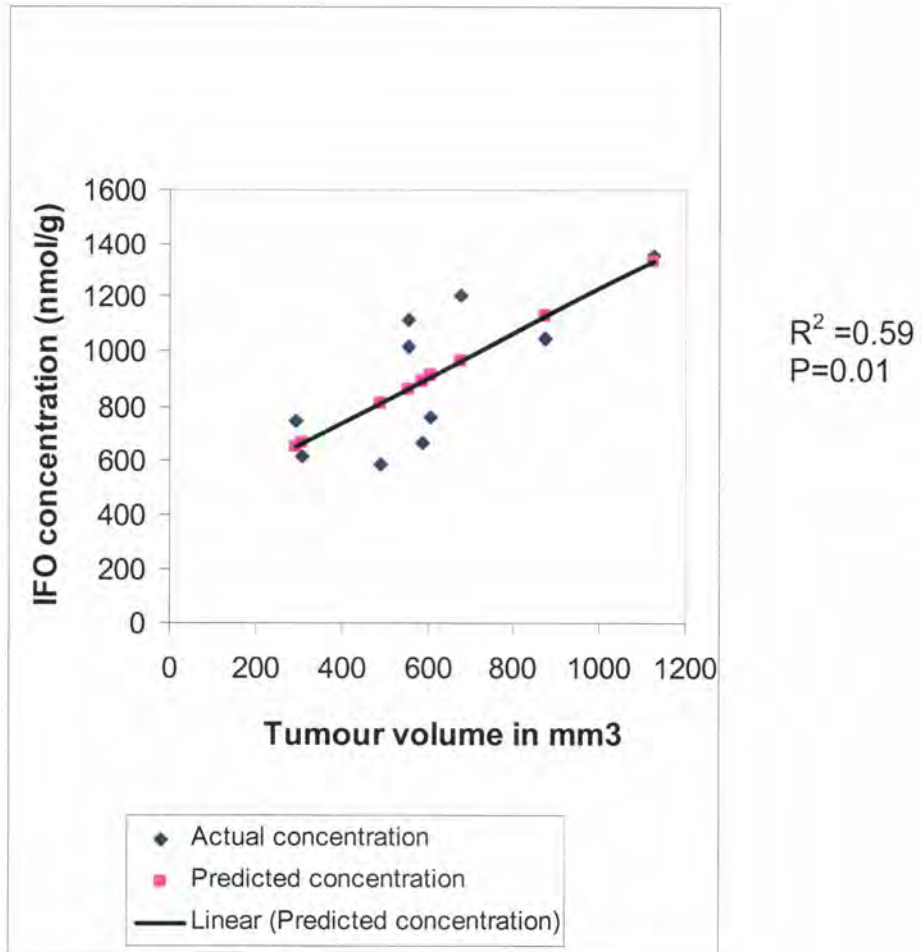
ND: Not determinable, 2-DCI: 2-dechloroethylifosfamide, 3-DCI: 3-dechloroethylifosfamide, Keto: keto ifosfamide, CXI: carboxyifosfamide

Table 3.2: Concentrations of ifosfamide and its metabolites in tumour extracts based on HPLC-MS measurements in nmol/g wet weight.

Tumour from animal no.	Time from injection (min)	2-DCI	3-DCI	Ifosfamide	Keto	CXI
7	150	99	100	1360	22	36
8	225	148	144	760	29	14
9	240	135	134	1200	39	19
10	200	43	444	660	267	13
11	180	107	98	1016	46	27
12	195	132	133	1044	13	ND
13	135	113	110	1116	36	20
14	190	7	43	612	17	ND
15	230	96	104	745	7	36
17	190	48	56	583	6	96
Mean ± S.E.M	194±10	93±14	137±36	910±86	48±25	33±9

ND: Not determinable, 2-DCI: 2-dechloroethylifosfamide, 3-DCI: 3-dechloroethylifosfamide, Keto: keto ifosfamide, CXI: carboxyifosfamide

Figure 3.13: Relationship of tumour volume with ifosfamide concentration as obtained by HPLC-MS.



3.5.6 Comparison of HPLC-MS data between liver and tumour

It was possible to compare concentrations of ifosfamide and its metabolites in livers and tumours in 10 animals. All metabolites except keto-ifosfamide were found to be higher in the liver extract when compared to tumour extract (Table 3.3).

Dechloroethylation pathway: Higher concentration of metabolites of dechloroethylation pathway (2-DCI and 3-DCI) were found in livers as compared to tumour in 7 out of 10 animals. The average ratio of liver metabolites/ tumour metabolites was 1.7 ± 0.6 . However, the difference was not statistically significant ($p=0.27$).

Ifosfamide: Higher concentrations of the parent drug were detected in the liver in 7/10 animals. The mean ratio of liver to tumour was 1.3 ± 0.2 . The Difference was not statistically significant ($p=0.1$).

Keto-ifosfamide: Keto-ifosfamide was present in higher concentrations in the tumours in 8 out of 10 evaluable samples. This difference was however not statistically significant ($p=0.26$). In one liver extract it was undetectable. The average tumour keto-ifosfamide to liver keto-ifosfamide ratio was 8 ± 6.5 .

Carboxyifosfamide: The concentration of carboxyifosfamide was significantly higher in liver compared to tumour in all the 10 animals for whom data were available ($p=0.0004$). In 2 tumours it was undetectable. The mean ratio of liver/tumour concentration was 12.7 ± 4.5 .

Table 3.3: Concentrations of ifosfamide and its metabolites in paired liver and tumour extracts in nmol/g wet weight.

Tissue	2-DCI	3-DCI	Ifosfamide	Keto	CXI
Liver animal 7	141	138	1320	16	228
Tumour animal 7	99	100	1360	22	36
Liver animal 8	780	288	1560	34	374
Tumour animal 8	148	144	760	29	14
Liver animal 9	137	162	1640	17	179
Tumour animal 9	135	134	1200	39	19
Liver animal 10	37	38	744	ND	45
Tumour animal 10	43	444	660	267	13
Liver animal 11	105	123	1528	14	262
Tumour animal 11	107	98	1016	46	27
Liver animal 12	145	1576	1400	10	192
Tumour animal 12	132	133	1044	13	ND
Liver animal 13	106	124	1124	25	172
Tumour animal 13	113	110	1116	36	20
Liver animal 14	4	4	311	12	16
Tumour animal 14	7	43	612	17	ND
Liver animal 15	162	159	1243	35	287
Tumour animal 15	96	104	745	7	36
Liver animal 17	18	18	318	4	230
Tumour animal 17	48	56	583	6	96
Mean±S.E.M	1.7±0.6		1.3±0.2	1.15±0.46	12.7±4.5
liver/tumour ratio					
P value	0.27		0.1	0.26	0.0004

ND: Not determinable, 2-DCI: 2dechloroethylifosfamide, 3-DCI: 3-dechloroethylifosfamide, Keto: keto- ifosfamide, CXI: carboxyifosfamide.

Concentrations are expressed as nmol/g wet weight.

3.5.7 Correlation between HPLC-MS and MRS data

Relationship between time from ifosfamide injection and concentration of metabolites obtained by HPLC-MS

Time after ifosfamide injection to excision of the tumour was compared with concentration of metabolites obtained by HPLC-MS. There was no correlation between time from ifosfamide injection and the concentrations of ifosfamide or metabolites detected in the liver or tumour extracts. This is not surprising considering that majority of the samples were obtained at about 3 hours from ifosfamide injection.

We compared half-life, maximum amplitude of IFO as detected by in vivo MRS (C_{MAX}) and IFO amplitude at the end of the experiment with concentrations of ifosfamide and its metabolites detected by HPLC-MS. Table 3.4 compares data obtained by in vivo MRS, with ifosfamide concentration as obtained by HPLC-MS in liver and Table 3.5 gives details of tumour dimensions, C_{MAX}, T_{MAX}, half-life, final amplitude of IFO, and concentration of IFO obtained by HPLC-MS in tumours. No correlation was obtained between data obtained by spectroscopy and HPLC-MS (see Figures 3.14 and 3.15).

Table 3.4: Correlation of data obtained by in vivo MRS with ifosfamide concentration as obtained by HPLC-MS in liver

Animal No	CMAX	TMAX (min)	Half-life (min)	Final IFO amplitude	IFO concentration by HPLC-MS (nmol/g wet weight)
1	36.47	30-60	102	14.1	1120
3	48.59	60-90	46	10.7	1268
4	28.86	90-120	169	19.2	716
5	30.65	30-60	96	10.1	289
6	41.64	90-120	133	20.8	1292

N.B. CMAX, TMAX, Half-life and final IFO amplitude are obtained using MRS.

Table 3.5: Correlation of data obtained by in vivo MRS with ifosfamide concentration as obtained by HPLC-MS in tumour

Animal No	Tumour volume (mm³)	CMAX	TMAX (min)	Half-life (min)	Final IFO amplitude	IFO conc. by HPLC-MS (nmol/g wet weight)
7	1124	50.79	60-90	346	18.79	1360
8	609	28.13	0-30	166	11.24	760
9	676	31.68	60-90	205	21.32	1200
10	590	26.39	30-60	147	14.92	660
12	873	60.68	0-30	405	43.46	1044
13	554	48.56	0-30	50	12.55	1116
14	307	28.00	0-30	238	23.66	612
15	296	31.03	0-30	385	27.61	745
17	488	22.04	0-30	86	7.63	583

N.B. CMAX, TMAX, Half-life and final IFO amplitude are obtained using MRS

Figure 3.14 :Relationship of half-life as obtained by in vivo ^{31}P MRS with ifosfamide concentrations as obtained by HPLC-MS

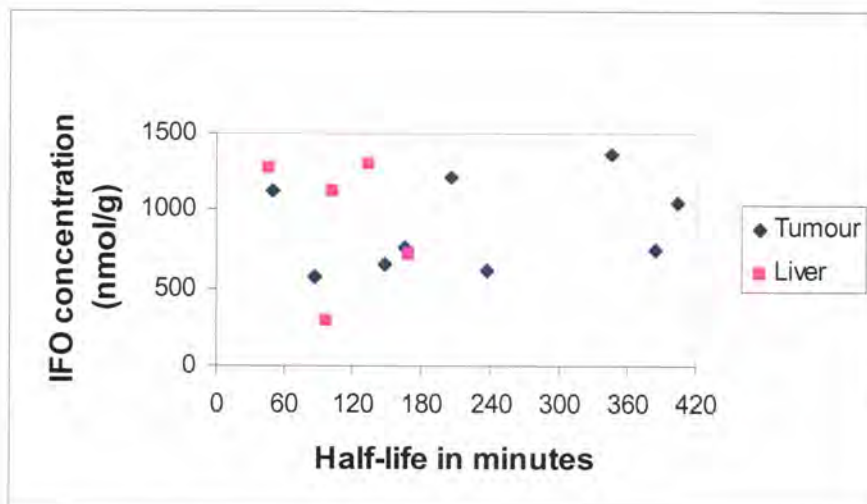
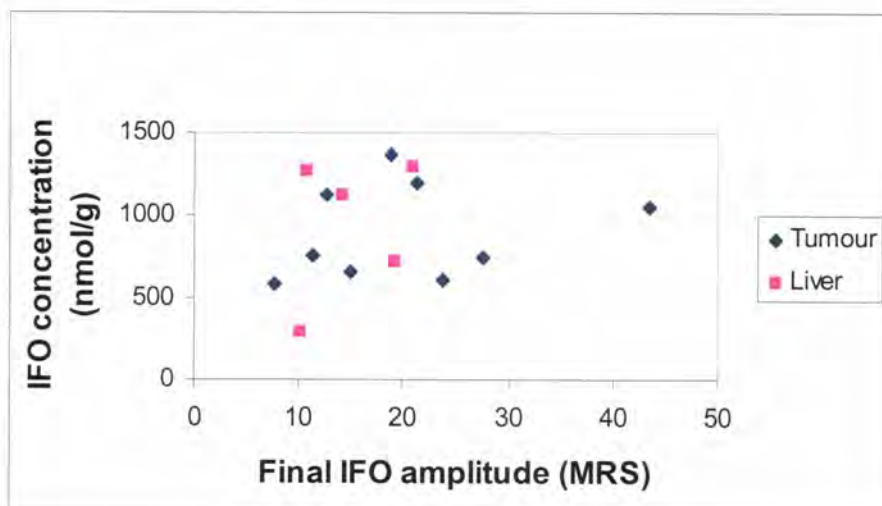


Figure 3.15: Relationship of final amplitude of ifosfamide measured by in vivo ^{31}P MRS with concentration as obtained by HPLC-MS



3.6 Discussion

In our MRS experiments we have used a non-invasive means to gain information regarding the tissue pharmacokinetics of ifosfamide. For the liver experiments, the MRI scans confirmed that the liver occupied a large proportion of the surface coil. For tumour experiments, MRI scans were not performed, as it was possible to place the mouse so that the superficial tumour was directly on the coil. The tumour diameters generally ranged from 10-15 mm as shown in Table 3.5. The surface coil had a diameter of 12mm and as these scans were non-localised some signal could have been obtained from the overlying skin. The advantage of using nude mice is that the skin is very thin and contains a smaller amount of muscle when compared to normal mice or rats and therefore contamination from muscle should be small.

The non-decoupled ^{31}P MRS spectrum from parent ifosfamide has a complex multiplet pattern. This is caused by J-coupling with neighbouring ^1H nuclei (through two bonds to the $-\text{NH}$ hydrogen and through 3 bonds to three sets of CH_2 groups). This may partly explain the large width of the 'ifosfamide' peak seen *in vivo*. However, we can not exclude the possibility that it is made of more than 1 metabolite. The fact that only a single peak was observed by using perchloric acid extraction and high resolution MRS suggests that at these time points (approximately 2-3 hours from injection of ifosfamide), any other metabolite could have been at very low concentration.

From Tables 3.1 and 3.2 it is evident that the concentrations of 2-DCI, 3-DCI, keto-ifosfamide and carboxy-ifosfamide as measured by HPLC-MS at 2-3 hours from IFO injection are significantly lower in tissues when compared to

the concentration of ifosfamide. Therefore, considering the small size of the peak that was observed in the ifosfamide region, it is not surprising that we could not confidently identify other metabolites in vitro.

Using HPLC-MS it was possible to measure the concentrations of several inactive metabolites. The active metabolites or those that yield active metabolites i.e. 4-hydroxyifosfamide, aldo-ifosfamide and the ifosfamide mustard were not quantified as they are very labile and extraction from tissue is difficult.

Unlike cyclophosphamide, about 50% of IFO is metabolised by the dechloroethylation pathway [Boddy et al., 1995b]. We can assume that quantifying the inactive metabolites would give an indirect indication of the active metabolites.

The measured carboxyifosfamide concentration was significantly higher in liver extracts compared to tumour extracts. This supports the argument that the peak observed at 21 ppm in 2 out of our 5 animals was carboxyifosfamide. The enzyme aldehyde dehydrogenase, which converts aldo-ifosfamide to carboxyifosfamide, is more active in liver than tumour. Some tumour cell lines may have increased aldehyde dehydrogenase activity leading to chemo-resistance [Brock, 1989]. Although there are no studies related to ifosfamide, there are studies to suggest that cellular levels of aldehyde dehydrogenase could be potential predictors of therapeutic responses to cyclophosphamide based chemotherapy, for example in breast cancers [Sladek et al., 2002].

Although the concentration of IFO and most of its metabolites were higher in liver as compared to tumour, keto-ifosfamide was higher in tumours when

compared to liver in over two-thirds of animals. This is consistent with the observation that in 2 tumour experiments in vivo signals were identified at 11-12 ppm. In analysis of human body fluids by NMR, a signal 4.5 downfield from IFO was thought to be related to Keto-IFO [Martino et al., 1992; Martino et al., 1992] .

Marked intra-subject variations in the metabolism of both IFO and cyclophosphamide have been previously described [Boddy et al., 1992; Boddy et al., 1993; Boddy et al., 1995b; Boddy et al., 1996a; Yule et al., 1995]. This could reflect the variability in the levels of enzymes necessary for its metabolism. Variations in toxicity and efficacy could result due to the differences in its metabolism. From our data, we have seen variations in both half-life as detected by MRS and concentrations of metabolites as detected by HPLC-MS.

No relationship was observed between the final amplitude of IFO and concentration of IFO as obtained by HPLC-MS. A possible reason would be the small amount of contamination from overlying skin. Some loss during transportation or extraction of the in vitro samples cannot be ignored.

Half-life:

The half -life of ifosfamide has been previously studied in animal models and in clinical settings. Clinical studies rely on blood sampling and sampling of other body fluids to estimate decay of the drug. For example a half-life which ranged from 2.4 to 5 hours was measured in plasma in adults with bronchogenic carcinoma after short infusions of 1.5 g/m²/day for 3 days [Lind et al., 1989a]. In adults with breast cancer, in whom IFO was administered as a 24 hours continuous infusion at 5 g/m², the half-life ranged from 2.67 to

6.69 hours [Boddy et al., 1995b]. Half-life was also measured in 8 children receiving 5g/ m²/day of ifosfamide as a 24-hour infusion. The elimination half-life ranged from 2.9-5.2 hours [Pinkerton et al., 1985]. Table 3.6 gives a summary of half-life in clinical studies. Various studies have compared different IFO doses and schedules of administration as well as inter subject variations between courses.

Using MRS, the half-life of IFO in a rat model has been previously studied [Rodrigues et al., 1997]. The effect of carbogen breathing on the uptake of the drug in both liver and GH3 prolactinoma tumour was also studied. The half-life of IFO in liver was calculated to be 59±10 minutes without carbogen breathing and 71±16 minutes after carbogen breathing. A higher uptake of IFO was observed in the tumour in rats breathing carbogen. The half-life for elimination in tumours was reported to be 208±25 minutes in animals not breathing carbogen and 215±27 minutes for animals breathing carbogen. In our experimental animals the half-life of IFO in liver was longer (109±20 minutes), but comparable in tumour (225±43 minutes).

We found a positive correlation between half-life and size of tumour. Xenograft studies have shown a decrease in blood flow with increasing tumour volume [Okazaki et al., 1982; Lyng et al., 1992]. It is therefore possible that decreased blood flow causes a trapping of the drug in tumour thereby increasing the half-life. This is also supported by the observation that bigger tumours had higher ifosfamide concentration as measured by HPLC-MS. TMAX was delayed (60-90 minutes) in the largest tumour, possibly due to slow uptake by the poorly vascularised tumour. This observation could have an implication for scheduling of ifosfamide in clinical situations.

Table 3.6: Summary of half-life measurements of IFO obtained from clinical studies

Reference	Regimen	Number of patients	Elimination half-life (h)	Comments
[Allen and Creaven, 1975]	5 g/m ² /1h	5	15.2	Single dose of IFO
[Nelson et al., 1976]	1.6-2.4 g/m ² /dx3	3	6.9	Divided doses of IFO
[Cerny et al., 1986]	1g/d oral, iv	7	5.9	100% bioavailability
	2g/d oral, iv	7	5.3	
[Lind et al., 1989b]	1.5g/ m ² /0.5h x5			Half-life higher in obese patients
	Obese adults	4	6.4	
	Normal adults	12	5.0	
[Lind et al., 1990b]	1.5g/ m ² /0.5h x5			Positive correlation between half-life and age. No effect on auto-induction
	>60 years	11	6.0	
	<60 years	9	3.8	
[Lewis et al., 1991]	5 g/m ² /0.5h	6	5.4	Comparison between two schedules
	5 g/m ² /24h	4	4.5	
[Boddy et al., 1993]	9 g/m ² /72h	16	2.1	Paediatric study
[Boddy et al., 1995a]	9 g/m ² /72h	17	2.1	Paediatric study. Comparison between two schedules
	3 g/m ² /1hx3	17	3.2	
[Boddy et al., 1995b]	5 g/m ² /24h	15	4.7	Correlation with response
[Boddy et al., 1996a]	9 g/m ² /72h	11 (cycle 1)	2.1	Paediatric study. Intra-subject variation in metabolism studied.
		11 (cycle 2)	3.1	
[Singer et al., 1998]	3 g/m ² /h	14	6.9	No significant difference in the pharmacokinetics between 2 schedules.
	3 g/m ² /120h	14	7.0	
[Passe et al., 1999]	6 g/m ² /120h	12	5.2	Paediatric study

3.7 Summary and future directions

Several pharmacokinetic studies have been performed previously measuring concentrations of IFO or its metabolite in blood. These however, do not give a true estimate of uptake by tissues. We have attempted to measure elimination pharmacokinetics i.e. half-life non-invasively in liver and tumour in xenografted mice using ^{31}P MRS. It has been possible to demonstrate signal relating to some metabolites, but not all, due to the lower sensitivity of MRS when compared to HPLC-MS. Inactive metabolites could be detected in both livers and tumour extracts using HPLC-MS techniques. Comparison of metabolites in liver and tumours suggests that carboxyifosfamide is always higher in livers possibly related to higher levels of aldehyde dehydrogenase enzyme. The dechloroethylation pathway is predominant in liver whereas production of keto-ifosfamide may be more active in tumour. No biochemical-spectroscopic correlation could be obtained. The variability in half-life in liver and tumours obtained from our data confirms the inter-individual variations observed in pharmacokinetic analysis of sera. Longer half-life (as estimated by MR spectroscopy) and higher concentration of ifosfamide (as estimated by HPLC-MS.) were observed in larger tumours. Future prospective clinical studies should be done to assess whether half-life in liver or tumour correlates with response to chemotherapy. This could help identify potential patients who are non-responders to ifosfamide and help tailor therapy.

CHAPTER 4

MAGNETIC RESONANCE SPECTROSCOPY (MRS) TO ASSESS RESPONSE TO CHEMOTHERAPY IN A PAEDIATRIC EMBRYONAL RHABDOMYOSARCOMA MODEL.

4.1 Introduction

³¹P MRS is being evaluated as a potential tool for monitoring early response in a variety of tumour types. As detailed in Chapter 1, there are very few published studies relevant to paediatric tumours.

This study was designed to evaluate the role of MRS in assessing response to chemotherapy using a mouse tumour model clinically relevant to paediatric oncology. For the study, the rhabdomyosarcoma cell line (RD) was used [McAllister et al., 1969]. The technique to grow this tumour in nude mice has been previously established in our institution [HA Cocker, 2001]. Rhabdomyosarcoma is a highly malignant tumour and thought to arise from primitive mesenchymal cells committed to develop into striated muscle. It accounts for 4-8% of all solid tumours in children [Carli M et al., 1997]. Approximately 50 new cases of rhabdomyosarcoma are diagnosed every year in the U.K. in children under 15 years of age. A remarkable aspect of rhabdomyosarcoma cells grown in nude mice is that they retain their ability to differentiate [Nanni et al., 1989].

4.2 Aims and objectives

- i. To investigate the role of MRS to define early markers of tumour response in vivo using a paediatric tumour model.
- ii. To evaluate the metabolic changes in ifosfamide- and vehicle-treated tumours using in vivo ^{31}P MRS.
- iii. To complement in vivo findings with in vitro high-resolution ^1H and ^{31}P MRS on tumour extracts.

4.3 Materials and methods

The methods for tissue culture, tumour propagation, tumour volume measurements and animal preparation for in vivo experiments are described in Chapter 3.

4.3.1 Ifosfamide injection

An intra-peritoneal line primed with ifosfamide was established prior to placing the animal in the magnet. Ifosfamide was injected whilst the animal was still in the magnet after an initial localised ^{31}P MR spectrum had been acquired. We used a dose of 400 mg/kg in the first five mice as this dose was used in the pharmacokinetic study described in Chapter 3. Four animals died due to toxicity and, therefore, for subsequent experiments the ifosfamide dose was reduced to 250 mg/kg. For analysis purposes, only animals that were given 250 mg/kg of ifosfamide have been included. This dose is comparable to approximately 7.5 g/m^2 , within the dose range used in clinical practice for this tumour ($6\text{-}9 \text{ g/m}^2$).

4.3.2 Saline injection

For vehicle- treated animals (control group), an intra-peritoneal line primed with saline was established prior to placing the animal in the magnet. Saline was injected after the first localised spectrum was acquired.

4.3.3 *In vivo* experiments

The experimental conditions for *in vivo* ^{31}P MR spectroscopy are described in Chapter 3. Image selected *in vivo* spectroscopy (ISIS) of tumour was obtained using an adiabatic sincos pulse, a TR of 3 seconds and 600 scans. For each animal ISIS spectra were obtained pre, 30 minutes and 7-9 days post IFO or saline treatment.

The IFO treated animals were given the uro-protectant MESNA (Urometexan, 2-mercaptoethane sulphonate) at 250 mg/kg intra-peritoneally after the completion of spectroscopic measurements on Day 1.

4.3.4 Processing of tumours after spectroscopy experiments

The animal was killed by cervical dislocation and the tumour was excised. One half of the tumour was freeze clamped while the other half was freshly frozen. Both the samples were stored under liquid nitrogen.

Procedure for extraction of the tumour metabolites prior to high resolution

MRS

The freeze clamped samples were weighed and homogenised under liquid nitrogen. A volume of cold 6% perchloric acid equal to 4 times the weight of the tissue was added to the homogenised sample and allowed to stand on ice for 20 minutes. The sample was centrifuged at 2000 revolutions per minute for 10 minutes at 4°C and the supernatant was separated and neutralised to a pH of 7 using varying concentrations of potassium hydroxide and perchloric acid. The neutralised sample was again centrifuged and the supernatant was freeze-dried.

4.3.5 In vitro ^1H and ^{31}P MRS experiments

1ml of D_2O was added to the freeze-dried sample and centrifuged at 10,000 rpm for 5 minutes. 0.5ml was transferred to a 5mm NMR tube and 50 μl of 5 mM TSP (3-trimethylsilyl-2,2,3,3-tetradeutero propionate) was added as a chemical shift reference for quantification in ^1H MRS. 25 μl of 10 mM MNPA (methylene diphosphoric acid) was added as reference for ^{31}P MRS. The experiments were performed using a Bruker 11.74T magnet.

4.3.6 Data analysis of in vivo spectra

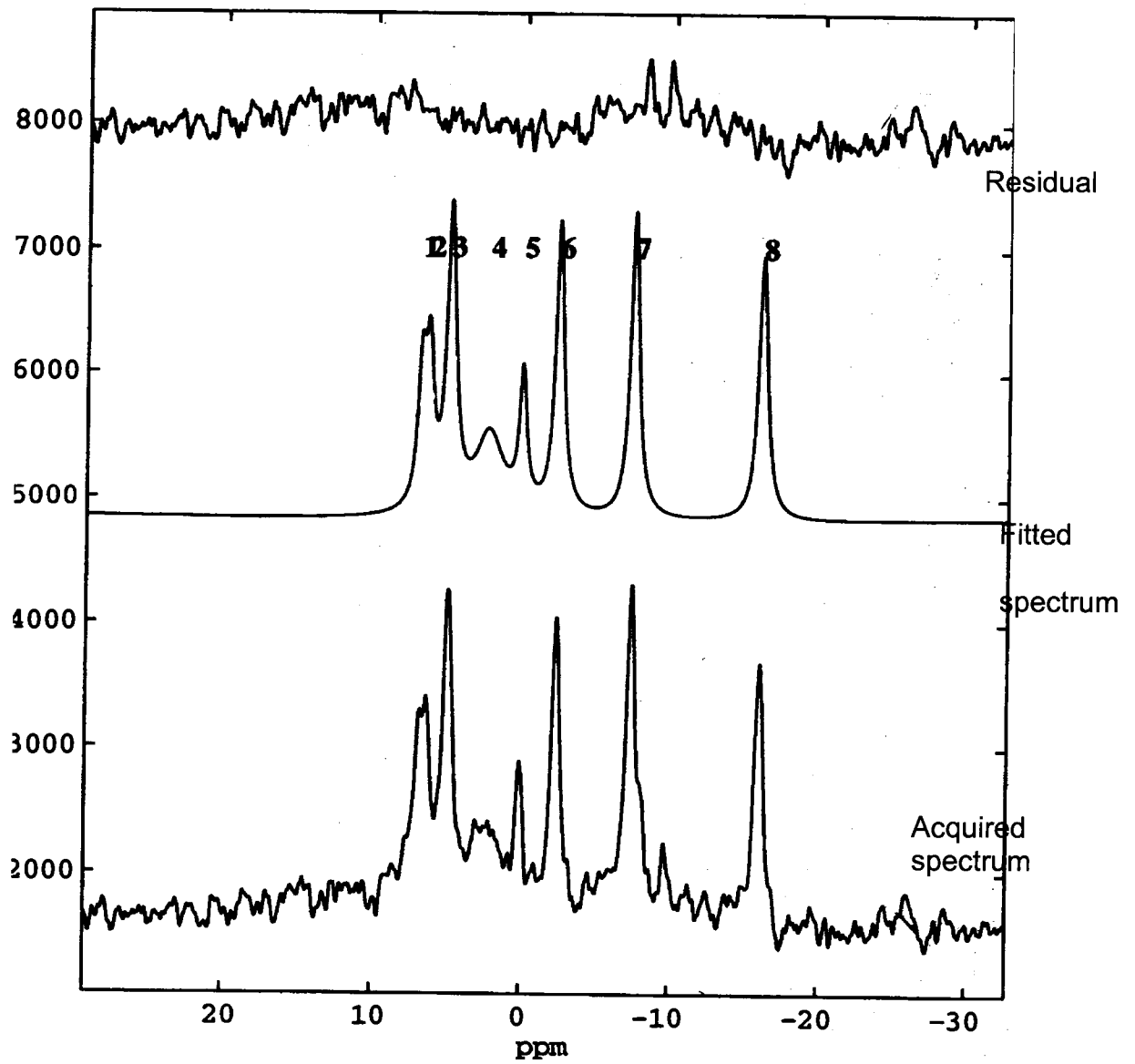
In vivo ^{31}P MR spectra were processed using MRUI (Magnetic Resonance User Interface). The spectral data was analysed using the VARPRO (VARiable PROjection) algorithm from within MRUI along with algorithm called AMARES (advanced method for accurate, robust, and efficient spectral fitting) [Vanhamme et al., 1997]. For intracellular pH (pH_i) calculations, the chemical shift difference between Pi and α -NTP resonances were used.

4.3.7 Data analysis of in vitro spectra

The spectral line heights were measured and concentrations of metabolites were calculated relative to the known concentration of the reference agent [Moreno et al., 1998]. This was obtained by dividing the spectral height of the metabolite with the spectral height of the known metabolite i.e. the reference agent. This was multiplied by the concentration of the reference agent.

Metabolites were expressed in $\mu\text{mol/g}$ of wet tissue.

Figure 4.1: An example of the results of the analysis of ^{31}P MR spectra.



4.3.8 Response measurements

Responses were measured by conventional methods.

Partial response was defined as decrease in the size of the tumour by $\geq 50\%$.

Stable disease was defined as change in tumour volume $\pm 25\%$.

Objective response was defined as decrease in volume $> 25\%$ and $< 50\%$.

Progressive disease was defined as tumour increase by $> 25\%$.

4.3.9 Statistical analysis

Data were expressed as mean \pm standard error of the mean (S.E.M). Paired t-tests were used to compare temporal changes within the IFO-treated and control groups of tumours. Unpaired t-tests were used to compare differences between the IFO-treated and control groups at a specific time point and to compare the data obtained by in vitro spectroscopy.

4.4 Results

Experiments were performed in 26 tumour bearing nude mice. Five were excluded from the analysis because the higher IFO dose had been used. Out of the remaining 21 animals, 6 were injected with saline and of these complete data sets (at 3 time points) were available in 5 animals. Of the 15 animals receiving the lower (250 mg/kg) dose, complete data were obtained in 11 animals.

4.4.1 Comparison of volume change of tumours in IFO- treated Vs vehicle -treated (control) animals

An increase in the tumour volume was found in all control animals. On average the tumours had doubled in size when measured between Day 7 and 9 (range 65-153%, mean $102 \pm 19\%$) (Figure 4.3). In the IFO treated mice, stable disease was observed in 9 mice and 2 had progressive disease. Decrease in tumour volume was seen in 5 animals. Overall, the percentage change in tumour volume ranged from -22% to $+57\%$ (mean $7 \pm 7\%$) (Figure 4.2). This difference between the IFO-treated and the control group was statistically significant ($p=0.006$).

Figure 4.2: Tumour volumes in ifosfamide-treated animals on Day 1 & Day 8

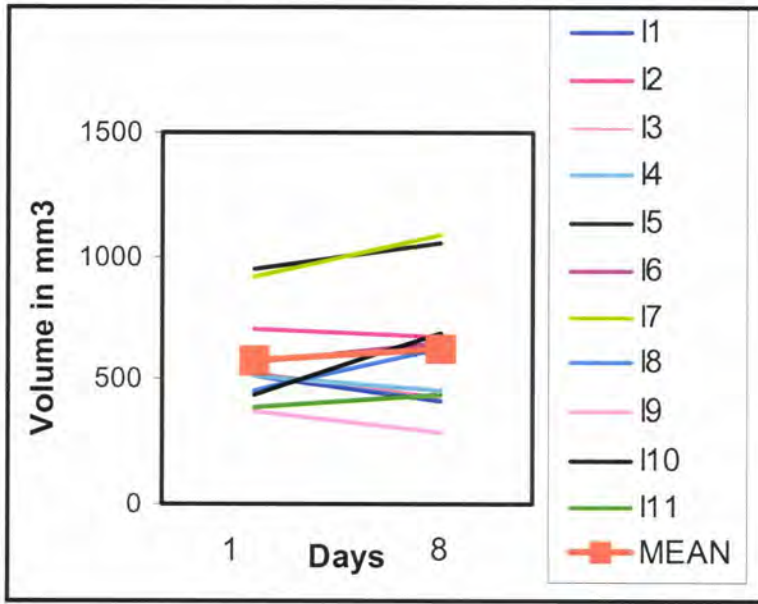
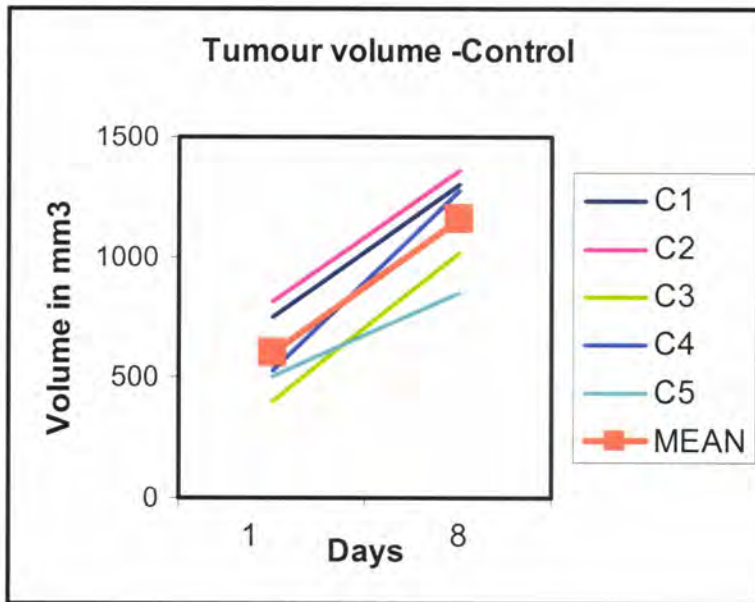


Figure 4.3: Tumour volumes in control animals on Day 1 & Day 8



4.4.2 In vivo ³¹P MRS data

Resonances for Phosphomonoesters (PME), inorganic phosphate (Pi), Phosphocreatine (PCr) and the three peaks of NTP i.e. γ -adenosine triphosphate (γ -NTP), α -adenosine triphosphate (α -NTP) and β -adenosine triphosphate (β -NTP) were readily identified in the in vivo ³¹P MR spectra. Phosphodiester (PDE) were observed in some spectra. However, the PDE peak had a broad line width and was often indistinguishable from noise and therefore is not included in the data analysis. For analysis purposes total phosphorus (Tot P) was calculated by addition of PME+Pi+PCr and the 3 NTP peaks. Intracellular pH was calculated by using the difference in chemical shift between Pi and α -NTP peaks.

For comparative analysis, ratios of following metabolites were obtained: β -NTP/Tot P, Pi/Tot P, PME/Tot P, PME/Pi, β -NTP/Pi, PME/ β -NTP. Ratios with PCr were not included in the analysis as characteristically malignant tumours lack PCr [Negendank, 1992] and the PCr signal seen could be due to contamination from the overlying skin or muscle. Signal at -2.5 ppm, which is characteristic of γ -NTP, could contain a contribution from the β -phosphate group of adenosine diphosphate and signal at -7.5 ppm could contain contributions from the α -phosphate groups of both ATP and adenosine diphosphate [Gadian D.G, 1982f]. Therefore ratios with α -NTP and γ -NTP have not been considered.

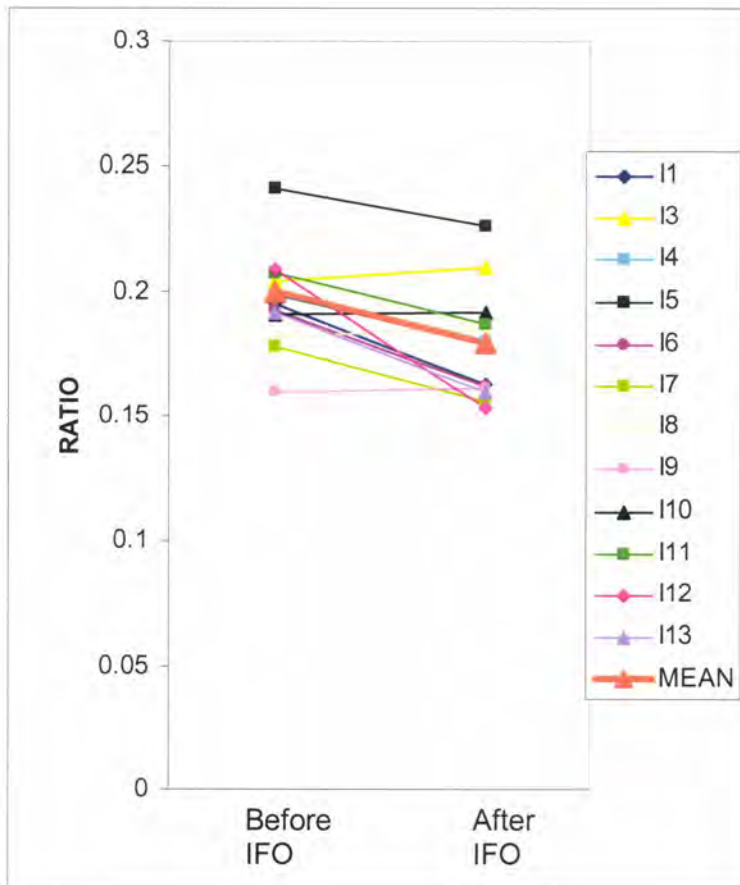
4.4.3 Effects of the treatment (IFO or saline) on ³¹P MRS ratios compared with pre-treatment values

A significant decrease in the β -NTP/Tot P and β -NTP/Pi ratios and an increase in PME/ β -NTP ratio were observed pre and post IFO (at 30 minutes) on Day 1 (Table 4.1). Figure 4.4 shows the changes in the β -NTP/Tot P ratio in the ifosfamide treated animals. A similar increase in the PME/ β -NTP ratio was also seen in control animals after saline injection. Comparison of ³¹P MR spectra obtained pre IFO and on Day 8 post IFO showed a significant increase in the ratio of PME/Pi and β -NTP/Pi. No significant change in the other ratios or pH was observed. In the control group no significant change was observed between Day 1 and Day 8

Table 4.1: Summary of the in vivo ³¹P MRS peak area ratios (mean ±S.E.M) for which, there was a significant change on Day 1 or Day 8 of treatment compared with the pre-treatment value

Metabolite ratio	Animal group	Pre (Day 1)	Post (Day 1)	Post (Day 8)	P value (Pre & Post Day 1)	P value (Pre & Day 8)
β-NTP/Total P	Ifosfamide	0.20±0.01	0.18±0.01	0.21±0.01	0.006*	0.14
	Control	0.18±0.01	0.17±0.01	0.18±0.01	0.21	0.81
β-NTP/Pi	Ifosfamide	1.48±0.18	1.22±0.19	2.18±0.29	0.04*	0.04*
	Control	1.12±0.25	1.05±0.26	0.87±0.06	0.46	0.32
PME/β-NTP	Ifosfamide	0.95±0.08	1.06±0.06	0.91±0.05	0.016*	0.39
	Control	0.92±0.08	1.06±0.10	0.94±0.03	0.014*	0.61
PME/Pi	Ifosfamide	1.38±0.17	1.22±0.12	1.85±0.16	0.46	0.04*
	Control	0.96±0.14	0.99±0.12	0.82±0.54	0.71	0.30

Figure 4.4: β -NTP/Tot P ratios in IFO-treated animals on day 1 (before and after IFO)—Acute effects



4.4.4 Comparison of changes in the ratios following IFO treatment with changes in ratios following saline treatment

Between Day 1 and Day 8 there were significant increases in the ratios of PME/Pi and β -NTP/Pi after IFO compared to control. Table 4.2 shows the mean \pm S.E.M of the change in the 2 metabolites obtained by subtracting Day 1 ratio from Day 8 ratio. Figures 4.5 and 4.6 show changes in β -NTP/Pi ratios in the 2 animal groups and Figures 4.7 and 4.8 show changes in PME/Pi ratios in the 2 animal groups. Figure 4.9 shows examples of in vivo ^{31}P MR spectra of ifosfamide-treated tumours on Day 1 and Day 8 and Figure 4.10 shows examples of in vivo ^{31}P MR spectra of saline-treated tumours on Day 1 and Day 8.

Table 4.2: Summary of significant changes in the ratios following IFO treatment with changes in the ratios following saline treatment (Day8-Day1 comparison)

Ratio	IFO-treated tumour (mean\pmS.E.M)	Saline-treated tumour (mean\pmS.E.M)	P value
PME/Pi	0.52 \pm 0.14	-0.23 \pm 0.15	0.021
β-NTP/Pi	0.85 \pm 0.33	-0.27 \pm 0.31	0.030

Figure 4.5: β -NTP/Pi ratios in IFO-treated animals on Day 1 and Day 8

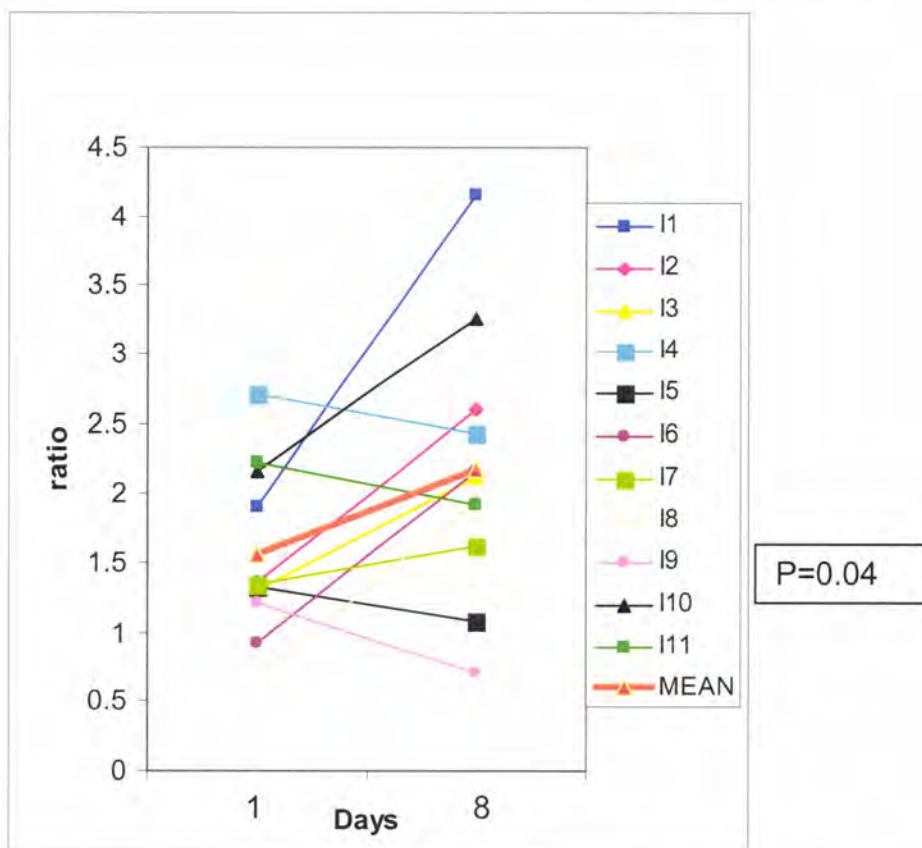


Figure 4.6: β -NTP/Pi ratios in control animals on Day 1 and Day 8

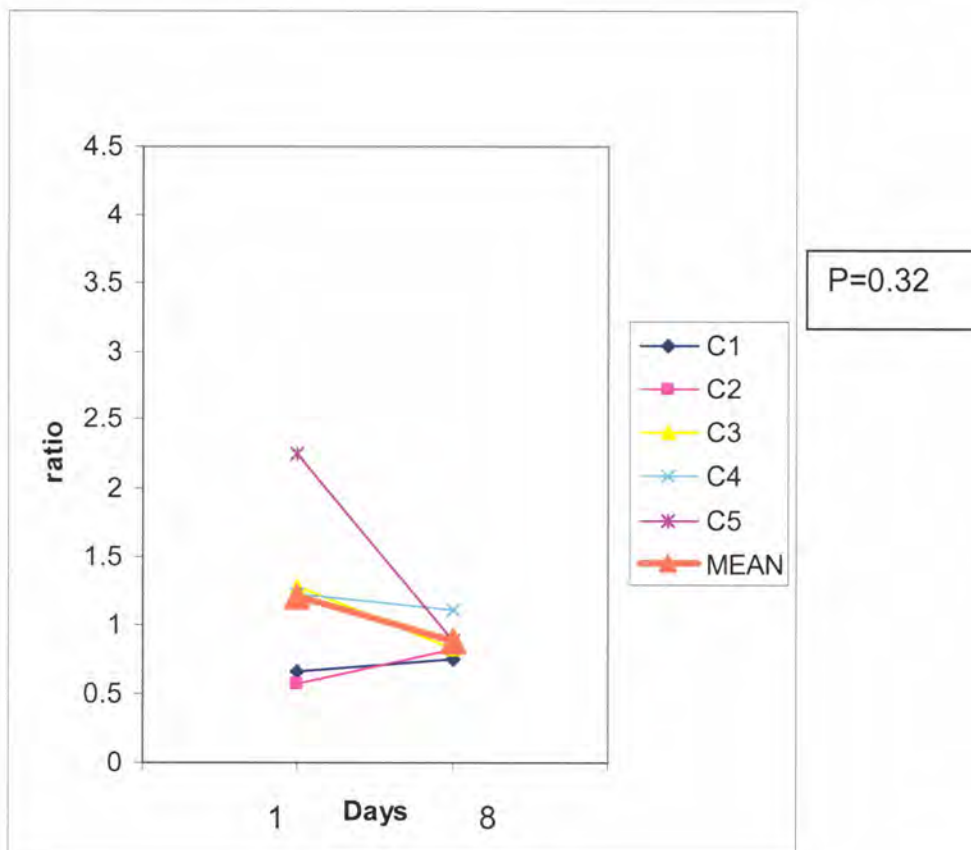


Figure 4.7: PME/Pi ratios in IFO-treated animals on Day 1 and Day 8

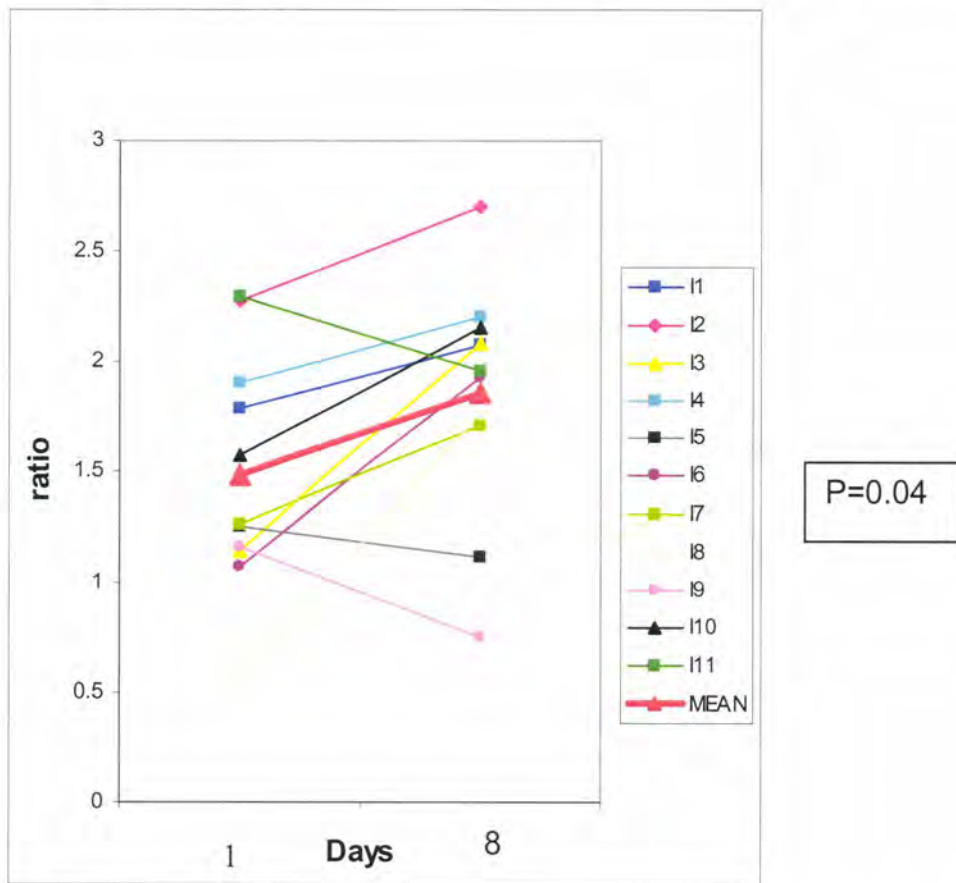
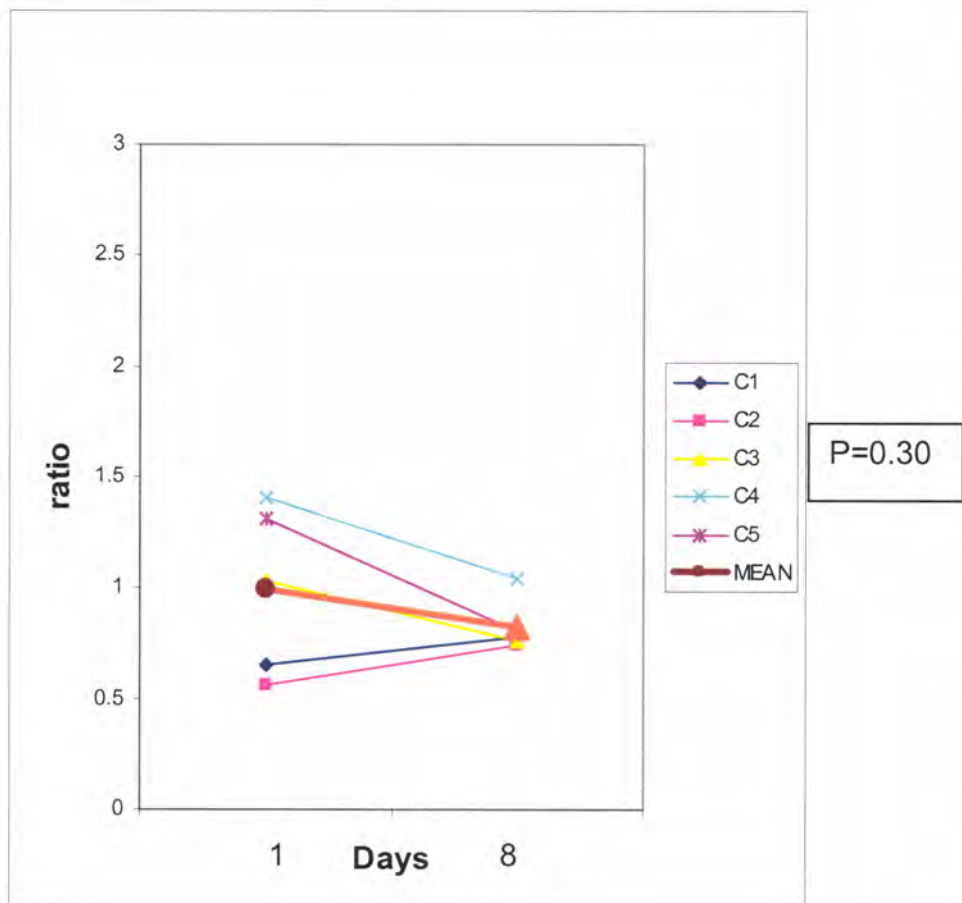


Figure 4.8: PME/Pi ratios in control animals on Day 1 and Day 8



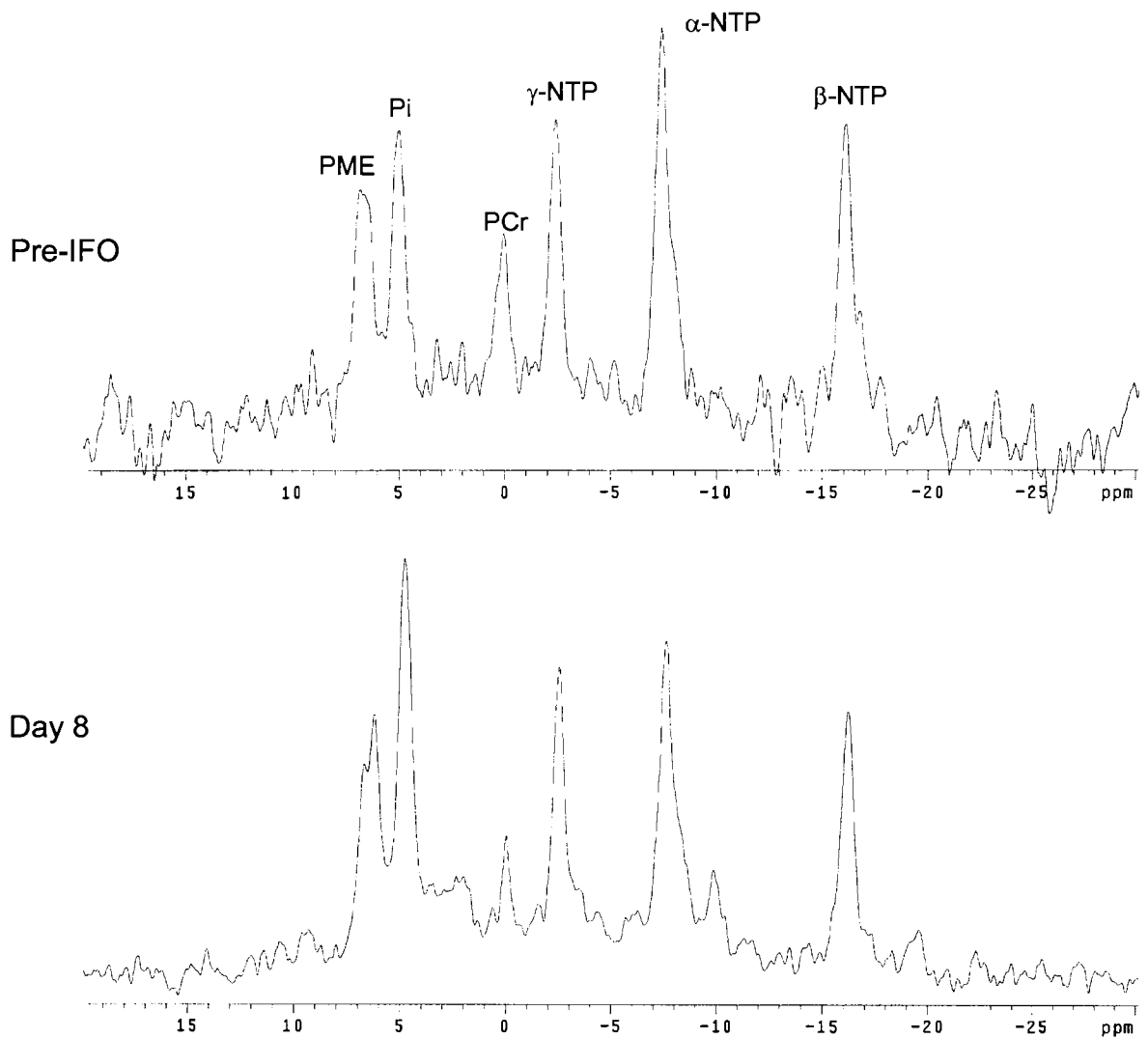


Figure 4.9: ISIS localised spectra of tumour treated with ifosfamide (Day 1 and Day 8).

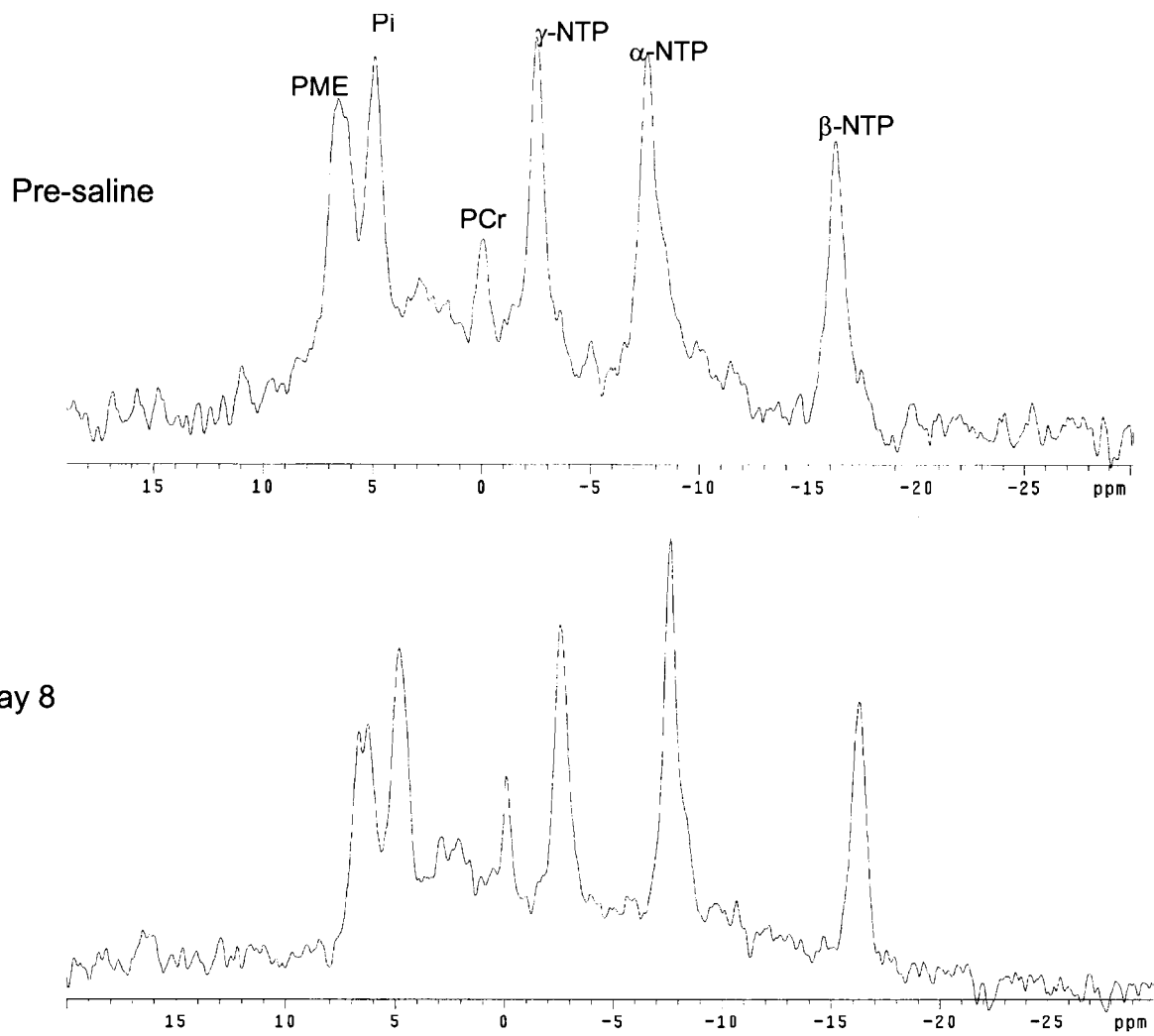


Figure 4.10: ISIS localised spectra of tumour treated with saline (Day 1 and Day 8)

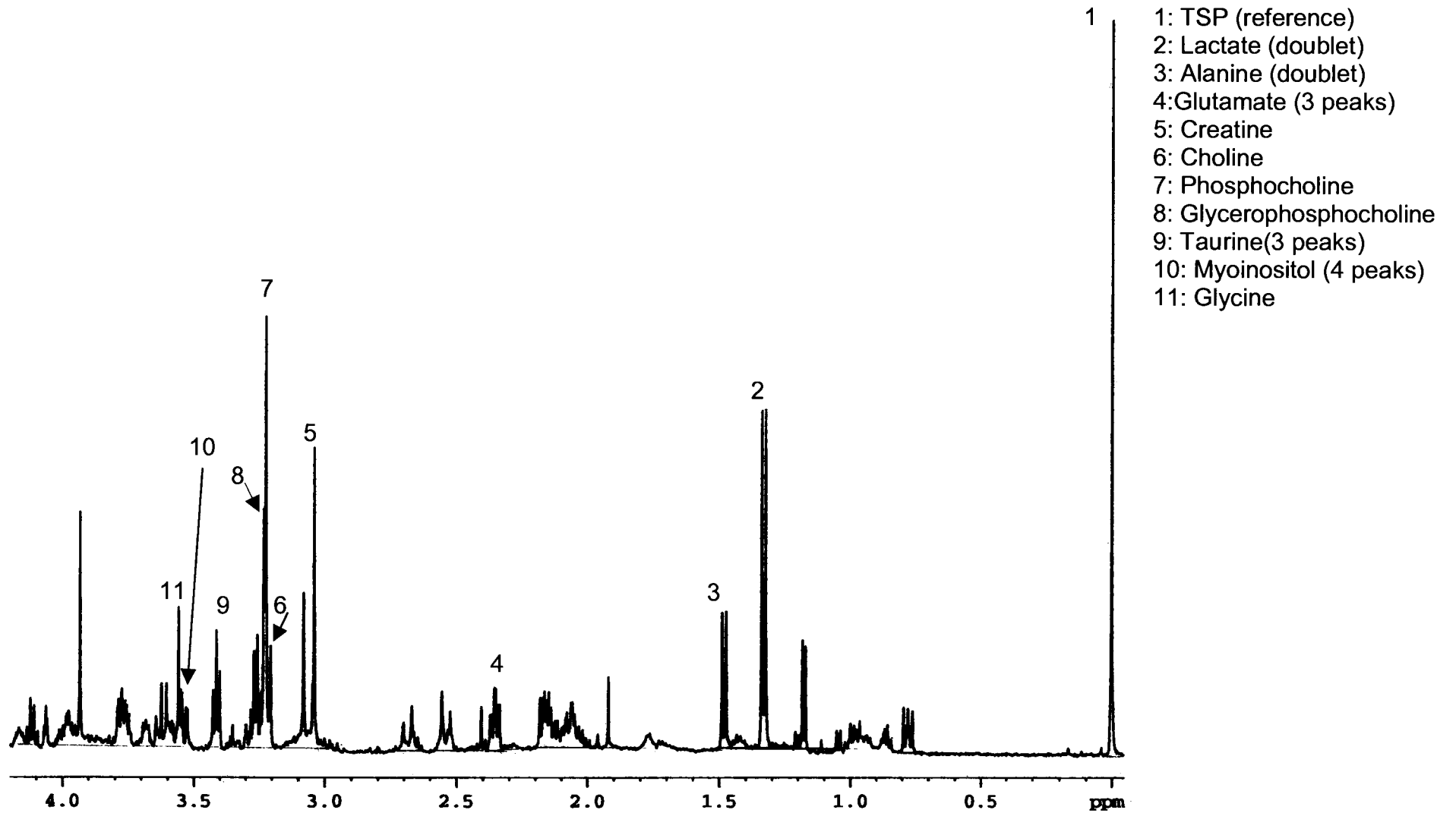
4.4.5 Comparison of in vitro ¹H MRS data between treated and control animals

Concentrations of lactate, alanine, glutamate, creatine, choline, phosphocholine, glycerophosphocholine, betaine, taurine, myoinositol, glycine were calculated from ¹H MRS spectra of the tumour extract on Day 8. Figure 4.11 shows an example of an in vitro ¹H MRS spectrum of a tumour extract. Comparison between IFO-treated and saline-treated tumours did not show any significant difference as shown in Table 4.3.

Table 4.3: Comparison of in vitro ¹H MRS data between treated and control animals expressed as mean ± S.E.M on Day 8.

	Treated (n=10) μmol/g wet weight	Control (n=5) μmol/g wet weight	P
Lactate	4.43±0.51	4.91±0.83	0.84
Alanine	1.78±0.28	1.89±0.52	0.64
Glutamate	2.11±0.32	1.90±0.74	0.70
Creatine	2.07±0.23	2.19±0.52	0.79
Choline	0.26±0.12	0.21±0.06	0.73
Phosphocholine	1.30±0.15	1.19±0.35	0.70
Glycerophosphocholine	0.71±0.07	0.47±0.11	0.12
Taurine	3.32±0.35	2.86±0.65	0.68
Myoinositol	1.99±0.22	1.56±0.23	0.64
Glycine	1.57±0.14	1.57±0.34	0.98

Figure 4.11: In vitro ^1H MR spectrum of a tumour extract



4.4.6 Comparisons of in vitro ³¹P MRS data between treated and control animals

Concentrations of PE, PC, Pi, Glycerophosphoethanolamine (GPE), Glycerophosphocholine (GPC) and PCr were determined from ³¹P MR spectra of the tumour extracts on Day 8. PE levels were found to be significantly higher in the IFO-treated group when compared with control tumours as shown in Table 4.4. Concentration of PME (as estimated by adding PE and PC) was significantly higher in the IFO-treated group when compared to the control group and the ratio of PE/PC was significantly higher in the IFO-treated group. There was no significant difference in the concentration of PDE (as estimated by adding GPE and GPC) between the two groups. Figures 4.12 and 4.13 show the in vitro ³¹P MR spectra obtained on Day 8 from IFO-treated and control tumour respectively.

Concentrations of phosphocholine and glycerophosphocholine were estimated by in vitro ¹H MRS and ³¹P MRS. Table 4.5 shows the concentrations of these metabolites by the two methods. A very close correlation was obtained.

Table 4.4: Comparison of in vitro ³¹P MRS data between treated and control animals expressed as mean ± S.E.M.

	Treated (n=10) μmol/g wet weight	Control (n=5) μmol/g wet weight	P
Phosphoethanolamine	2.09±0.23	0.97±0.23	0.005*
Phosphocholine	1.25±0.13	0.87±0.23	0.20
Inorganic Phosphate	2.51±0.43	1.96±0.87	0.59
Glycerophosphoethanolamine	0.24±0.04	0.19±0.06	0.45
Glycerophosphocholine	0.68±0.01	0.43±0.13	0.18
Phosphocreatine	0.20±0.05	0.10±0.05	0.17
PE/PC	1.72±0.16	1.19±0.09	0.01*
PE+PC (equivalent to PME in vivo)	3.34±0.33	1.84±0.45	0.02*
GPC+GPE (equivalent to PDE in vivo)	0.92±0.14	0.62±0.28	0.24
PE+PC/GPC+GPE	4.00±0.39	3.11±1.4	0.07

Table 4.5: Comparison of concentration of metabolites obtained by in vitro ¹H MRS and ³¹P MRS

Metabolite	In vitro ¹H MRS ($\mu\text{mol/g}$ wet weight)	In vitro ³¹P MRS ($\mu\text{mol/g}$ wet weight)
Glycerophosphocholine (IFO-treated tumour)	0.71 \pm 0.07	0.68 \pm 0.01
Glycerophosphocholine(control tumour)	0.47 \pm 0.11	0.43 \pm 0.13
Phosphocholine (IFO-treated tumour)	1.30 \pm 0.15	1.25 \pm 0.13
Phosphocholine (control tumour)	1.19 \pm 0.35	0.87 \pm 0.23

Figure 4.12: In vitro ^{31}P MR spectrum obtained from ifosfamide treated tumour on Day 8

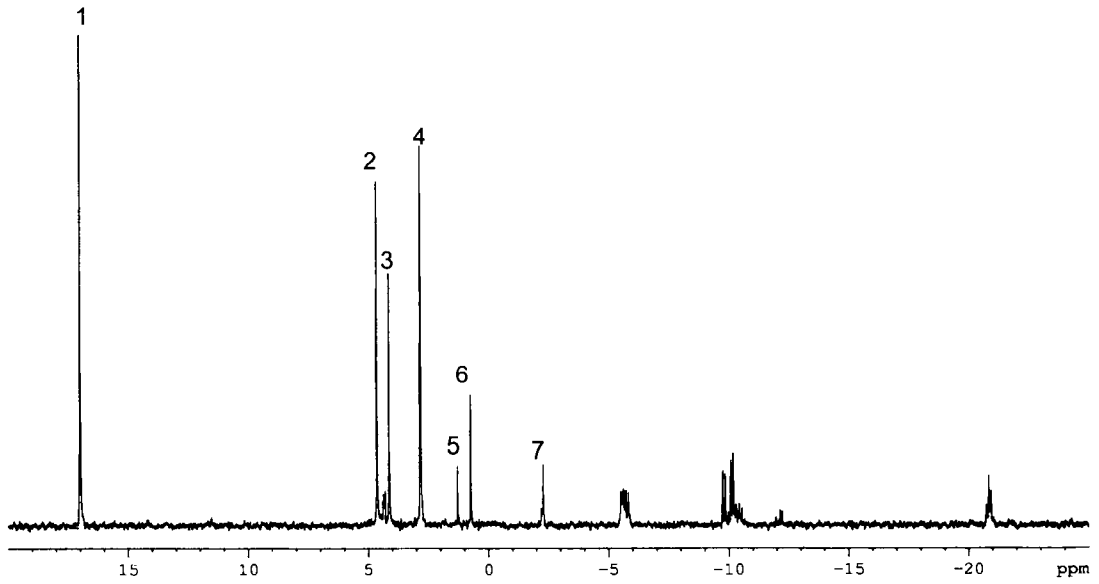
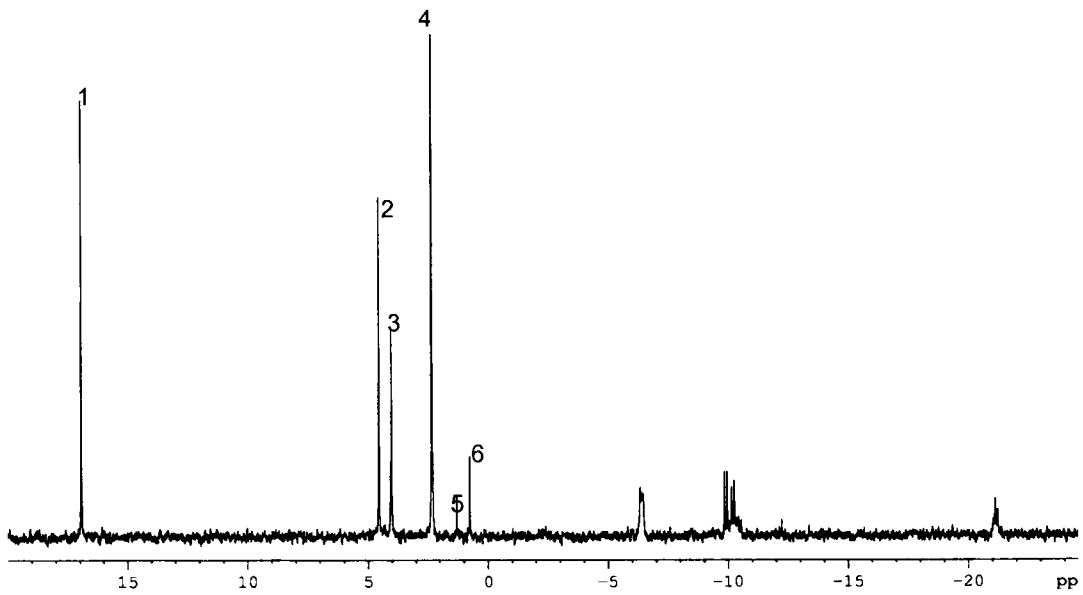


Figure 4.13: In vitro ^{31}P MR spectrum obtained from control tumour on Day 8



1: MNPA (reference); 2: PE; 3:PC; 4:Pi; 5:GPE; 6:GPC; 7:PCr

4.5 Discussion

Ifosfamide (IFO) is one of the most active agents in rhabdomyosarcoma. In a phase two window study, with newly diagnosed unresectable rhabdomyosarcomas, twenty-two children and adolescents were given 2 courses of single agent ifosfamide. Partial responses were seen in 86% patients [Pappo et al., 1993]. Combination chemotherapy with IFO has also been used as the first treatment in advanced rhabdomyosarcoma and 81% of the 152 patients showed a response [Sandler et al., 2001]. A randomised study compared ifosfamide and etoposide combination with melphalan and vincristine combination in newly diagnosed children and adolescents with metastatic rhabdomyosarcoma (phase II window therapy). Patients receiving ifosfamide containing regimen had significantly higher survival [Breitfeld et al., 2001]. Single agent IFO has also been used in a range of other solid tumours at relapse [Pinkerton and Pritchard, 1989; Schwartzman et al., 1989; Pinkerton et al., 1985; Magrath et al., 1986]. A large randomised study in adult patients tested the benefit of adding ifosfamide to a combination of doxorubicin and dacarbazine in advanced soft tissue and bone sarcomas. Response rates were significantly higher for the ifosfamide arm of the study. There was also a trend towards longer duration of response in ifosfamide-treated patients [Antman et al., 1993]. Currently, combination chemotherapy with IFO is being used as first line of management in several paediatric solid tumours including rhabdomyosarcoma.

The activity of ifosfamide was clearly demonstrated in this study. On average the tumours doubled in size in control animals whereas stable disease was

observed in over 80% of ifosfamide treated tumours. Although the cell line implanted in all these animals was the same, the variation in volume responses following IFO treatment could be due to host factors such as blood supply to the tumour. We have also seen variability in the half-life of ifosfamide in the tumours (discussed previously in Chapter 3) which could affect clinical response.

4.5.1 Acute effects of chemotherapy/ saline

Immediately after treatment all β -NTP related ratios were consistent with a decrease in β -NTP. An increase in PME/ β -NTP ratio was observed in both saline-treated and IFO-treated groups. This could be due to effects of injection. A decrease in NTP/Pi ratio has been previously observed in GH3 prolactinoma and N-methyl-N-nitrosourea induced mammary tumours at 30 minutes after IFO injection and this was confirmed to be due to drug induced hypotension [Rodrigues et al., 1997].

4.5.2 Changes in PME and β -NTP

The most striking change observed between Day 1 and Day 8 was an increased ratio of PME/Pi and β -NTP/Pi in ifosfamide treated tumours. The in vivo spectroscopic method alone does not allow one to conclude whether the increase in the ratio is due to increase in PME (or β -NTP) or decrease in Pi. Further analysis of tumour extract data using high resolution ^{31}P MRS confirmed that the level of PE on Day 8 was significantly higher in the IFO-treated group when compared to the controls. PME is mainly composed of

PE and PC and therefore we can conclude that the increase in PME/Pi ratio is mainly due to an increase in the PE levels. We cannot reliably estimate Pi in extracts. It is also difficult to estimate β -NTP levels using in vitro high-resolution spectroscopy as it degrades very rapidly in vitro. One could speculate that the increase in β -NTP/Pi is due to an increase in β -NTP.

Three patterns of variations have been described after chemotherapy or radiotherapy [de Certaines et al., 1993].

1. The spectrum changes to that of severely hypoxic tissue i.e. decrease of PCr/Pi and NTP/ Pi ratio. This is an acceleration of the process, which occurs in untreated tumour, where progressive depletion in oxygen and nutrient supply causes a decrease in the NTP/Pi ratio. This phenomenon is mainly observed following cytokines, hyperthermia or photodynamic therapy, which are known to induce ischemic injury.

2. A paradoxical enhancement of the bioenergetic activity i.e. increases in PCr and/or NTP and a decrease in Pi is usually observed after chemotherapy or radiation therapy. This process, called 'activation' by Steen (1989) has several possible reasons [Steen, 1989].
 - i) Tumour cell death produces inflammatory response and recruits macrophages into the tumour so that the fraction of normal cells contributing to the tumour spectrum is increased.
 - ii) Tumour cell death enables the surviving cells to obtain more oxygen and nutrients.
 - iii) Preferentially low energy cells are killed.
 - iv) The intratumoural hydrostatic pressure decreases due to cell killing and so blood flow is generally improved.
 - v) Therapy directly affects blood flow or causes increased capillary permeability within the tumour.

3. Successive transition from low energy status to high-energy status is sometimes observed after radiation therapy.

4.5.3 Phosphomonoesters (PME)

Role in cells:

The PME resonance mainly comprises signals from phospholipid metabolites phosphoethanolamine (PE) and phosphocholine (PC). These are precursors of phosphatidylethanolamine (PtdEtn) and phosphatidylcholine (PtdCho); important components of cell membrane. The concept of plasma membrane function has recently evolved from that of a simple permeable bag to that of an important site of the regulation of cancer cells and specifically of cancer cell/host interactions [Podo and de Certaines, 1996]. The synthetic and degradation pathway of these phospholipids contributes towards regulation of cell growth and function [Kiss, 1999;Podo, 1999]. Diacylglycerol and phosphatidate are produced from hydrolysis of PtdCho and PtdEtn and function as second messengers [Daniel et al., 1999]. Diacylglycerol also induces activation of protein kinase C [Nishizuka, 2003]. Phosphatidate is also a potent mutagen.

The first clinical study in neuroblastoma suggested that PME/ β -NTP ratio may be a useful marker of tumour growth or regression with higher ratio signifying tumour growth [Maris et al., 1985]. A multi-centre study in non-Hodgkin' s lymphoma in adults has suggested that the pre-treatment ratio of PME/NTP could correlate with subsequent treatment outcome. The data also revealed that the PME/NTP ratio decreased significantly after treatment in complete and partial responders but not in non-responders [Griffiths et al., 2002]. Similarly, in breast cancer patients, response to therapy was associated with a decrease in PME content in 14 out of 17 patients [Leach et

al., 1998]. In this study the response was assessed at 3 weeks from start of chemotherapy.

We have demonstrated an increase in the PME/Pi ratio between Day 8 and Day 1 in the ifosfamide treated tumours. Tumours treated with IFO when compared to control group had significantly higher PE on Day 8. Therefore the increase in PME/Pi ratio was probably due to an increase in phosphoethanolamine. This has been previously described following cyclophosphamide. The mechanism by which both increased and decreased levels of PME can be associated with cells having decreased cell growth rates is not known [Steen, 1989]. This could reflect differences in tumour types, model or treatments.

Following cyclophosphamide therapy in radiation induced fibrosarcoma in mouse, an increase in the ratio of PME/Pi and β -NTP/Pi has been seen from Day 3 onwards. The authors attribute this to a decrease in Pi and no data is available on in vitro extracts [Li et al., 1988].

The response to cyclophosphamide therapy has also been studied in mouse mammary carcinoma to determine whether changes previously described due to radiation were specific or could be reproduced by an alternative alkylating agent. Cyclophosphamide treated tumours showed a significant increase in NTP/Pi and PCr/Pi ratios when compared with a control group from 48 hours to 168 hours. This was preceded by a significant drop in the first 24 hours. The PME/Pi ratio was significantly higher for treated tumours compared with the control group from Day 4 onwards [Street et al., 1995].

4.5.4 Significance of phosphoethanolamine and phosphocholine

In most human tumours, PE is present in higher concentrations when compared with PC [Podo, 1999] and this has also been observed in our study. A PE/PC ratio of less than 1 has been observed in a number of cultured malignant cells. The predominance of PE over PC in tumours in vivo compared to cultured cells, could be because the tumour is mainly in the 'stationary' phase and the S phase fraction is usually low [Podo, 1999]. Several enzymes are involved in the metabolism of PE. Activity of ethanolamine kinase enzyme has been studied in tumours treated with cyclophosphamide and no change was observed in its specific activity when compared to the control group [Street et al., 1995]. There could be 2 possible mechanisms for increased PE in ifosfamide-treated tumours.

- 1) Accumulation of PE due to a decreased demand for cell membrane (PtdEtn) synthesis in non-proliferating cells.
- 2) Increased hydrolysis of phosphatidylethanolamine due to cell membrane damage by chemotherapy.

The PE/PC ratio has been previously studied in cell cultures, multicellular spheroids and xenograft models. Several studies have suggested that an increase in PE is associated with quiescent cells, or with a reduced proportion of cells in 'S' phase. A summary of the studies is given in Table 5 and is described below.

1) Cultured cells

Rat glioma cells were studied in bioreactors. PE levels remained low and constant during lag and log phases and increased dramatically upon cessation of culture growth. Levels of PC were found to be high in log phase and declined to low levels in the stationary phase [Gillies et al., 1994b]. Studies on different cell lines in bioreactors showed consistent and dramatically higher PE/PC ratio in stationary cultures compared to actively proliferating cultures [Aiken and Gillies, 1996].

2) Multicellular spheroids

Perfused multicellular spheroids represent a particularly useful in vitro tumour model for studying metabolic and spectral alterations associated with different conditions of cell proliferation and viability. As their size increases, they develop a necrotic core surrounded by quiescent cells (middle layer) and proliferating cells (external layers) [Podo, 1999]. In mammary carcinoma spheroids, a negative correlation between PE/PC ratio and the S phase cell fraction was observed and PE/PC correlated positively with the extent of central necrosis [Freyer et al., 1991]. An increase in PE/PC due to a decrease in PC has also been previously described with increasing T47D human breast cancer spheroid size, consistent with a reduction in proliferative fraction [Ronen et al., 1990].

3) Xenograft model

An increase in PE/PC has been previously shown post radiation in a mouse mammary carcinoma [Mahmood et al., 1994]. These changes were similar to those observed after radiation in cell cultures. The authors suggest that these changes could be due to intrinsic effects of radiation on cellular metabolism and could be due to membrane damage or inhibition of cellular proliferation [Mahmood et al., 1995]. An increase in the ratio of PE/PC with treatment was also observed in cyclophosphamide-treated mammary carcinoma and this supports the hypothesis that the PE/PC ratio reflects cell kill or cessation of cellular proliferation. However, in that case, the change was due to a decrease in PC and no change in ethanolamine kinase enzyme activity was observed [Street et al., 1995]. The same group studied in vivo and ex vivo changes in mouse mammary carcinoma following 5 fluorouracil (5-FU) therapy, which causes cells to accumulate in S phase. The changes observed were similar to those observed after cyclophosphamide with an increase in PE/PC ratio in treated groups. This was confirmed, by study of the extract, to be related to an increase in PE [Street et al., 1997]. In a more recent study, effects of 17-AAG were studied in mice HT29 xenografts. A significant increase in PME/ total P was observed following treatment. This was confirmed on the extract study to be due to an increase in both PC and PE [Chung YL et al., 2002].

Table 4.6: Summary of studies showing effects on PE/PC ratio

No	Study	Experimental conditions	Results and comments
1	[Freyer et al., 1991]	Mouse mammary carcinoma (EMT6/R0) multicellular tumour spheroids	Bigger spheroids had smaller proportion of cells in S phase. PE/PC ratio had a strong negative correlation with S phase fraction.
2	[Ronen et al., 1990]	Human breast cancer (T47D) spheroids	Larger spheroids contained smaller proliferative cell fraction. Increased PE/PC ratio in larger spheroids due to reduced PC.
3	[Gillies et al., 1994b]	Rat glioma cells in bioreactors.	PC levels were lower and PE levels were higher in stationary phase (non-proliferating cells).
4	[Aiken and Gillies, 1996]	Various cell lines grown in bioreactors	PC/PE ratio was lower in stationary phase compared to log phase. Increased PE was associated with decreased culture growth.
5	[Mahmood et al., 1994]	Murine mammary carcinoma- in vivo study. Radiation therapy-Doses 4-17Gray.	Post radiation PE/PC ratio increased in a dose dependant manner and reached a maximum at 7 days.
6	[Mahmood et al., 1995]	Radiation induced fibrosarcoma –1 tumour. Single dose of 17G radiotherapy. In vivo and in vitro (cell culture) data.	PE/PC ratio increased significantly in RT treated as compared to control group due to increase in PE levels. Similar changes in vivo and vitro suggest changes at cellular level and are likely to be due to cell death or growth inhibition due to RT. Possibly membrane damage
7	[Street et al., 1995]	Mouse mammary carcinoma treated with cyclophosphamide (150 mg/kg). In vivo and in vitro tumour study.	PE/PC ratio increased in cyclophosphamide treated animals. In vitro study confirmed decrease in PC levels. PE/PC ratio reflects cell kill or cessation of cellular proliferation.
8	[Street et al., 1997]	Mouse mammary carcinoma treated with 5-fluorouracil	PE/PC significantly increased for treated tumours, due to increase in PE. Tumour response could be independent of mechanism of action and/or cell cycle phase specificity.
9	[Chung YL et al., 2002]	Mouse HT 29 tumour. Treated with 17-AAG	Increased PME/PDE, PME/Tot P, PME/ β -NTP in vivo. In vitro data showed an increased PE & PC.

4.5.5 β -NTP

Nucleotide tri phosphates are the building blocks for nucleic acid synthesis.

Increase in β -NTP could be due to 'activation' as described by Steen (see earlier) or due to:

Reduced DNA synthesis.

Improved tumour oxygenation.

Reduced DNA synthesis: In regenerating rat liver after partial hepatectomy, the content of hepatic NTP was reduced 48 hours after resection i.e. at the time of active DNA synthesis. In animals treated with 5-FU, a smaller drop in NTP was observed. Direct measure of DNA synthesis and nuclear proliferation confirmed that chemotherapy inhibited thymidine incorporation and Ki67 proliferation suggesting that interruption of DNA synthesis leads to a reduced utilisation of NTP [Kooby et al., 2000].

The hypothesis that tumour bioenergetics are sensitive to metabolic hypoxia was suggested first by tumour ligation experiments, in which tumour blood supply was clamped. ^{31}P MRS characteristically showed a decrease in PCr and NTP and an increase in Pi [Lilly et al., 1985]. It was concluded that an absence of metabolic substrate or accumulation of metabolic waste products could be the cause of these MRS changes. Subsequent experiments studied effects of different inhalation of gas mixtures which confirmed that bioenergetics of tumour were dependent on oxygen supply [Steen, 1991].

Agents that decrease blood flow such as hydralazine and flunarazine produce a decrease in high-energy phosphates whereas agents which increase blood flow produce an opposite effect [Bhujwalla et al., 1990].

During the growth of untreated tumour, with increasing hypoxia, the levels of energy-rich phosphates decline and Pi increases [Steen, 1989]. In rat gliosarcoma treated with carmustine, this was associated with a significant increase in high-energy phosphates. Both tumour oxygenation and perfusion were significantly increased after treatment.

In murine fibrosarcoma, a progressive loss of PCr and NTP with increasing Pi and PME signal was noted during growth. Ratios of PCr/Pi, PME/Pi, NTP/Pi and PDE/Pi declined as the tumour size increased. When mean tissue PO₂ was plotted against the pH, NTP/Pi, PCr/Pi, PME/Pi and PDE/Pi, highly significant positive correlations were observed. The only ratio which increased with tumour growth was PME/NTP, for which a negative correlation was observed with mean tissue pO₂ [Vaupel et al., 1989].

4.6 Summary and future directions

Significant changes in the tumour bioenergetics and membrane metabolisms are seen after chemotherapy. Our data are consistent with other xenograft studies with cyclophosphamide, suggesting that the changes may be consistent across tumour types. An increase in the PE component of PME could reflect quiescent cells or smaller proportion of cells in the 'S' phase fraction. An increase in β -NTP could be related to improved blood supply and decreasing hypoxia of a treated tumour or reduced DNA synthesis caused by this alkylating agent. This suggests measurements with ^{31}P MRS may have potential to define markers of tumour response in clinical studies.

CONCLUSIONS AND POTENTIAL FUTURE STUDIES

From our study we conclude that

- 1) It is possible to study pharmacokinetics of ifosfamide non-invasively using ^{31}P MRS in an animal model.
- 2) Ifosfamide causes detectable changes in the bioenergetic status and metabolism of the membrane precursor molecules (phosphoethanolamine) in tumours and this can be studied in vivo using MRS.
- 3) It is possible to observe spectroscopic signal related to ifosfamide and cyclophosphamide in liver of adults and children.

Based on these findings, it would be possible to design studies with the following aims:

- a) To define the relationship between ifosfamide pharmacokinetics and clinical response: If a correlation was confirmed, this could facilitate dose adjustment and individualise therapy.
- b) To define the relationship between changes observed by MRS and clinical response: multicentre studies would be needed to confirm the role of MRS in different paediatric tumour types. This could help evaluate early activity of drugs in phase II studies and aid treatment decisions for children who are non-responders.
- c) To define the relationship between MRS changes and histological response at surgery. If pre-operative spectral findings can be correlated with histological outcome, this could guide decisions regarding timing of surgery and the nature of pre-surgical therapy.

APPENDIX

APPENDIX 3.1

Standard Operating Procedure for measurement of ifosfamide and metabolites, in tissues, using LC/MS/MS
Pharmacology Section, CRU

ASOP 31

Revision 1

Effective date: 13/02/02

Review date: 01/12/02

Signature

Edited by:
Approved by:
Reviewed by:

Northern Institute of Cancer Research
University of Newcastle upon Tyne
Framlington Place
Newcastle upon Tyne
NE2 4HH

Associated SOPs: -

SOP 1 Use of pH meter
SOP 4 Weighing out of potent carcinogens
SOP 6 HPLC columns
SOP 7 Preparation of HPLC mobile phases
SOP 10 Packing of HPLC precolumns
SOP 23 Setting up LC/MS/MS
SOP 18 Validation of an analytical method
SOP 19 Transfer of data from analytical software to study files
SOP 22 Filling in instrument logs
SOP 25 Preparation and storage of reagents and solutions
SOP 27 Use of Zymark evaporator

Caution!

1. Wear a lab coat and gloves at all times

2. Fill in a COSHH form and ensure you are registered for the appropriate carcinogens

Materials

Chemicals

Cyclophosphamide	Sigma Chemical Co., Poole, Dorset
Ifosfamide	Degussa
2-DCI	ASTA
3-DCI	ASTA
CXIP	ASTA
Keto	ASTA
Ethyl Acetate (HPLC grade)	FSA Laboratory Supplies, Loughborough, UK.
Methanol (HPLC grade)	FSA Laboratory Supplies, Loughborough, UK
Glacial Acetic Acid	FSA Laboratory Supplies, Loughborough, UK
Ammonia Hydroxide Solution	FSA Laboratory Supplies, Loughborough, UK

Equipment and Supplies

Disposable Polypropylene Universals, 20 and 5 ml,	Sterilin, Feltham, UK.
Magnetic Stirrer & Hot Plate, SM3	Stuart Scientific Co Ltd, UK
Pipettes,	Models P20, P100, P200, P1000, P5000, Gilson, Anachem, Luton, UK.
Disposable Pipette Tips	P100, P200, P1000, P5000, Gilson, Anachem, Luton, UK.
10 ml Disposable Borosilicate Glass Tubes	Baxter Healthcare Corporation, USA.
15ml Polypropylene screw-capped tubes	FSA Laboratory supplies, Loughborough, UK

1.5ml eppendorfs	FSA Laboratory supplies, Loughborough, UK
Autosampler vials	Jones Chromatography, UK
Top Loading Balance, Salter XF3200	SH Scientific, Blyth, UK
Microbalance, Salter FX-40	SH Scientific, Blyth, UK
Vortex mixer	FSA Laboratory Supplies, Loughborough, UK
Evaporator	Zymark, Runcorn, Cheshire, UK
Centrifuge	Falcon 6/300, Fisons, Crawley, Surrey, UK
Multitube vortexer	Janke & Kuntel, IKA laboratechnik, Germany
Homogeniser	Ultra-turrax T25, Janke & Kuntel, IKA laboratechnik, Germany
pH meter	model pH302, Hanna instruments, UK
Solvent Filtration Apparatus	Alltech, Carnforth, UK.
Filters	0.5 μ m PTFE & 0.45 μ m cellulose nitrate filters, Whatman Ltd., Maidstone, Kent, UK.
LC/MS/MS Apparatus	
Luna C18, 50 x 2 mm column	Phenomenex, Macclesfield, Cheshire, UK.
Series 200 Micro pump	Perkin Elmer Ltd., Post Office Lane, Beckonsfield, Bucks, UK.
Series 200 Autosampler	
Series 200 Peltier column oven	
API 2000 LC/MS/MS	Applied Biosystems, Foster City, CA., USA.
Analyst Software 1.1	

Methods

Preparation of 1 mg/ml cyclophosphamide solution

(see SOP4 and cyclophosphamide carcinogen protocol):

Remove cyclophosphamide from 40C carcinogen cupboard and allow to equilibrate for approximately 60 minutes.

In the carcinogen hood accurately weigh approximately 5 mg into a 7ml bijou container.

Dissolve the cyclophosphamide in the appropriate amount of methanol to yield a 1 mg/ml solution. Aliquot and store at -20oC.

Record the details in your lab book (include batch and amount weighed out).

Record details in the appropriate sheet in the carcinogen excel file (pklabdocs/potent carc/carcinog.xls).

Preparation of 100 μ g/ml cyclophosphamide solution for use as internal standard

Dilute 1 mg/ml solution above 1 in 10: -in an eppendorf, combine 100 μ l of 1 mg/ml stock and 900 μ l of dH₂O.

Preparation of 4 mg/ml ifosfamide solution

(see SOP4 and ifosfamide carcinogen protocol):

Remove ifosfamide from 40C carcinogen cupboard and allow to equilibrate for approximately 60 minutes.

In the carcinogen hood accurately weigh approximately 5 mg into a 7ml bijou container.

Dissolve the ifosfamide in the appropriate amount of methanol to yield a 4 mg/ml solution.

Aliquot and store at -20oC.

Record the details in your lab book (include batch and amount weighed out).

Record details in the appropriate sheet in the carcinogen excel file (pklabdocs/potent carc/carcinog.xls).

Preparation of 1 mg/ml 3-DCI solution

(see SOP4 and ifosfamide carcinogen protocol):

Remove 3-DCI from -20oC carcinogen cupboard and allow to equilibrate for approximately 60 minutes.

In the carcinogen hood accurately weigh approximately 5 mg into a 7ml bijou container.

Dissolve the 3-DCI in the appropriate amount of methanol to yield a 1 mg/ml solution. Aliquot and store at -20oC.

Record the details in your lab book (include batch and amount weighed out).

Record details in the appropriate sheet in the carcinogen excel file (pklabdocs/potent carc/carcinog.xls).

Preparation of 1 mg/ml 2-DCI solution

(see SOP4 and ifosfamide carcinogen protocol):

Remove 2-DCI from -20°C carcinogen cupboard and allow to equilibrate for approximately 60 minutes.

In the carcinogen hood accurately weigh approximately 5 mg into a 7ml bijou container.

Dissolve the 2-DCI in the appropriate amount of methanol to yield a 1 mg/ml solution. Aliquot and store at -20°C.

Record the details in your lab book (include batch and amount weighed out).

Record details in the appropriate sheet in the carcinogen excel file (pklabdocs/potent carc/carcinog.xls).

Preparation of 1 mg/ml Keto solution

(see SOP4 and ifosfamide carcinogen protocol):

Remove Keto from -20°C carcinogen cupboard and allow to equilibrate for approximately 60 minutes.

In the carcinogen hood accurately weigh approximately 5 mg into a 7ml bijou container.

Dissolve the Keto in the appropriate amount of methanol to yield a 1 mg/ml solution. Aliquot and store at -20°C.

Record the details in your lab book (include batch and amount weighed out).

Record details in the appropriate sheet in the carcinogen excel file (pklabdocs/potent carc/carcinog.xls).

Preparation of 1 mg/ml CXIP solution

(see SOP4 and ifosfamide carcinogen protocol):

Remove CXIP from -20°C carcinogen cupboard and allow to equilibrate for approximately 60 minutes.

In the carcinogen hood accurately weigh approximately 5 mg into a 7ml bijou container.

Dissolve the CXIP in the appropriate amount of methanol to yield a 1 mg/ml solution. Aliquot and store at -20°C.

Record the details in your lab book (include batch and amount weighed out).

Record details in the appropriate sheet in the carcinogen excel file (pklabdocs/potent carc/carcinog.xls).

Preparation of spiking solutions

Conc A (800 µg/ml Ifosfamide and 200µg/ml metabolites)

100µl of 4 mg/ml ifosfamide and 100µl each of 1 mg/ml 3-DCI, 2-DCI, Keto, CXIP.

Conc B (400µg/ml Ifosfamide and 100µg/ml metabolites)

400µl of Conc A + 400µl dH₂O

Conc C (200µg/ml Ifosfamide and 50µg/ml metabolites)

400µl of Conc B + 400µl dH₂O

Tissue Homogenisation

Weigh the tissue in a tared bijou.

Add three times the weight in volume of PBS.

Homogenise the tissue to remove all lumps.

Homogenised tissues can be stored at -80°C until required.

Extraction

Label 12 x15ml orange capped polypropylene tubes for each tissue (i.e. 3 x blank, 3 x conc A, 3 x conc B, 3 x conc C).

Add 50µl of tissue homogenate.

Add 10µl of spike – either water or Conc A or Conc B or Conc C.

Add 10µl of I.S. (100µg/ml cyclophosphamide).

Add 1ml of ethyl acetate.

Vortex the tubes on the multitube vortexer for 15 minutes.

Centrifuge at 2500rpm for 10 minutes at 4°C.

Using a Gilson pipette remove 0.9ml of supernatant and place in a borosilicate tube.

Evaporate to dryness under N₂ at 37°C.

Reconstitute in 200µl mobile phase.

Vortex.

Centrifuge at 1000rpm for 10 minutes at 4°C.

Transfer to a limited volume insert.

Inject 50µl onto LC/MS/MS.

The sample will be injected twice using two separate LC/MS/MS acquisition methods.

LC/MS/MS conditions

Preparation of LC/MS/MS Mobile Phase

Preparation of 0.02M Ammonium Acetate (pH 4)

Mix 1.2g of glacial acetic acid with about 850g of distilled water.

Adjust the pH to 4.0 with strong ammonia solution.

Add water to a final weight of 1000g

Filter through a 4.5 µm cellulose nitrate filter.

Filter sufficient HPLC methanol (~1L) and deionised water (~500mL) to make the following:

~500ml of methanol – transfer to a labelled reagent bottle

~ 500 ml of a 50/50 (v/v) solution of methanol and dH₂O – transfer to a labelled reagent bottle

Place the filtered Ammonium acetate on line A, the filtered methanol on line B and the 50/50 methanol/water mix on the needlewash.

Set up the LC/MS/MS system according to SOP 23.

Chromatographic Conditions for Ifosfamide and positive ion metabolites

Hardware configuration: Melanie1_1

Acquisition method: Ifo + metab + CP pos.dam

Mobile phase: 50/50 MeOH/Ammonium acetate pH4

Flow Rate: 300 µl/min

Column: Phenomenex Luna C18 50x2mm 3µ

Pre-column: Phenomenex security guard C18 4x2mm

Injection volume: 50µl

Retention times:

Compound	Mass ratio	Approx. Retention time (mins)
Ifosfamide	260/154	2.4
Cyclophosphamide	260/139	2.8
3-DCI	199/120	1.7
2-DCI	199/171	1.7
Keto	274/141	2.0

Chromatographic conditions for CXIP

Hardware configuration: Melanie1_1

Acquisition method: CXIP 290_219 MRM neg.dam

Mobile phase: 35/65 MeOH/Ammonium acetate pH4

Flow Rate: 300 µl/min

Column: Phenomenex Luna C18 50x2mm 3µ

Pre-column: Phenomenex security guard C18 4x2mm

Injection volume: 50µl

Retention times: CXIP 2.7mins

Remember to fill in the instrument log book after use.

Calculations

Mean all the peak area ratios for each of the positive compounds at each of the spiked concentrations (i.e. blank, conc A, conc B, conc C).and the peak areas for CXIP.

Sample	Mean Peak Area or area ratio	Conc of ifosfamide spike (µg/ml)	Conc of metabolite spike (µg/ml)
Blank		0	0
Conc A		160	40
Conc B		80	20
Conc C		40	10

1. Perform linear regression analysis for each compound (make sure the correct concs are used for the metabolite and ifosfamide (table above)).
2. Calculate the Adjusted Area = mean area for each conc –intercept.
3. Calculate the measured conc = mean area for each conc/slope
4. Calculate the adjusted conc = adjusted area/slope
5. Calculate the concentration in the tissue = measured conc – adjusted conc
6. See example overleaf.

Example

Peak Areas

Sample	Mean 2DCI	Mean DCCP	Mean Ifosfamide	Mean Keto	conc mets (µg/ml)	conc ifos (µg/ml)
Liver	0.0612	0.0409	1.77	0.000934	0	0
Liver A	0.523	0.337	6.17	0.191	40	160
Liver B	0.262	0.172	4.21	0.0981	20	80
Liver C	0.193	0.131	3.22	0.0596	10	40
Adj ratio ratio-intercept						
Sample	2DCI	DCCP	Ifos	Keto		
Liver	-0.00052	-0.03784		-0.188	-0.004886	
Liver A	0.46128	0.02106		4.212	0.18518	
Liver B	0.20028	-0.00094		2.252	0.09228	
Liver C	0.13128	-0.03294		1.262	0.05378	
conc ratio/slope						
Sample	2DCI	DCCP	Ifos	Keto		
Liver	5.40683806	0.845343681	65.74792913	0.2003432		
Liver A	46.2054952	9.007760532	229.1891089	40.969541		
Liver B	23.1469211	5.958980044	156.3834924	21.042471		
Liver C	17.0509762	1.524390244	119.609227	12.7842128		
adj conc adj ratio/slope						
Sample	2DCI	DCCP	Ifos	Keto		
Liver	-0.0459405	-5.243902439	-6.983395862	-1.04804805		
Liver A	40.7527167	2.918514412	156.4577839	39.7211497		
Liver B	17.6941426	-0.130266075	83.65216745	19.7940798		
Liver C	11.5981977	-4.564855876	46.87790201	11.5358215		
conc conc -adj conc						
Sample	2DCI	DCCP	Ifos	Keto		
Liver	5.45277851	6.08924612	72.73132499	1.24839125		
Liver A	5.45277851	6.08924612	72.73132499	1.24839125		
Liver B	5.45277851	6.08924612	72.73132499	1.24839125		
Liver C	5.45277851	6.08924612	72.73132499	1.24839125		

Regressions –Intercept and slope (X variable) used in the calculations above

Liver 2DCI		Liver DCCP		liver ifos		liver Keto	
Regression Statistics		Regression Statistics		Regression Statistics		Regression Statistics	
Multiple R	0.99521169	Multiple R	0.994394351	Multiple R	0.995672712	Multiple R	0.997962224
R Square	0.9904463	R Square	0.988820125	R Square	0.99136415	R Square	0.995928601
Adjusted R	0.98566945	Adjusted R Sq	0.983230188	Adjusted R Sr	0.987046225	Adjusted R Square	0.993892901
Standard E	0.02325208	Standard Error	0.016049539	Standard Errc	0.21022437	Standard Error	0.006234987
Observatio	4	Observations	4	Observations	4	Observations	4
ANOVA		ANOVA		ANOVA		ANOVA	
df		df		df		df	
Regressor	1	Regression	1	Regression	1	Regression	1
Residual	2	Residual	2	Residual	2	Residual	2
Total	3	Total	3	Total	3	Total	3
Coefficients		Coefficients		Coefficients		Coefficients	
Intercept	0.06172	Intercept	0.04394	Intercept	1.958	Intercept	0.0058204
X Variable	0.01131886	X Variable 1	0.007216286	X Variable 1	0.026921429	X Variable 1	0.004662177

REFERENCE LIST

Ackerman JJ, Grove TH, Wong GG, Gadian DG, Radda GK (1980) Mapping of metabolites in whole animals by ^{31}P NMR using surface coils. *Nature* 283: 167-170

Aeschlimann C, Kupfer A, Schefer H, Cerny T (1998) Comparative pharmacokinetics of oral and intravenous ifosfamide/mesna/methylene blue therapy. *Drug Metab Dispos* 26: 883-890

Aiken NR, Gillies RJ (1996) Phosphomonoester metabolism as a function of cell proliferative status and exogenous precursors. *Anticancer Res* 16: 1393-1397

Allen LM, Creaven PJ (1975) Pharmacokinetics of ifosfamide. *Clin Pharmacol Ther* 17: 492-498

Allen LM, Creaven PJ, Nelson RL (1976) Studies on the human pharmacokinetics of isophosphamide (NSC-109724). *Cancer Treat Rep* 60: 451-458

Antman K, Crowley J, Balcerzak SP, Rivkin SE, Weiss GR, Elias A, Natale RB, Cooper RM, Barlogie B, Trump DL., (1993) An intergroup phase III randomized study of doxorubicin and dacarbazine with or without ifosfamide and mesna in advanced soft tissue and bone sarcomas. *J Clin Oncol* 11: 1276-1285

Arias-Mendoza F, Brown TR, Charles HC, Zakian K, Schwarz A J, Doyle VL, Nelson SJ, Rijpkema M, Glickson JD, and Evelhoch JL (1999) Methodological standardization for a multi-institutional in vivo trial of localized

³¹P MR Spectroscopy in human cancer research. Proceedings of the 7th Annual Meeting of the International Society of Magnetic Resonance in Medicine, 1585.

Arias-Mendoza F, Brown TR, Schwartz AJ, Leach MO, Zakian K, Koutcher JA, Stubbs M, Griffiths JR, Nelson SJ, Heerschap A, Glickson JD, Charles HC, and Evelhoch JL (2000). Preliminary results of a multi-institutional trial to demonstrate clinical predictive value of in vivo localized ³¹P MR spectroscopy data in human non-Hodgkin's lymphoma. Proceedings of the 8th Annual Meeting of the International Society of Magnetic Resonance in Medicine, 98.

Arias-Mendoza F, Zakian K, Stubbs M, Collins DJ, Payne G, Brown TR, Leach MO, Griffiths JR, Koutcher JA, Glickson JD, Evelhoch JL, Heerschap A, Charles HC, and Nelson SJ (2001). Investigation of the predictive value of the pretreatment tumour content of phosphoethanolamine and phosphocholine measured by in vivo ³¹P MR spectroscopy in non-hodgkin's lymphoma in a multi-institutional setting. Proceedings of the 9th Annual Meeting of the International Society of Magnetic Resonance in Medicine, 274

Artemov D, Bhujwala ZM, Maxwell RJ, Griffiths JR, Judson IR, Leach MO, Glickson JD (1995) Pharmacokinetics of the ¹³C labeled anticancer agent temozolomide detected in vivo by selective cross-polarization transfer. *Magn Reson Med* 34: 338-342

Bates TE, Williams SR, Gadian DG (1989) Phosphodiesterases in the liver: the effect of field strength on the ³¹P signal. *Magn Reson Med* 12: 145-150

Becker R, Ritter A, Eichhorn U, Lips J, Bertram B, Wiessler M, Zdzienicka MZ, Kaina B (2002) Induction of DNA breaks and apoptosis in crosslink-hypersensitive V79 cells by the cytostatic drug beta-D-glucosyl-ifosfamide mustard. *Br J Cancer* 86: 130-135

Bhujwalla AM, Tozer GM, Field SB, Proctor E, Busza A, Williams SR (1990) The combined measurement of blood flow and metabolism in RIF-1 tumours in vivo. A study using H₂ flow and ³¹P NMR spectroscopy. *NMR Biomed* 3: 178-183

Bizzi A, Movsas B, Tedeschi G, Phillips CL, Okunieff P, Alger JR, Di Chiro G (1995) Response of non-Hodgkin lymphoma to radiation therapy: early and long-term assessment with ¹H MR spectroscopic imaging. *Radiology* 194: 271-276

Block F, Hansen WW, Packard M (1946) The nuclear induction experiment. *Physical Reviews* 70: 474-485

Boddy AV, Cole M, Pearson AD, Idle JR (1995c) The kinetics of the auto-induction of ifosfamide metabolism during continuous infusion. *Cancer Chemother Pharmacol* 36: 53-60

Boddy AV, English M, Pearson AD, Idle JR, Skinner R (1996b) Ifosfamide nephrotoxicity: limited influence of metabolism and mode of administration during repeated therapy in paediatrics. *Eur J Cancer* 32A: 1179-1184

Boddy AV, Furtun Y, Sardas S, Sardas O, Idle JR (1992) Individual variation in the activation and inactivation of metabolic pathways of cyclophosphamide. *J Natl Cancer Inst* 84: 1744-1748

Boddy AV, Proctor M, Simmonds D, Lind MJ, Idle JR (1995b)

Pharmacokinetics, metabolism and clinical effect of ifosfamide in breast cancer patients. *Eur J Cancer* 31A: 69-76

Boddy AV, Yule SM (2000) Metabolism and pharmacokinetics of oxazaphosphorines. *Clin Pharmacokinet* 38: 291-304

Boddy AV, Yule SM, Wyllie R, Price L, Pearson AD, Idle JR (1993)

Pharmacokinetics and metabolism of ifosfamide administered as a continuous infusion in children. *Cancer Res* 53: 3758-3764

Boddy AV, Yule SM, Wyllie R, Price L, Pearson AD, Idle JR (1995a)

Comparison of continuous infusion and bolus administration of ifosfamide in children. *Eur J Cancer* 31A: 785-790

Boddy AV, Yule SM, Wyllie R, Price L, Pearson AD, Idle JR (1996a)

Intrasubject variation in children of ifosfamide pharmacokinetics and metabolism during repeated administration. *Cancer Chemother Pharmacol* 38: 147-154

Borner K, Kisro J, Bruggemann SK, Hagenah W, Peters SO, Wagner T

(2000) Metabolism of ifosfamide to chloroacetaldehyde contributes to antitumor activity in vivo. *Drug Metab Dispos* 28: 573-576

Bottomley PA (1987) Spatial localization in NMR spectroscopy in vivo. *Ann N*

Y Acad Sci 508: 333-348

Brain EG, Yu LJ, Gustafsson K, Drewes P, Waxman DJ (1998) Modulation of P450-dependent ifosfamide pharmacokinetics: a better understanding of drug activation in vivo. *Br J Cancer* 77: 1768-1776

Breitfeld PP, Lyden E, Raney RB, Teot LA, Wharam M, Lobe T, Crist WM, Maurer HM, Donaldson SS, Ruymann FB (2001) Ifosfamide and etoposide are superior to vincristine and melphalan for pediatric metastatic rhabdomyosarcoma when administered with irradiation and combination chemotherapy: a report from the Intergroup Rhabdomyosarcoma Study Group. *J Pediatr Hematol Oncol* 23: 225-233

Brock N (1983) The oxazaphosphorines. *Cancer Treat Rev* 10 Suppl A: 3-15

Brock N (1989) Oxazaphosphorine cytostatics: past-present-future. Seventh Cain Memorial Award lecture. *Cancer Res* 49: 1-7

Brock N, Pohl J (1983) The development of mesna for regional detoxification. *Cancer Treat Rev* 10 Suppl A: 33-43

Brock N, Pohl J (1986) Prevention of urotoxic side effects by regional detoxification with increased selectivity of oxazaphosphorine cytostatics. *IARC Sci Publ* 269-279

Brock N, Pohl J, Stekar J (1981a) Studies on the urotoxicity of oxazaphosphorine cytostatics and its prevention--I. Experimental studies on the urotoxicity of alkylating compounds. *Eur J Cancer* 17: 595-607

Brock N, Pohl J, Stekar J (1981b) Studies on the urotoxicity of oxazaphosphorine cytostatics and its prevention. 2. Comparative study on

the uroprotective efficacy of thiols and other sulfur compounds. *Eur J Cancer Clin Oncol* 17: 1155-1163

Brock N, Pohl J, Stekar J, Scheef W (1982) Studies on the urotoxicity of oxazaphosphorine cytostatics and its prevention--III. Profile of action of sodium 2-mercaptoethane sulfonate (mesna). *Eur J Cancer Clin Oncol* 18: 1377-1387

Brock N, Stekar J, Pohl J, Niemeyer U, Scheffler G (1979) Acrolein, the causative factor of urotoxic side-effects of cyclophosphamide, ifosfamide, trofosfamide and sufosfamide. *Arzneimittelforschung* 29: 659-661

Brown TR (1992) Practical applications of chemical shift imaging. *NMR Biomed* 5: 238-243

Brown TR, Kincaid BM, Ugurbil K (1982) NMR chemical shift imaging in three dimensions. *Proc Natl Acad Sci U S A* 79: 3523-3526

Bryant DJ, Bydder GM, Case HA, Collins AG, Cox IJ, Makepeace A, Pennock JM (1988) Use of ³¹phosphorus MR spectroscopy to monitor response to chemotherapy in non-Hodgkin lymphoma. *J Comput Assist Tomogr* 12: 770-774

Budach V, Bamberg M, Scheulen M, Niederle N, and Krause U (1987). Preclinical chemosensitivity studies with human soft tissue sarcomas in nude mice. Contributions to Oncology (Proceedings of the satellite symposium ' Ifosfamide in tumor therapy' 18th National cancer Congress of the German Cancer society 26, 168-175.

Burtscher IM, Stahlberg F, Holtas S (1997) Proton (1H) MR spectroscopy for routine diagnostic evaluation of brain lesions. *Acta Radiol* 38: 953-960

Calvert AH, Newell DR, Gumbrell LA, O'Reilly S, Burnell M, Boxall FE, Siddik ZH, Judson IR, Gore ME, Wiltshaw E (1989) Carboplatin dosage: prospective evaluation of a simple formula based on renal function. *J Clin Oncol* 7: 1748-1756

Carli M, Guglielmi M, Sotti G, Cecchetto G, Ninfo V (1997) Soft tissue sarcomas. In *Paediatric Oncology -Clinical practice and controversies*, Pinkerton CR, Plowman PN (eds) pp 380-416. Chapman & Hall: London

Castillo M, Kwock L, Mukherji SK (1996) Clinical applications of proton MR spectroscopy. *AJNR Am J Neuroradiol* 17: 1-15

Cerny T, Leyvraz S, von Briel T, Kupfer A, Schaad R, Schmitz SF, Honegger P, Sessa C, Brunner J, Boddy AV (1999) Saturable metabolism of continuous high-dose ifosfamide with mesna and GM-CSF: a pharmacokinetic study in advanced sarcoma patients. Swiss Group for Clinical Cancer Research (SAKK). *Ann Oncol* 10: 1087-1094

Cerny T, Margison JM, Thatcher N, Wilkinson PM (1986) Bioavailability of ifosfamide in patients with bronchial carcinoma. *Cancer Chemother Pharmacol* 18: 261-264

Chung YL, Troy H, Banerji U, Judson I, Leach MO, Stubbs M, Ronen SM, Workman P, and Griffiths JR (2002). The pharmacodynamic effects of 17-AAG on HT29 xenografts in mice monitored by magnetic resonance spectroscopy. *Proceedings of the AACR* , 371.

Colvin M, Russo JE, Hilton J, Dulik DM, Fenselau C (1988) Enzymatic mechanisms of resistance to alkylating agents in tumor cells and normal tissues. *Adv Enzyme Regul* 27: 211-221

Connors TA, Cox PJ, Farmer PB, Foster AB, Jarman M (1974) Some studies of the active intermediates formed in the microsomal metabolism of cyclophosphamide and isophosphamide. *Biochem Pharmacol* 23: 115-129

Cocker HA (2001). Drug resistance in Paediatric rhabdomyosarcoma- Pathway and Circumvention. Theses, Doctoral, University of London .

Damadian R (1971) Tumour detection by nuclear magnetic resonance. *Science* 1151-1153

Daniel LW, Sciorra VA, Ghosh S (1999) Phospholipase D, tumor promoters, proliferation and prostaglandins. *Biochim Biophys Acta* 1439: 265-276

de Certaines JD, Albrechtsen J, Larsen VA, Xie X, Rygaard J, Henriksen O (1992) In vivo ³¹P magnetic resonance spectroscopy and ¹H magnetic resonance imaging of human bladder carcinoma on nude mice: effects of tumour growth and treatment with cis-dichloro-diamine platinum. *In Vivo* 6: 611-616

de Certaines JD, Larsen VA, Podo F, Carpinelli G, Briot O, Henriksen O (1993) In vivo ³¹P MRS of experimental tumours. *NMR Biomed* 6: 345-365

Dillon WP, Nelson S (1999) What is the role of MR spectroscopy in the evaluation and treatment of brain neoplasms? *AJNR Am J Neuroradiol* 20: 2-3

Dowling C, Bollen AW, Noworolski SM, McDermott MW, Barbaro NM, Day MR, Henry RG, Chang SM, Dillon WP, Nelson SJ, Vigneron DB (2001) Preoperative proton mr spectroscopic imaging of brain tumors: correlation with histopathologic analysis of resection specimens. *AJNR Am J Neuroradiol* 22: 604-612

Dubourg L, Michoudet C, Cochat P, Baverel G (2001) Human kidney tubules detoxify chloroacetaldehyde, a presumed nephrotoxic metabolite of ifosfamide. *J Am Soc Nephrol* 12: 1615-1623

Engle TW, Zon G, Egan W (1979) ^{31}P NMR investigations of phosphoramidate mustard: evaluation of pH control over the rate of intramolecular cyclization to an aziridinium ion and the hydrolysis of this reactive alkylator. *J Med Chem* 22: 897-899

Evanochko WT, Sakai TT, Ng TC, Krishna NR, Kim HD, Zeidler RB, Ghanta VK, Brockman RW, Schiffer LM, Braunschweiger PG, (1984) NMR study of in vivo RIF-1 tumors. Analysis of perchloric acid extracts and identification of ^1H , ^{31}P and ^{13}C resonances. *Biochim Biophys Acta* 805: 104-116

Evans WE, Relling MV, Rodman JH, Crom WR, Boyett JM, Pui CH (1998) Conventional compared with individualized chemotherapy for childhood acute lymphoblastic leukemia. *N Engl J Med* 338: 499-505

Evelhoch JL, Gillies RJ, Karczmar GS, Koutcher JA, Maxwell RJ, Nalcioglu O, Raghunand N, Ronen SM, Ross BD, Swartz HM (2000) Applications of magnetic resonance in model systems: cancer therapeutics. *Neoplasia* 2: 152-165

Findlay MP, Leach MO (1994) In vivo monitoring of fluoropyrimidine metabolites: magnetic resonance spectroscopy in the evaluation of 5-fluorouracil. *Anticancer Drugs* 5: 260-280

Findlay MP, Leach MO, Cunningham D, Collins DJ, Payne GS, Glaholm J, Mansi JL, McCready VR (1993) The non-invasive monitoring of low dose, infusional 5-fluorouracil and its modulation by interferon-alpha using in vivo ¹⁹F magnetic resonance spectroscopy in patients with colorectal cancer: a pilot study. *Ann Oncol* 4: 597-602

Frahm J, Bruhn H, Gyngell ML, Merboldt KD, Hanicke W, Sauter R (1989) Localized high-resolution proton NMR spectroscopy using stimulated echoes: initial applications to human brain in vivo. *Magn Reson Med* 9: 79-93

Frahm J, Merboldt KD, Hanicke W (1987) Localized proton spectroscopy using stimulated echoes. *Journal of Magnetic Resonance* 72: 502-508

Freeman DM, Hurd R (1997) Decoupling: theory and practice. II. State of the art: in vivo applications of decoupling. *NMR Biomed* 10: 381-393

Freeman R, Kupce E (1997) Decoupling: theory and practice. I. Current methods and recent concepts. *NMR Biomed* 10: 372-380

Freyer JP, Schor PL, Jarrett KA, Neeman M, Sillerud LO (1991) Cellular energetics measured by phosphorous nuclear magnetic resonance spectroscopy are not correlated with chronic nutrient deficiency in multicellular tumor spheroids. *Cancer Res* 51: 3831-3837

Gadian D.G (1982c) Applications to animals and human beings. In *Nuclear magnetic resonance and its applications to living systems*, Gadian D.G (ed) pp 62-77. Oxford University Press: UK

Gadian D.G (1982e) Applications to cells and tissues. In *Nuclear magnetic resonance and its applications to living systems*, Gadian D.G (ed) pp 43-77. Oxford University Press: UK

Gadian D.G (1982a) Introduction. In *Nuclear magnetic resonance and its applications to living systems*, Gadian D.G (ed) pp 1-22. Oxford University Press: U.K.

Gadian D.G (1982d) The n.m.r.parameters and their measurements. In *Nuclear magnetic resonance and its applications to living systems*, Gadian D.G (ed) pp 99-132. Oxford University press: UK

Gadian D.G (1982b) The theoretical basis of the n.m.r. experiments. In *Nuclear magnetic resonance and its applications to living systems*, Gadian D.G (ed) pp 78-98. Oxford University Press: UK

Gadian D.G (1982f) The type of information available from n.m.r. In *Nuclear magnetic resonance and its applications to living systems*, Gadian D.G (ed) pp 23-42. Oxford University Press: UK

Gilard V, Malet-Martino MC, de Forni M, Niemeyer U, Ader JC, Martino R (1993) Determination of the urinary excretion of ifosfamide and its phosphorylated metabolites by ^{31}P phosphorus nuclear magnetic resonance spectroscopy. *Cancer Chemother Pharmacol* 31: 387-394

Gillies RJ, Barry JA, Ross BD (1994b) In vitro and in vivo ^{13}C and ^{31}P NMR analyses of phosphocholine metabolism in rat glioma cells. *Magn Reson Med* 32: 310-318

Gillies RJ, Liu Z, Bhujwala Z (1994a) ^{31}P -MRS measurements of extracellular pH of tumors using 3-aminopropylphosphonate. *Am J Physiol* 267: C195-C203

Girard N, Wang ZJ, Erbetta A, Sutton LN, Phillips PC, Rorke LB, Zimmerman RA (1998) Prognostic value of proton MR spectroscopy of cerebral hemisphere tumors in children. *Neuroradiology* 40: 121-125

Glaholm J, Leach MO, Collins D, al Jehazi B, Sharp JC, Smith TA, Adach J, Hind A, McCready VR, White H (1990) Comparison of 5-fluorouracil pharmacokinetics following intraperitoneal and intravenous administration using in vivo ^{19}F magnetic resonance spectroscopy. *Br J Radiol* 63: 547-553

Griffiths JR (1991) Are cancer cells acidic? *Br J Cancer* 64: 425-427

Griffiths JR, Cady E, Edwards RH, McCready VR, Wilkie DR, Wiltshaw E (1983) ^{31}P -NMR studies of a human tumour in situ. *Lancet* 1: 1435-1436

Griffiths JR, Glickson JD (2000) Monitoring pharmacokinetics of anticancer drugs: non-invasive investigation using magnetic resonance spectroscopy. *Adv Drug Deliv Rev* 41: 75-89

Griffiths JR, Stevens AN, Iles RA, Gordon RE, Shaw D (1981) ^{31}P -NMR investigation of solid tumours in the living rat. *Biosci Rep* 1: 319-325

Griffiths JR, Tate AR, Howe FA, Stubbs M (2002) Magnetic Resonance Spectroscopy of cancer-practicalities of multi-centre trials and early results in non-Hodgkin's lymphoma. *Eur J Cancer* 38: 2085-2093

Haberkorn U, Krems B, Gerlach L, Bachert P, Morr I, Wiessler M, van Kaick G (1998) Assessment of glucosylifosfamide mustard biodistribution in rats with prostate adenocarcinomas by means of in vivo ^{31}P NMR and in vitro uptake experiments. *Magn Reson Med* 39: 754-761

Hadidi AH, Coulter CE, Idle JR (1988) Phenotypically deficient urinary elimination of carboxyphosphamide after cyclophosphamide administration to cancer patients. *Cancer Res* 48: 5167-5171

Hanaoka H, Yoshioka Y, Ito I, Niitu K, Yasuda N (1993) In vitro characterization of lung cancers by the use of ^1H nuclear magnetic resonance spectroscopy of tissue extracts and discriminant factor analysis. *Magn Reson Med* 29: 436-440

Hartley JM, Spanswick VJ, Gander M, Giacomini G, Whelan J, Souhami RL, Hartley JA (1999) Measurement of DNA cross-linking in patients on ifosfamide therapy using the single cell gel electrophoresis (comet) assay. *Clin Cancer Res* 5: 507-512

Heesters MA, Kamman RL, Mooyaart EL, Go KG (1993) Localized proton spectroscopy of inoperable brain gliomas. Response to radiation therapy. *J Neurooncol* 17: 27-35

Highley MS, Momerency G, Van Cauwenberghe K, Van Oosterom AT, De Bruijn EA, Maes RA, Blake P, Mansi J, Harper PG (1995) Formation of chloroethylamine and 1,3-oxazolidine-2-one following ifosfamide administration in humans. *Drug Metab Dispos* 23: 433-437

Highley MS, Schrijvers D, Van Oosterom AT, Harper PG, Momerency G, Van Cauwenberghe K, Maes RA, De Bruijn EA, Edelstein MB (1997) Activated oxazaphosphorines are transported predominantly by erythrocytes. *Ann Oncol* 8: 1139-1144

Hilton J (1984) Role of aldehyde dehydrogenase in cyclophosphamide-resistant L1210 leukemia. *Cancer Res* 44: 5156-5160

Hoult DI, Busby SJ, Gadian DG, Radda GK, Richards RE, Seeley PJ (1974) Observation of tissue metabolites using ³¹P nuclear magnetic resonance. *Nature* 252: 285-287

Huang Z, Roy P, Waxman DJ (2000) Role of human liver microsomal CYP3A4 and CYP2B6 in catalyzing N-dechloroethylation of cyclophosphamide and ifosfamide. *Biochem Pharmacol* 59: 961-972

Hwang JH, Egnaczyk GF, Ballard E, Dunn RS, Holland SK, Ball WS, Jr. (1998) Proton MR spectroscopic characteristics of pediatric pilocytic astrocytomas. *AJNR Am J Neuroradiol* 19: 535-540

Innocenti F, Ratain MJ (2002) Update on pharmacogenetics in cancer chemotherapy. *Eur J Cancer* 38: 639-644

Iyer L, Ratain MJ (1998) Pharmacogenetics and cancer chemotherapy. *Eur J Cancer* 34: 1493-1499

Jackel MC, Kopf-Maier P, Baumgart F, Ziessow D, Tausch-Treml R (2000) Value of ³¹P NMR spectroscopy in predicting the response of a xenografted human hypopharynx carcinoma to irradiation. *J Cancer Res Clin Oncol* 126: 325-331

Johnstone EC, Lind MJ, Griffin MJ, Boddy AV (2000) Ifosfamide metabolism and DNA damage in tumour and peripheral blood lymphocytes of breast cancer patients. *Cancer Chemother Pharmacol* 46: 433-441

Joqueviel C, Gilard V, Martino R, Malet-Martino M, Niemeyer U (1997) Urinary stability of carboxycyclophosphamide and carboxyifosfamide, two major metabolites of the anticancer drugs cyclophosphamide and ifosfamide. *Cancer Chemother Pharmacol* 40: 391-399

Kaijser GP, Beijnen JH, Bult A, Underberg WJ (1994) Ifosfamide metabolism and pharmacokinetics (review). *Anticancer Res* 14: 517-531

Kaijser GP, de Kraker J, Bult A, Underberg WJ, Beijnen JH (1998) Pharmacokinetics of ifosfamide and some metabolites in children. *Anticancer Res* 18: 1941-1949

Kaijser GP, Keizer HJ, Beijnen JH, Bult A, Underberg WJ (1996) Pharmacokinetics of ifosfamide, 2- and 3-dechloroethylifosfamide in plasma

and urine of cancer patients treated with a 10-day continuous infusion of ifosfamide. *Anticancer Res* 16: 3247-3257

Kaijser GP, Korst A, Beijnen JH, Bult A, Underberg WJ (1993) The analysis of ifosfamide and its metabolites (review). *Anticancer Res* 13: 1311-1324

Kamada K, Houkin K, Abe H, Sawamura Y, Kashiwaba T (1997)

Differentiation of cerebral radiation necrosis from tumor recurrence by proton magnetic resonance spectroscopy. *Neurol Med Chir (Tokyo)* 37: 250-256

Kamen BA, Frenkel E, Colvin OM (1995) Ifosfamide: should the honeymoon be over? *J Clin Oncol* 13: 307-309

Kerbusch T, de Kraker J, Keizer HJ, van Putten JW, Groen HJ, Jansen RL, Schellens JH, Beijnen JH (2001a) Clinical pharmacokinetics and pharmacodynamics of ifosfamide and its metabolites. *Clin Pharmacokinet* 40: 41-62

Kerbusch T, Huitema AD, Ouwerkerk J, Keizer HJ, Mathot RA, Schellens JH, Beijnen JH (2000) Evaluation of the autoinduction of ifosfamide metabolism by a population pharmacokinetic approach using NONMEM. *Br J Clin Pharmacol* 49: 555-561

Kerbusch T, Jansen RL, Mathot RA, Huitema AD, Jansen M, van Rijswijk RE, Beijnen JH (2001c) Modulation of the cytochrome P450-mediated metabolism of ifosfamide by ketoconazole and rifampin. *Clin Pharmacol Ther* 70: 132-141

Kerbusch T, Mathot RA, Keizer HJ, Kaijser GP, Schellens JH, Beijnen JH (2001b) Influence of dose and infusion duration on pharmacokinetics of ifosfamide and metabolites. *Drug Metab Dispos* 29: 967-975

Kim RB (2002) Pharmacogenetics of CYP enzymes and drug transporters: remarkable recent advances. *Adv Drug Deliv Rev* 54: 1241-1242

Kiss Z (1999) Regulation of mitogenesis by water-soluble phospholipid intermediates. *Cell Signal* 11: 149-157

Kooby DA, Zakian KL, Challa SN, Matei C, Petrowsky H, Yoo HH, Koutcher JA, Fong Y (2000) Use of phosphorous-31 nuclear magnetic resonance spectroscopy to determine safe timing of chemotherapy after hepatic resection. *Cancer Res* 60: 3800-3806

Koutcher JA, Alfieri AA, Devitt ML, Rhee JG, Kornblith AB, Mahmood U, Merchant TE, Cowburn D (1992) Quantitative changes in tumor metabolism, partial pressure of oxygen, and radiobiological oxygenation status postradiation. *Cancer Res* 52: 4620-4627

Koutcher JA, Ballon D, Graham M, Healey JH, Casper ES, Heelan R, Gerweck LE (1990) ³¹P NMR spectra of extremity sarcomas: diversity of metabolic profiles and changes in response to chemotherapy. *Magn Reson Med* 16: 19-34

Kurowski V, Wagner T (1993) Comparative pharmacokinetics of ifosfamide, 4-hydroxyifosfamide, chloroacetaldehyde, a. *Cancer Chemother Pharmacol* 33: 36-42

Kwock LA (2001) Tuning in on tumor activity with proton MR spectroscopy. *AJNR Am J Neuroradiol* 22: 807-808

Lauterbur PC (1973) Image formation by induced local interactions. *Nature* 242: 190-191

Lazareff JA, Gupta RK, Alger J (1999) Variation of post-treatment H-MRSI choline intensity in pediatric gliomas. *J Neurooncol* 41: 291-298

Leach MO (1992) Practicalities of localization in animal and human tumours. *NMR Biomed* 5: 244-252

Leach M., Le Moyec L, and Podo F (1992). MRS of tumours: Basic Principles. de Certaines JD, Bovee W, and Podo F. First. Magnetic Resonance Spectroscopy in Biology and Medicine. (ed 1st) Pergamon Press Ltd. 295-344 UK

Leach MO, Verrill M, Glaholm J, Smith TA, Collins DJ, Payne GS, Sharp JC, Ronen SM, McCready VR, Powles TJ, Smith IE (1998) Measurements of human breast cancer using magnetic resonance spectroscopy: a review of clinical measurements and a report of localized ³¹P measurements of response to treatment. *NMR Biomed* 11: 314-340

Lean CL, Newland RC, Ende DA, Bokey EL, Smith IC, Mountford CE (1993) Assessment of human colorectal biopsies by ¹H MRS: correlation with histopathology. *Magn Reson Med* 30: 525-533

Lee PL, Gonzalez RG (2000) Magnetic resonance spectroscopy of brain tumors. *Curr Opin Oncol* 12: 199-204

Lewis LD (1996) A study of 5 day fractionated ifosfamide pharmacokinetics in consecutive treatment cycles. *Br J Clin Pharmacol* 42: 179-186

Lewis LD, Fitzgerald DL, Mohan P, Thatcher N, Harper PG, Rogers HJ (1991) The pharmacokinetics of ifosfamide given as short and long intravenous infusions in cancer patients. *Br J Clin Pharmacol* 31: 77-82

Li SJ, Wehrle JP, Rajan SS, Steen RG, Glickson JD, Hilton J (1988) Response of radiation-induced fibrosarcoma-1 in mice to cyclophosphamide monitored by in vivo ³¹P nuclear magnetic resonance spectroscopy. *Cancer Res* 48: 4736-4742

Lilleyman JS, Lennard L (1994) Mercaptopurine metabolism and risk of relapse in childhood lymphoblastic leukaemia. *Lancet* 343: 1188-1190

Lilly MB, Katholi CR, Ng TC (1985) Direct relationship between high-energy phosphate content and blood flow in thermally treated murine tumors. *J Natl Cancer Inst* 75: 885-889

Lin A, Bluml S, Mamelak AN (1999) Efficacy of proton magnetic resonance spectroscopy in clinical decision making for patients with suspected malignant brain tumors. *J Neurooncol* 45: 69-81

Lind MJ, Margison JM, Cerny T, Thatcher N, Wilkinson PM (1989a) Comparative pharmacokinetics and alkylating activity of fractionated

intravenous and oral ifosfamide in patients with bronchogenic carcinoma.

Cancer Res 49: 753-757

Lind MJ, Margison JM, Cerny T, Thatcher N, Wilkinson PM (1989b)

Prolongation of ifosfamide elimination half-life in obese patients due to altered drug distribution. *Cancer Chemother Pharmacol* 25: 139-142

Lind MJ, Margison JM, Cerny T, Thatcher N, Wilkinson PM (1990b) The

effect of age on the pharmacokinetics of ifosfamide. *Br J Clin Pharmacol* 30: 140-143

Lind MJ, Roberts HL, Thatcher N, Idle JR (1990a) The effect of route of administration and fractionation of dose on the metabolism of ifosfamide.

Cancer Chemother Pharmacol 26: 105-111

Loehrer PJ, Sr. (1992) The history of ifosfamide. *Semin Oncol* 19: 2-6

Low JE, Borch RF, Sladek NE (1983) Further studies on the conversion of 4-hydroxyoxazaphosphorines to reactive mustards and acrolein in inorganic buffers. *Cancer Res* 43: 5815-5820

Luyten PR, Bruntink G, Sloff FM, Vermeulen JW, van der Heijden JI, den Hollander JA, Heerschap A (1989) Broadband proton decoupling in human ³¹P NMR spectroscopy. *NMR Biomed* 1: 177-183

Lyng H, Skretting A, Rofstad EK (1992) Blood flow in six human melanoma xenograft lines with different growth characteristics. *Cancer Res* 52: 584-592

Magrath I, Sandlund J, Raynor A, Rosenberg S, Arasi V, Miser J (1986) A phase II study of ifosfamide in the treatment of recurrent sarcomas in young people. *Cancer Chemother Pharmacol* 18 Suppl 2: S25-S28

Mahmood U, Alfieri AA, Ballon D, Traganos F, Koutcher JA (1995) In vitro and in vivo ^{31}P nuclear magnetic resonance measurements of metabolic changes post radiation. *Cancer Res* 55: 1248-1254

Mahmood U, Alfieri AA, Thaler H, Cowburn D, Koutcher JA (1994) Radiation dose-dependent changes in tumor metabolism measured by ^{31}P nuclear magnetic resonance spectroscopy. *Cancer Res* 54: 4885-4891

Maris JM, Evans AE, McLaughlin AC, D'Angio GJ, Bolinger L, Manos H, Chance B (1985) ^{31}P nuclear magnetic resonance spectroscopic investigation of human neuroblastoma in situ. *N Engl J Med* 312: 1500-1505

Martin AJ, Liu H, Hall WA, Truwit CL (2001) Preliminary assessment of turbo spectroscopic imaging for targeting in brain biopsy. *AJNR Am J Neuroradiol* 22: 959-968

Martino R, Crasnier F, Chouini-Lalanne N, Gilard V, Niemeyer U, de Forni M, Malet-Martino MC (1992) A new approach to the study of ifosfamide metabolism by the analysis of human body fluids with ^{31}P nuclear magnetic resonance spectroscopy. *J Pharmacol Exp Ther* 260: 1133-1144

McAllister RM, Melnyk J, Finkelstein JZ, Adams EC, Jr., Gardner MB (1969) Cultivation in vitro of cells derived from a human rhabdomyosarcoma. *Cancer* 24: 520-526

Meyerand ME, Pipas JM, Mamourian A, Tosteson TD, Dunn JF (1999) Classification of biopsy-confirmed brain tumors using single-voxel MR spectroscopy. *AJNR Am J Neuroradiol* 20: 117-123

Misiura K, Okruszek A, Pankiewicz K, Stec WJ, Czownicki Z, Utracka B (1983) Stereospecific synthesis of chiral metabolites of ifosfamide and their determination in the urine. *J Med Chem* 26: 674-679

Moller HE, Vermathen P, Rummeny E, Wortler K, Wuisman P, Rossner A, Wormann B, Ritter J, Peters PE (1996) In vivo ^{31}P NMR spectroscopy of human musculoskeletal tumors as a measure of response to chemotherapy. *NMR Biomed* 9: 347-358

Momerency G, Van Cauwenberghe K, Highley MS, Harper PG, Van Oosterom AT, De Bruijn EA (1996) Partitioning of ifosfamide and its metabolites between red blood cells and plasma. *J Pharm Sci* 85: 262-265

Moon RB, Richards JH (1973) Determination of intracellular pH by ^{31}P Magnetic resonance. *J Biol Chem* 248: 7276-7278

Moreno A, Lopez LA, Fabra A, Arus C (1998) ^1H MRS markers of tumour growth in intrasplenic tumours and liver metastasis induced by injection of HT-29 cells in nude mice spleen. *NMR Biomed* 11: 93-106

Moretti JL, Rapin JR, Hamberger C, Lautie JP, Mathieu E, Renault H (1979) Radiopharmacological studies of ^{125}I -labeled ifosfamide in rats. *Int J Nucl Med Biol* 6: 145-151

Murphy EJ, Rajagopalan B, Brindle KM, Radda GK (1989) Phospholipid bilayer contribution to ^{31}P NMR spectra in vivo. *Magn Reson Med* 12: 282-289

Murray GI, Taylor MC, Burke MD, Melvin WT (1998) Enhanced expression of cytochrome P450 in stomach cancer. *Br J Cancer* 77: 1040-1044

Murray GI, Weaver RJ, Paterson PJ, Ewen SW, Melvin WT, Burke MD (1993) Expression of xenobiotic metabolizing enzymes in breast cancer. *J Pathol* 169: 347-353

Nanni P, De Giovanni C, Nicoletti G, Del Re B, Scotlandi K, Lollini PL (1989) Human rhabdomyosarcoma cells in nude mice as a model for metastasis and differentiation. *Invasion Metastasis* 9: 231-241

Narayan P, Jajodia P, Kurhanewicz J, Thomas A, MacDonald J, Hubesch B, Hedgcock M, Anderson CM, James TL, Tanagho EA. (1991) Characterization of prostate cancer, benign prostatic hyperplasia and normal prostates using transrectal ^{31}P phosphorus magnetic resonance spectroscopy: a preliminary report. *J Urol* 146: 66-74

Negendank W (1992) Studies of human tumors by MRS: a review. *NMR Biomed* 5: 303-324

Negendank WG, Crowley MG, Ryan JR, Keller NA, Evelhoch JL (1989) Bone and soft-tissue lesions: diagnosis with combined H-1 MR imaging and P-31 MR spectroscopy. *Radiology* 173: 181-188

Negendank WG, Padavic-Shaller KA, Li CW, Murphy-Boesch J, Stoyanova R, Krigel RL, Schilder RJ, Smith MR, Brown TR (1995) Metabolic characterization of human non-Hodgkin's lymphomas in vivo with the use of proton-decoupled phosphorus magnetic resonance spectroscopy. *Cancer Res* 55: 3286-3294

Negendank WG, Sauter R, Brown TR, Evelhoch JL, Falini A, Gotsis ED, Heerschap A, Kamada K, Lee BC, Mingeot MM, Moser E, Padavic-Shaller KA, Sanders JA, Spraggins TA, Stillman AE, Terwey B, Vogl TJ, Wicklow K, Zimmerman RA (1996) Proton magnetic resonance spectroscopy in patients with glial tumors: a multicenter study. *J Neurosurg* 84: 449-458

Nelson RL, Allen LM, Creaven PJ (1976) Pharmacokinetics of divided-dose ifosfamide. *Clin Pharmacol Ther* 19: 365-370

Nishizuka Y (2003) Discovery and prospect of protein kinase C research: epilogue. *J Biochem (Tokyo)* 133: 155-158

Norpoth K (1976) Studies on the metabolism of isopnosphamide (NSC-109724) in man. *Cancer Treat Rep* 60: 437-443

Norpoth K, Muller G, Raidt H (1976) [Isolation and characterisation of two main metabolites of ifosfamide from human urine (author's transl)]. *Arzneimittelforschung* 26: 1376-1377

Nowrousian MR, Burkert H, Herdrich K, Pohl J, Seeber S. (1993) *Ifosfamide in cancer therapy-A comparison with cyclophosphamide*. Universitätsverlag Jena GmbH: Germany

Ojugo AS, McSheehy PM, McIntyre DJ, McCoy C, Stubbs M, Leach MO, Judson IR, Griffiths JR (1999) Measurement of the extracellular pH of solid tumours in mice by magnetic resonance spectroscopy: a comparison of exogenous (19)F and (31)P probes. *NMR Biomed* 12: 495-504

Ojugo AS, McSheehy PM, Stubbs M, Alder G, Bashford CL, Maxwell RJ, Leach MO, Judson IR, Griffiths JR (1998) Influence of pH on the uptake of 5-fluorouracil into isolated tumour cells. *Br J Cancer* 77: 873-879

Okazaki M, Kubota T, Hanatani Y, Maruyama K, Tsuyuki K, Nakada M, Asanuma F, Ishibiki K, Abe O (1982) [Microvascular architecture of human tumors transplanted in nude mice--its relationship to sensitivity to antineoplastic agents]. *Gan To Kagaku Ryoho* 9: 1433-1441

Ordidge R, Connelly A, Lohman J. (1986) Image -selected in vivo spectroscopy (ISIS). a new technique for spatially selective NMR spectroscopy. *Journal of Magnetic Resonance* 66: 283-294

Pappo AS, Etcubanas E, Santana VM, Rao BN, Kun LE, Fontanesi J, Roberson PK, Bowman LC, Crist WM, Shapiro DN (1993) A phase II trial of ifosfamide in previously untreated children and adolescents with unresectable rhabdomyosarcoma. *Cancer* 71: 2119-2125

Passe P, Delepine N, Arnaud P, Urien S, Delepine G, Traore F, Desbois JC, Brion F (1999) Pharmacokinetic modelling of ifosfamide administered by continuous infusion on 5 days at the dose of 6 g/m². *Anticancer Res* 19: 837-842

Payne GS, Pinkerton CR, Bouffet E, Leach MO (2000) Initial measurements of ifosfamide and cyclophosphamide in patients using (31)P MRS: pulse-and-acquire, decoupling, and polarization transfer. *Magn Reson Med* 44: 180-184

Pinkerton CR, Pritchard J (1989) A phase II study of ifosfamide in paediatric solid tumours. *Cancer Chemother Pharmacol* 24 Suppl 1: S13-S15

Pinkerton CR, Rogers H, James C, Bowman A, Barbor PR, Eden OB, Pritchard J (1985) A phase II study of ifosfamide in children with recurrent solid tumours. *Cancer Chemother Pharmacol* 15: 258-262

Podo F (1999) Tumour phospholipid metabolism. *NMR Biomed* 12: 413-439

Podo F, de Certaines JD (1996) Magnetic resonance spectroscopy in cancer: phospholipid, neutral lipid and lipoprotein metabolism and function. *Anticancer Res* 16: 1305-1315

Poptani H, Gupta RK, Roy R, Pandey R, Jain VK, Chhabra DK (1995) Characterization of intracranial mass lesions with in vivo proton MR spectroscopy. *AJNR Am J Neuroradiol* 16: 1593-1603

Presant CA, Wolf W, Albright MJ, Servis KL, Ring R, III, Atkinson D, Ong RL, Wiseman C, King M, Blayney D, . (1990) Human tumor fluorouracil trapping: clinical correlations of in vivo 19F nuclear magnetic resonance spectroscopy pharmacokinetics. *J Clin Oncol* 8: 1868-1873

Presant CA, Wolf W, Waluch V, Wiseman C, Kennedy P, Blayney D, Brechner RR (1994) Association of intratumoral pharmacokinetics of fluorouracil with clinical response. *Lancet* 343: 1184-1187

Preul MC, Caramanos Z, Collins DL, Villemure JG, LeBlanc R, Olivier A, Pokrupa R, Arnold DL (1996) Accurate, noninvasive diagnosis of human brain tumors by using proton magnetic resonance spectroscopy. *Nat Med* 2: 323-325

Preul MC, Caramanos Z, Villemure JG, Shenouda G, LeBlanc R, Langleben A, Arnold DL (2000) Using proton magnetic resonance spectroscopic imaging to predict in vivo the response of recurrent malignant gliomas to tamoxifen chemotherapy. *Neurosurgery* 46: 306-318

Purcell EM, Torrey HC, Pound RV (1946) Resonance absorption by nuclear magnetic moments in a solid. *Physical Reviews* 69: 37-38

Redmond OM, Bell E, Stack JP, Dervan PA, Carney DN, Hurson B, Ennis JT (1992) Tissue characterization and assessment of preoperative chemotherapeutic response in musculoskeletal tumors by in vivo ³¹P magnetic resonance spectroscopy. *Magn Reson Med* 27: 226-237

Roberts J.E, Griffin R.G (1987) Solid state NMR techniques. In *Phosphorus NMR in biology*, Burt CT (ed) pp 63-83. CRC Press: Florida

Rodrigues LM, Maxwell RJ, McSheehy PM, Pinkerton CR, Robinson SP, Stubbs M, Griffiths JR (1997) In vivo detection of ifosfamide by ³¹P-MRS in rat tumours: increased uptake and cytotoxicity induced by carbogen breathing in GH3 prolactinomas. *Br J Cancer* 75: 62-68

Rodrigues LM, Robinson SP, McSheehy PM, Stubbs M, Griffiths JR (2002) Enhanced uptake of ifosfamide into GH3 prolactinomas with hypercapnic hyperoxic gases monitored in vivo by (³¹)P MRS. *Neoplasia* 4: 539-543

Ronen SM, Jackson LE, Belouèche M, Leach MO (2001) Magnetic resonance detects changes in phosphocholine associated with Ras activation and inhibition in NIH 3T3 cells. *Br J Cancer* 84: 691-696

Ronen SM, Stier A, Degani H (1990) NMR studies of the lipid metabolism of T47D human breast cancer spheroids. *FEBS Lett* 266: 147-149

Rousseau A, Marquet P (2002) Application of pharmacokinetic modelling to the routine therapeutic drug monitoring of anticancer drugs. *Fundam Clin Pharmacol* 16: 253-262

Sandler E, Lyden E, Ruymann F, Maurer H, Wharam M, Parham D, Link M, Crist W (2001) Efficacy of ifosfamide and doxorubicin given as a phase II "window" in children with newly diagnosed metastatic rhabdomyosarcoma: a report from the Intergroup Rhabdomyosarcoma Study Group. *Med Pediatr Oncol* 37: 442-448

Sarosy G (1989) Ifosfamide--pharmacologic overview. *Semin Oncol* 16: 2-8

Schwartz PS, Waxman DJ (2001) Cyclophosphamide induces caspase 9-dependent apoptosis in 9L tumor cells. *Mol Pharmacol* 60: 1268-1279

Schwartzman E, Scopinaro M, Angueyra N (1989) Phase II study of ifosfamide as a single drug for relapsed paediatric patients. *Cancer Chemother Pharmacol* 24 Suppl 1: S11-S12

Sharkey FE, Fogh J (1984) Considerations in the use of nude mice for cancer research. *Cancer Metastasis Rev* 3: 341-360

Singer JM, Hartley JM, Brennan C, Nicholson PW, Souhami RL (1998) The pharmacokinetics and metabolism of ifosfamide during bolus and infusional administration: a randomized cross-over study. *Br J Cancer* 77: 978-984

Skinner R, Sharkey IM, Pearson AD, Craft AW (1993) Ifosfamide, mesna, and nephrotoxicity in children. *J Clin Oncol* 11: 173-190

Sladek NE (1988) Metabolism of oxazaphosphorines. *Pharmacol Ther* 37: 301-355

Sladek NE, Kollander R, Sreerama L, Kiang DT (2002) Cellular levels of aldehyde dehydrogenases (ALDH1A1 and ALDH3A1) as predictors of therapeutic responses to cyclophosphamide-based chemotherapy of breast cancer: a retrospective study. Rational individualization of oxazaphosphorine-based cancer chemotherapeutic regimens. *Cancer Chemother Pharmacol* 49: 309-321

Smith SR, Martin PA, Davies JM, Edwards RH, Stevens AN (1990) The assessment of treatment response in non-Hodgkin's lymphoma by image guided ^{31}P magnetic resonance spectroscopy. *Br J Cancer* 61: 485-490

Springate JE (1997) Ifosfamide metabolite chloroacetaldehyde causes renal dysfunction in vivo. *J Appl Toxicol* 17: 75-79

Steen RG (1989) Response of solid tumors to chemotherapy monitored by in vivo ^{31}P nuclear magnetic resonance spectroscopy: a review. *Cancer Res* 49: 4075-4085

- Steen RG (1991) Characterization of tumor hypoxia by ^{31}P MR spectroscopy. *AJR Am J Roentgenol* 157: 243-248
- Stevens AN, Morris PG, Iles RA, Sheldon PW, Griffiths JR (1984) 5-fluorouracil metabolism monitored in vivo by ^{19}F NMR. *Br J Cancer* 50: 113-117
- Street JC, Alfieri AA, Traganos F, Koutcher JA (1997) In vivo and ex vivo study of metabolic and cellular effects of 5-fluorouracil chemotherapy in a mouse mammary carcinoma. *Magn Reson Imaging* 15: 587-596
- Street JC, Mahmood U, Matei C, Koutcher JA (1995) In vivo and in vitro studies of cyclophosphamide chemotherapy in a mouse mammary carcinoma by ^{31}P NMR spectroscopy. *NMR Biomed* 8: 149-158
- Stubbs M (1999) Application of magnetic resonance techniques for imaging tumour physiology. *Acta Oncol* 38: 845-853
- Tausch-Treml R, Kopf-Maier P, Baumgart F, Gewiese B, Ziessow D, Scherer H, Wolf KJ (1991) ^{31}P nuclear magnetic resonance spectroscopy, histology and cytokinetics of a xenografted hypopharynx carcinoma following treatment with cisplatin: comparison in three sublines with increasing resistance. *Br J Cancer* 64: 485-493
- Taylor JS, Langston JW, Reddick WE, Kingsley PB, Ogg RJ, Pui MH, Kun LE, Jenkins JJ, III, Chen G, Ochs JJ, Sanford RA, Heideman RL (1996) Clinical value of proton magnetic resonance spectroscopy for differentiating recurrent or residual brain tumor from delayed cerebral necrosis. *Int J Radiat Oncol Biol Phys* 36: 1251-1261

Tedeschi G, Lundbom N, Raman R, Bonavita S, Duyn JH, Alger JR, Di Chiro G (1997) Increased choline signal coinciding with malignant degeneration of cerebral gliomas: a serial proton magnetic resonance spectroscopy imaging study. *J Neurosurg* 87: 516-524

Vaidya SJ, Payne GS, Leach MO, Pinkerton CR (2003) Potential role of magnetic resonance in assessment of tumour response in childhood cancer. *Eur J Cancer* 39: 728-735

Vanhamme L, van den BA, Van Huffel S (1997) Improved method for accurate and efficient quantification of MRS data with use of prior knowledge. *J Magn Reson* 129: 35-43

Vaupel P, Okunieff P, Kallinowski F, Neuringer LJ (1989) Correlations between ³¹P-NMR spectroscopy and tissue O₂ tension measurements in a murine fibrosarcoma. *Radiat Res* 120: 477-493

Wagner T, Peter G, Voelcker G, Hohorst HJ (1977) Characterization and quantitative estimation of activated cyclophosphamide in blood and urine. *Cancer Res* 37: 2592-2596

Walker D, Flinois JP, Monkman SC, Beloc C, Boddy AV, Cholerton S, Daly AK, Lind MJ, Pearson AD, Beaune PH, . (1994) Identification of the major human hepatic cytochrome P450 involved in activation and N-dechloroethylation of ifosfamide. *Biochem Pharmacol* 47: 1157-1163

Wang Z, Sutton LN, Cnaan A, Haselgrove JC, Rorke LB, Zhao H, Bilaniuk LT, Zimmerman RA (1995) Proton MR spectroscopy of pediatric cerebellar tumors. *AJNR Am J Neuroradiol* 16: 1821-1833

Warren KE, Frank JA, Black JL, Hill RS, Duyn JH, Aikin AA, Lewis BK, Adamson PC, Balis FM (2000) Proton magnetic resonance spectroscopic imaging in children with recurrent primary brain tumors. *J Clin Oncol* 18: 1020-1026

Watters JW, McLeod HL (2003) Cancer pharmacogenomics: current and future applications. *Biochim Biophys Acta* 1603: 99-111

Wolf W, Presant CA, Waluch V (2000) ¹⁹F-MRS studies of fluorinated drugs in humans. *Adv Drug Deliv Rev* 41: 55-74

Wolf W, Waluch V, Presant CA (1998) Non-invasive ¹⁹F-NMRS of 5-fluorouracil in pharmacokinetics and pharmacodynamic studies. *NMR Biomed* 11: 380-387

Woodland C, Ito S, Granvil CP, Wainer IW, Klein J, Koren G (2000) Evidence of renal metabolism of ifosfamide to nephrotoxic metabolites. *Life Sci* 68: 109-117

Yu LJ, Drewes P, Gustafsson K, Brain EG, Hecht JE, Waxman DJ (1999) In vivo modulation of alternative pathways of P-450-catalyzed cyclophosphamide metabolism: impact on pharmacokinetics and antitumor activity. *J Pharmacol Exp Ther* 288: 928-937

Yule SM, Boddy AV, Cole M, Price L, Wyllie R, Tasso MJ, Pearson AD, Idle JR (1995) Cyclophosphamide metabolism in children. *Cancer Res* 55: 803-809

Yule SM, Boddy AV, Cole M, Price L, Wyllie R, Tasso MJ, Pearson AD, Idle JR (1996) Cyclophosphamide pharmacokinetics in children. *Br J Clin Pharmacol* 41: 13-19

Yule SM, Price L, Cole M, Pearson AD, Boddy AV (2001) Cyclophosphamide metabolism in children following a 1-h and a 24-h infusion. *Cancer Chemother Pharmacol* 47: 222-228

Yule SM, Price L, Pearson AD, Boddy AV (1997) Cyclophosphamide and ifosfamide metabolites in the cerebrospinal fluid of children. *Clin Cancer Res* 3: 1985-1992

Yule SM, Walker D, Cole M, McSorley L, Cholerton S, Daly AK, Pearson AD, Boddy AV (1999) The effect of fluconazole on cyclophosphamide metabolism in children. *Drug Metab Dispos* 27: 417-421